The Circadian Clock-Cell Cycle Connection and its Implication for Cancer

Elham(Aida)Farshadi

The Circadian Clock-Cell Cycle Connection and its Implication for Cancer

De circadiane klok-celcyclus connectie en de implicaties voor kanker

Proefschrift

ter verkrijging van de graad van doctor aan de
Erasmus Universiteit Rotterdam
op gezag van de rector magnificus

Prof. dr. H.A.P. Pols

en volgens besluit van het College voor Promoties

De openbare verdediging zal plaatsvinden op
dinsdag 22 mei 2018 om 15:30 uur

door

Elham (Aida) Farshadi
geboren te Ahvaz, Iran

ERASMUS UNIVERSITEIT ROTTERDAM

Promotiecommissie:

Promotor:	Prof. dr. G.T.J. van der Horst
Overige leden:	Prof. dr. W. Vermeulen Prof. dr. F. Lêvi Dr. R.W.F. de Bruin
Copromotoren:	Dr. I. Chaves

In memory of my father who tought me
the meaning of life and the will to explore
and then went

| Table of contents

Chapter 1	General introduction	12
Chapter 2	The positive circadian regulators CLOCK and BMAL1 heterodimer control G2/M cell cycle transition through Cyclin B1	34
Chapter 3	The Circadian Clock Proteins CRY1 and CRY2 Control the Cell Cycle G1/S Transition and Mitotic Progression	74
Chapter 4	Loss of coupling between the circadian clock and the cell cycle in a mouse breast carcinoma cell line	98
Chapter 5	Circadian clock genes differentially modulate the cancer properties of H1299 human non-small lung carcinoma cells	114
Chapter 6	General discussion	146
Appendix	Summary	156
	Samenvatting (Dutch summary)	158
	PhD Portfolio	160
	List of puplications	161
	Curriculum vitae	162
	Acknowledgments	163

CHAPTER 1

General introduction

Physiology in harmony with nature

The day/night cycle is the consequence of the rotation of the earth around its own axis on its path around the sun. This daily cycle has a period of 24 hours. As a result of the earth movement, living organisms are exposed to environmental changes, such as daily cycles of light and darkness and diurnal changes in temperature, that are associated with the day and night. Almost all the species have developed an internal timing system or "biological clock" to adapt to such external changes (Pittendrigh 1996). The biological clock generates a circadian rhythm that regulates physiological processes in order to optimize them to a particular time of the day. Harmony of an organism with itself, internally, and with the environmental changes is crucial for both survival and well-being of an organism. For example, at an early evolutionary stage various species developed the clock system to limit sunlight-sensitive processes, such as DNA replication, to the night (Khapre et al., 2010). Lack of internal synchrony, which is caused by shift work, and jet lag, may have long or short term health consequences for the body. For instance, shift work is considered as a carcinogenic factor, and the risk of cancer is enhanced by the number of the years an individual spends working at night (Schernhammer et al.,2003; Lee et al., 2010). Other complications that are related to circadian dysfunction have been reported by different studies (e.g., de-regulated hormonal function, fatigue, gastrointestinal disturbance, diabetes) (Takahashi et al.,2008; Preuss et al., 2008; Arble et al., 2010).

Circadian rhythms

The endogenous circadian oscillation was first reported by the French scientist "Jean-Jacques d'Ortous de Mairan" in 1729. He first noticed the daily movements of "Mimosa pudica" or "sensitive plant" leaves in response to the day and night. Interestingly, he discovered that these daily movements persist when the plant is kept in constant darkness (Kuhlman et al., 2007). The leaves were open during the day and closed at a certain time in the evening. Although de Mairan related these rhythms to passive reactions, his observation was the hallmark of the circadian rhythm discovery. The term circadian derives from the latin words of circa (around) and diem (day).

A circadian rhythm is a selfsustained biological event with a period of approximately 24 hours (Pittendrigh, 1960). One of the main characteristics of a circadian rhythm is its endogenous property (Wever et al., 1986). In the absence of synchronizing signals, the clock system will "free-fun" and oscillate with a period that is close to 24 hours but not exactly 24 hours. These endogenous rhythms are entrained to the exact 24 hour period of earth rotation by external environmental cues, notably light (Sharma et al., 2003; Ko et al., 2006). The external cues that are able to reset or synchronize the circadian rhythms are called "time givers" or by its original German name "Zeitgebers". In circadian biology, timing under entrained conditions is expressed in Zeitgeber Time (ZT), where ZT0 corresponds to lights on. Circadian time (CT) is a term used to refer to the internal physiological time in free-running conditions, i.e. in the absence of Zeitgebers, and, the start of a subjective day is called CT0. Living

organisms respond differently to the light pulses depending on when they were exposed to the light (Boulos et al., 2002). Responses to light pulses throughout the day can be plotted in order to generate a phase response curve (PRC). For example, if the light pulse is given at the beginning of the subjective night, a phase delay is seen in the circadian rhythm. In contrast, if the light stimuli are given at the end of the subjective night, a phase advance is observed (Pittendrigh et al.,1988). Light pulses during the subjective day have no effect on the rhythm.

I The mammalian circadian clock

The SCN master clock

The circadian clock system is conserved among all the species from prokaryotes, such as cyanobacteria (Iwasaka et al., 2000; Mori et al., 2000), to eukaryotes such as mammals (Reppert et al., 2001). Circadian systems are characterized by three basic features: 1. An environmental input (such as light), 2. An internal and self-sustained oscillator (circadian clock), and 3. An output (rhythmic oscillation in physiology or behavior). In animals, the circadian system is organized in a hierarchical manner, with a central brain clock at the top of hierarchy and peripheral clocks all over the body (Ku et al., 2006).

In mammals, the master clock is centrally located in the superchiasmatic nucleus of the hypothalamus (SCN). Damaging the SCN in rats disrupts both the activity/rest cycle and drinking behavior rhythms (Stephan et al.,1972). The role of the SCN in the circadian system has been further studied by the tau mutant golden hamsters. These mutant animals display a dramatic short circadian period of about 20 hours, compared to the wild type animals with a 24 hour circadian period (Ralph et al., 1990). Researchers could restore some of the circadian behavior by transplanting the SCN from the wild type hamsters in to the mutant hamsters (Ralph et al., 1990). In contrast, transplantation of the SCN from tau mutant hamsters in to the wild type animals results in a short circadian period in the wild type hamsters. These experiments indicated the importance of the SCN as the master circadian clock.

The SCN is composed of approximately 20,000 neurons. Each individual SCN neuron has a self-sustained and cell autonomous circadian oscillator with a broad range in circadian periodicity varying between 22 to 30 hours (Welsh et al., 1995; Mohawk et al., 2012). SCN clocks are constantly entrained (synchronized) to the day-night cycle of 24 hours. The photic information is received by photoreceptors located in the retina. Subsequently, the light information is transmitted to the SCN via the retinohypothalamic tract (RHT) (Meijer et al., 2007). A subset of ganglion cells in the inner layer of the retina that express the melanopsin photopigment are considered as the main circadian photoreceptors (Berson et al., 2002). The other photoreceptors, rods and cones, play an accessory role in maintaining circadian entrainment (Hattar et al., 2003). The SCN neurons keep synchrony and stay coupled to each other through synaptic connections (Aton et al., 2005). This intracellular coupling between the SCN neurons is critical for robust circadian rhythmicity, that leads to robust circadian outputs. Accordingly, synchronizing signals are transmitted to the peripheral clocks to achieve coherent rhythm in the entire organism.

Peripheral clocks

Rhythmic clock gene expression and protein expression has been identified in the peripheral tissues or non-SCN cells throughout the body (Yamazaki et al., 2000). Importantly, circadian rhythmicity persists in isolated tissues *in vitro,* where no control of the SCN exists, indicating the endogenous nature of the circadian oscillation at the periphery (Yamazaki et al., 2000). *In vivo*, these cellular clocks receive entraining signals via neural and hormonal stimuli from the SCN to maintain synchrony (Welsh et al., 2004). However, the circadian oscillation in isolated tissues or cell cultures dampens in time due to desynchronization between the cells in the absence of SCN signals. On the other hand, clock synchronizers such as as forskolin or dexamethasone can be used to temporarily resynchronize the cellular clocks in cell cultures (Yagita et al., 2001; Yamazaki et al., 2000). Upon treatment with clock synchronizers, several signal transduction pathways are activated, such as Mitogen-Activated Protein Kinase (MAPK) cascade and cAMP pathway, that lead to re-setting and synchronizing of the circadian oscillator (Balsalobre et., 2000). The peripheral and SCN clocks share the same molecular mechanisms to drive their circadian oscillation. However, there are differences in the manner in which these two clock systems get synchronized (Mohawk et al., 2012). For instance, while the prominent synchronizing signal for the SCN is the light signal, the peripheral clocks are sensitive to the feeding rhythm (Stokkan et al., 2001; Damiola et al., 2000). The hormones secreted upon feeding or fasting are the main phase entraining factors for the peripheral clocks. Circadian oscillation in the peripheral cells gives rhythmicity to mRNA expression of about 10% of the whole genome in each specific tissue (Panda et al., 2002; Miller et al., 2007).

Molecular mechanism of the mammalian circadian clock

The core molecular oscillator

The molecular mechanism of the circadian clock is based on auto-regulatoy transcriptional-translational feedback loops (TTFL) composed of positive (activating) and negative (inhibitory) elements (Reppert et al., 2002). The TTFL drives cyclic gene expression and protein expression of the clock genes with a period of approximately 24 hours (Lowery et al., 2004).

The activator (positive) elements of the circadian system are Brain Muscle Arnt-Like protein-1 (*Bmal1*) and Circadian Locomotor receptor Cycles Output Kaput (*Clock*) (Lowery et al., 2004). (Fig. 1). *Clock* mutant mice showed lengthened circadian period with gradual loss of circadian rhythmicity (Vitaterna et al., 1994). Mice lacking *Bmal1* were unable to generate endogenous circadian rhythms (Bunger et al., 2000), indicating a key role of BMAL1 and CLOCK proteins in circadian rhythm generation. CLOCK and BMAL1 belong to helix-loop-helix, Per Arntl Sim (bHLH-PAS) domain containing proteins (Bunger et al., 2000) and heterodimerize to form an active transcription factor that binds to the Enhancer-box (E-box) elements (5'-CACGTG-3') of their target genes (Takahashi et al., 2008). Period

(*Per 1,2*) and Cryptocrome (*Cry 1,2*) comprise the negative feedback loop of the circadian machinery (Takahashi et al., 2008). Homozygous *Per1* mutant mice show a shorter circadian period (Zheng et al., 2001; Cermakian et al., 2001). *Per2* mutant mice also exhibit a shorter circadian period, but gradually lose the circadian rhythmicity in constant darkness (Zheng et al.,1999). On the other hand, *Cry1* and *Cry2* deficient mice display a shortened and lengthened circadian period, respectively (Van der Horst et al., 1999). In the absence of both cryptochromes (*Cry1*$^{-/-}$, *Cry2*$^{-/-}$) a complete and immediate loss of rhythmicity is reported (van der Horst et al., 1999). These studies show that PER and CRY proteins are core circadian elements. Transcription of *Per* and *Cry* genes is induced by the CLOCK/BMAL1 complex. CRY/PER proteins are synthesized, accumulate in the cytoplasm, and after heterodimeriztion shuttle between the cytoplasm and the nucleus (Yagita et al., 2002). Once nuclear levels of PER/CRY complexes are sufficiently high, they inhibit transcription of E-box genes (including their own genes) by blocking CLOCK/BMAL1-mediated transcription (Shearman et al., 2000; Sato et al., 2006) (Fig. 1).

Posttranslational modifications, such as phosphorylation, acetylation, and ubiquitination, are equally important for stabilization or degradation and cellular translocation of the clock proteins. Phosphorylation of PER and CRY proteins regulates the circadian period (tau) in mammals (Lee et al.,2001). PER/CRY complexes are phosphorylated mainly by casein kinase 1 delta (CK1 δ) and epsilon (CK1 ε), and are degraded by 26S proteasome complexes, which allows reactivation of CLOCK/BMAL1-driven transcription (Takahashi et al., 2008). It has been shown that CRY proteins are crucial for the stabilization of phosphorylated PER2, but are not required for stabilization of phosphorylated PER1, suggesting fine tuning in the interaction between clock proteins. PER1 phosphorylation appears instead to be mainly important for nuclear translocation rather than stabilization of the protein (Lee et al.,2001). In addition, BMAL1 undergoes extensive post translational modifications, such as phosphorylation (Tamaru et al., 2009), acetylation (Hirayama et al., 2007), and ubiquitination (Kwon et al.,2006). These post translational modifications define activity and stability of the BMAL1 protein which is crucial for circadian function. For instance, it has been shown that the CLOCK protein possesses histone acetyl transferase activity (HAT) and acetylates its own partner, BMAL1 protein (Doi et al., 2006; Hirayama et al., 2007). Acetylation of BMAL1 in turn facilitates recruitment of CRY1 protein to nucleus facilitating transcription repression of CLOCK/BMAL1 heterodimer. Therefore, posttranslational modifications of the core clock proteins define the period of the circadian system and contribute to the stability and activity of these proteins.

There are additional feedback loops that reinforce the strength of the CLOCK/BMAL1 and PER/CRY loop (Lowery et al., 2004). CLOCK/BMAL1 heterodimers also drive the transcription of two nuclear receptors: *Rev-Erbα,* and RORα. REV-ERBα inhibits gene expression of *Bmal1,* and to a lesser extent of *Clock*, by binding to ROR responsive elements (ROREs) that are located in the promoters of these genes (Preitner et al. 2002; Lowrey et al., 2004). While REV-ERBα inhibits transcription of *Bmal1*, RORα activates it.

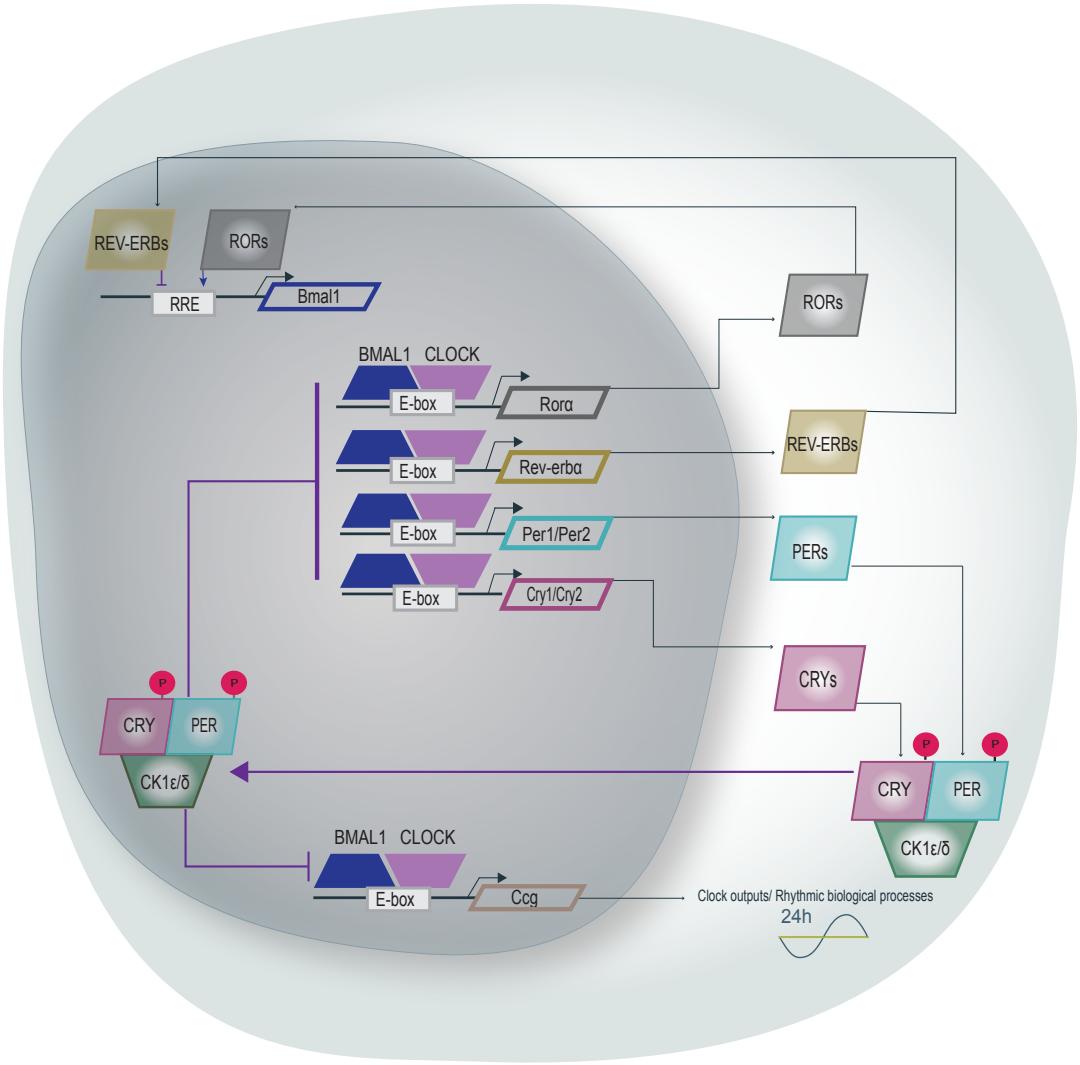

Figure 1. Transcriptional-translational network of the mammalian circadian oscillator. Diagram showing the molecular mechanism of the mammalian circadian system composed of a primary negative feedback loop, and a secondary auto-regulatory feedback loop. The primary negative feedback loop of the circadian oscillator involves *Clock*, *Bmal1*, *Per1*, *Per2*, *Cry1*, *Cry2* genes. CLOCK/BMAL1 heterodimer activates E-box transcription of *Per* and *Cry* genes. Subsequently, PER and CRY proteins heterodimerize and translocate to the nucleus to inhibit CLOCK/BMAL1-driven transcription. The secondary auto-regulatory feedback loop composed of *Rev-erbα* and *Rorα* elements that are the direct target of CLOCK/BMAL1 transcription factor. REV-ERBα competes with RORα to the bind retinoic acid-related orphan receptor response elements (RRE) located in the promoter of the *Bmal1* gene. REV-ERBα feedback to repress *Bmal1* transcription and RORα inhibit expression of *Bmal1*. PER and CRY proteins are mainly phosphorylated by Casein Kinase 1 Delta (CK1 δ) and Casein Kinase 1 Epsilon, (CK1 ε) an important regulatory mechanism to define the circadian periodicity.

This results in a high amplitude oscillation of *Bmal1* mRNA during a circadian cycle. A number of other clock components can be noted such as *Timeless (Tim)*, *Dec1*, *Dec2* and *E4BP4* but their roles have not been clearly specified. (Lowrey et al., 2004; Takahashi et al 2008).

Clock-controlled outputs

Circadian transcription of the core clock genes gives rhythmicity to the expression of numerous genes that are involved in various biological processes. These so-called Clock Controlled Genes (CCG) comprise over 10% of a tissue's transcriptome (Panda et al., 2002; Miller et al., 2007). Importantly, CCGs that are under circadian transcription differ in each specific tissue, which means that the cellular physiology and metabolism is tissue specific (Mohawk et al., 2012). These oscillating genes bring rhythmicity to many of the physiological processes, including hormone secretion, drug and xenobiotic metabolism, glucose homeostasis and cell proliferation (Takahashi et al., 2008). Considering the importance of the circadian clock and the wide range of physiological events that are regulated in a circadian manner, it is no surprise that environmental disturbance (such as jet lag) or genetic disruption of circadian rhythmicity predispose to a range of diseases including metabolic syndrome, cardiovascular disease and cancer (Arble et al., 2010; Fu et al., 2013).

Cell cycle control

The cell cycle represents another oscillatory system that co-exists with the circadian clock in dividing cells. The circadian clock and the cell cycle share many common features to drive their oscillatory events. Sequential rounds of transcription, translation, post translational modification, and degradation govern their cyclic events. The cell cycle follows a sequence of events in which cells copy their genome during S phase, and divide the genome into two daughter cells during mitosis (M phase). The S phase and Mitosis are separated by two gap phases (G1 and G2). During the G1 and G2 phases cells are prepared for the next step by cell growth, protein synthesis, and DNA repair (Norbury et al., 1992). The molecular events controlling the cell cycle are ordered and unidirectional. Cell cycle check points ensure the successful completion of each step, and allow transition to the next step (Noijma et al., 1997).

Progression through the cell cycle relies on the rhythmic activity of cyclin-CDK kinase complexes. Within these complexes, cyclins form the regulatory subunits and CDKs the catalytic subunits. (Tyson & Novak, 2008). Specific combination of cyclin-CDK complexes triggers various cell cycle events, such as DNA replication and mitosis, at a particular time during the cell cycle. Cyclin D is synthesized in response to growth stimuli in early G1 phase. It associates with the CDK4 and CDK6 kinases (Guillemot et al., 2001). The active cyclin D and CDK4 complex phosphorylates tumor suppressor RB protein in G1. The RB molecule is required to inhibit transcription of the genes required for G1 to S transition (Giacinti et al., 2006; Henley et al.,2012). Hyperphosphorylated Rb dissociates from the Rb/E2F complex resulting in activation of E2F complex. The E2F complex is a positive regulator of the cell cycle (Magnaghi-Jaulin et al., 1998). Activation of E2F as a transcriptional factor induces transcription of the genes regulating G1/S transition, such as cyclin E (Geng et al., 1996). In mid-G1, cyclin E is transcribed, along with CDK2, facilitating G1/S transition (Koff et al., 1992). Cyclin A2 transcription rises at the beginning of S phase and, in complex with its catalytic subunit CDK2, is essential for DNA replication and S phase progression (Erlandsson

et al., 2000; Coverley et al., 2002; Kalaszczynska et al., 2009). Cyclin B1 levels rise from the late S phase till late G2 phase allowing the protein to form complexes with CDK1 (Pines et al.,1989) (Fig. 2).

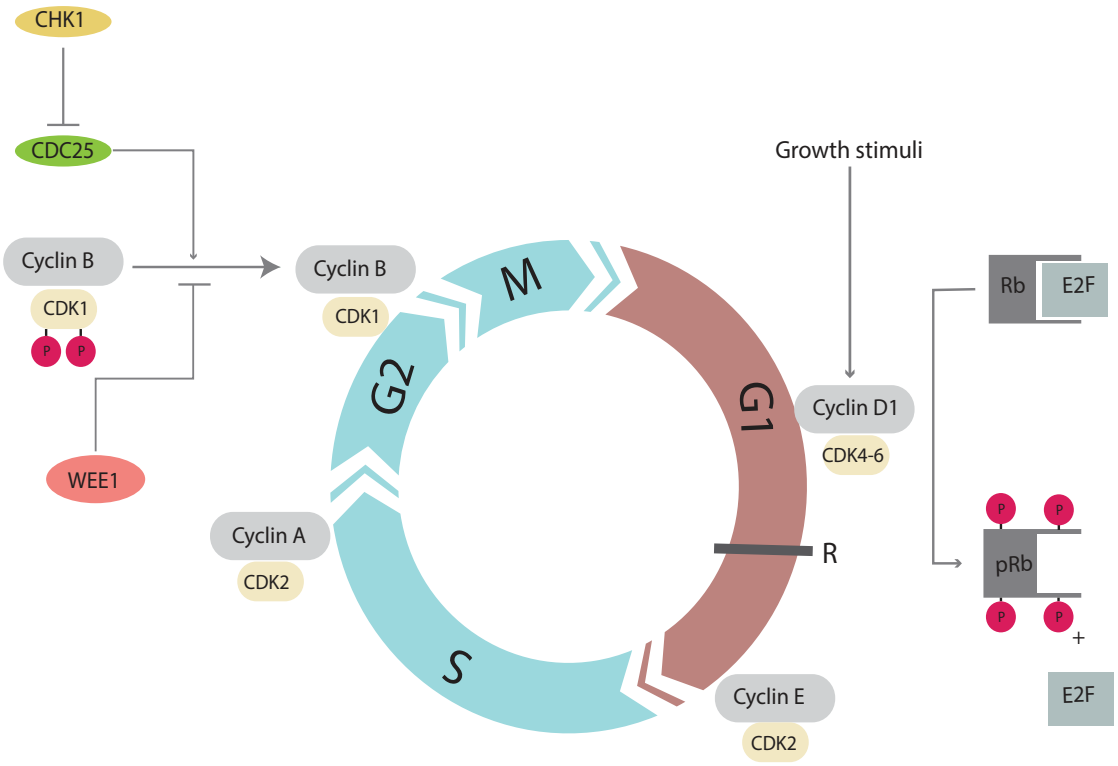

Figure 2. Schematic representation of the cell division cycle. Cyclin-CDK complexes regulating progression of the cells through different cell cycle phases. Phosphorylation of RB molecule by Cyclin D/CDK4-6 complexes in early or mid G1 phase results in dissociation of RB and E2F. E2F molecule triggers transition of the cells from G1 to S. Mitosis is initiated by Cyclin B1-CDK1 complex. Inhibitory phosphorylation of CDK1 by Wee1 kinase avoids premature mitosis. Cyclin B1-CDK1 complex is activated by CDC25 phosphatase. DNA damage check point molecules act mainly on CDC25 to prevent the activation of Cyclin B1-CDK1 complex.

CyclinB1-CDK1 initially should be kept in an inactive state to avoid premature mitosis. WEE1 and MYT1 kinases are responsible for the inhibitory phosphorylation of the CDK1 subunit, consequently CyclinB1-CDK1 complex is kept in a low or inactive state as a result of this phosphorylation (Mueller et al., 1995; Parker et al.,1992). A high level of Cyclin B1, and high level of Cyclin B1-CDK1 complex, generate sufficient activity for this protein complex to set off the double feedback loop in which Cyclin B1-CDK1 can inhibit its inhibitor (*Wee1*) and activate its activator (*Cdc25*), resulting in a rapid activation of Cyclin B1-Cdk1 and mitotic entry (Boutros et al., 2006; Lindqvist et al., 2009) (Fig. 2)

Cyclic expression of the cyclins is highly timed and scheduled, and their disappearance is regulated through induced proteolysis by the 26S proteasome. Timed degradation of the Cy-

clins is equally important for cell cycle progression as their timed expression. For instance, Cyclin B1 destruction is essential for mitotic exit (Pines et al., 2006;). Activity of Cyclin B1-CDK1 complex stops the segregation of chromosomes and stalls the cells at the end of anaphase (Holloway et al., 1993; Pines et al.,2006). Moreover, destruction of Cyclin A2 starts right after nuclear envelope break down, being almost completely degraded before metaphase (Den-Elzen et al., 2001; Geley et al., 2001). Overexpression of Cyclin A2 in late G2 phase cells delays chromosome alignment, subsequently delaying mitosis (Den Elzen et al., 2001).

Transition of the cells from one phase to another is tightly regulated by cell cycle checkpoints. Restriction point R in the late G1 phase is an important check point in the mammalian cell cycle. Before this restriction point, the cell cycle depends on external stimuli (growth factors) to proceed through G1. After the restriction point, the cell becomes independent of external mitogenic stimuli and can complete the cell division cycle autonomously (Pardee et al., 1974; Johnson et al., 2013). One other important cell cycle checkpoint is the G2/M checkpoint. This checkpoint ensures genome stability before cells enter M phase, avoiding that a defective genome passes to the next generation of the cells. When cells are exposed to genotoxic agents, or in case of defective replication in S phase, DNA damage response pathways are activated (Kastan et al., 2004). As it is mentioned before, the main driver of mitotic entry is the activity of Cyclin B1-Cdk1. Therefore, DNA damage response pathways modulate regulators of Cyclin B1-CDK1 complex to pause the cells in G2 (Stark et al., 2004). The DNA damage response is mainly triggered by two signaling cascades: Ataxia-Telangiectasia Mutated and Check Point Kinase 2 (ATM/CHK2), and ATM-Rad3-related and CheckPoint Kinase 1 (ATR/CHK1) (Sancar et al., 2010). The G2/M check point is regulated by CHK1-dependent phosphorylation of CDC25 phosphatase which is an important activator of CyclinB-CDK2 complex (Figure 2). Phosphorylation of CDC25 prevents activation of Cyclin B-CDK2 complex and stalls the cells in G2 phase (Boutros., 2007).

The interaction between the circadian oscillator and the cell cycle machinery

Initial studies suggest a cross-talk between the circadian clock and the cell cycle. For instance, it has been shown that a light-induced phase shift in mouse behavior leads to a corresponding shift in the proliferation timing of cells in the intestine (Scheving et al., 1983). On the other hand, DNA damage phase advanced circadian rhythms in a dose and time dependent manner (Oklejewicz et al., 2008). These studies indicate mutual influences of these two systems on each other. Research on human oral mucosa and skin has provided a first clue to on association between clock gene expression and cell cycle phase (Bjarnason et al., 1999 and 2001). This was achieved through the analysis of rhythmic expression of clock genes and cell cycle proteins in human oral mucosa and skin biopsies over 24 hours. Expression of *Per1* mRNA was shown to peak in the morning, and to coincide with the peak of p53 expression as a G1 marker. In contrast, *Bmal1* transcripts reached their highest level at night, showing synchrony with the peak expression of CyclinB1, a marker of G2 and M phase. Rhythmicity

in DNA synthesis and mitosis has also been demonstrated in hematopoietic, immune system, gastro-intestinal tract, liver, and skin cells of rodents (Lévi et al., 2007).

In a study by Matsuo and colleagues it has been shown that, in critical situations such as partial hepatectomy, the circadian rhythm affects the timing of cell division in vivo (Matsuo et al., 2003). This was shown by a partial hepatectomy in wild type mice, which caused the hepatocytes to enter M phase at a specific time of the day. This M phase gating was not seen in *Cry* deficient mice that displayed loss of circadian rhythmicity. (Matsuo et al., 2003). Circadian gating of cell division has been also proposed in other studies. For instance, it has been reported that approximately 16% of human epidermal cells undergo mitosis mainly at night (Scheving et al.,1959).

The dynamics of the circadian clock and cell cycle machineries and the interaction between these oscillators has also been addressed at the level of the individual cell by the use of a fluorescent circadian reporter (Rev-Erbα-VNP) which is under the direct control of CLOCK/BMAL1 complex. Using the Rev-Erbα reporter in a mouse fibroblast cell line (NIH3T3), the dynamic interaction between the circadian clock and cell cycle has been determined (Nagoshi et al., 2004; Bieler et al., 2014; Feillet et al., 2014). In the study by Nagoshi and coworkers, it was shown that there are three specific and non-random circadian time windows in which cell division occurs in the NIH3T3 cells. However, at the same time, the period and phase of the circadian clock were influenced and altered after each cell division event (Nagoshi et al., 2004). Later, using the same circadian clock reporter (Rev-Erbα-VNP) (Bieler et al., 2014) in combination with two cell cycle markers (FUCCI reporter system: hCDT1-mKOrange for G1, and hGeminin-CFP for S/G2/M) (Feillet et al., 2014), a tight synchrony between the circadian clock and the cell cycle has been reported at the single cell level. It has been shown that the circadian clock and the cell cycle are tightly phase coupled, and are oscillating with the same frequencies (1:1 ratio). A remarkable shortening of the circadian period was observed in dividing cells compared to non-dividing cells, indicating the influence of the cell cycle on the circadian clock (Bieler et al.,2014; Feillet et al., 2014). Bieler and colleagues reported a uni-directional link between the circadian clock and the cell cycle, suggesting that in the absence of external cues (clock synchronizers), the effect of the cell cycle on circadian period is dominant (Bieler et al., 2014). In contrast, in the study by Feillet and coworkers, a bi-directional link between these two oscillatory systems has been uncovered (Feillet et al.,2015). They have shown that synchronization of the circadian clock by physiological cues, such as dexamethasone, clustered cell division. This indicates that when the circadian oscillator is exposed to synchronizing cues, the effect of the circadian system on the cell cycle is dominant. In contrast, in the absence of clock sysnchronizers, the influence of the cell cycle on the circadian clock is dominant.

Our knowledge regarding the molecular mechanisms underlying the interaction between these two oscillatory systems is gradually increasing. Circadian clock genes regulate important cell cycle check points by either transcriptional control of critical regulatory genes, or by direct protein-protein interactions. For instance, oncogene *c-Myc* (G0/G1 transition) is negatively regulated by the BMAL1/CLOCK transcription factor (Fu et al., 2002). G1 and G1/S

checkpoints are under circadian control through cyclic transcription of the tumor suppressor genes *p21WAF1/CIP1* and *p16-Ink4A* (Gréchez-Cassiau et al., 2008; Kowalska et al., 2013). *p21* is negatively regulated by BMAL1, as suggested by a high level of P21 protein reported in *Bmal1*$^{-/-}$ hepatocytes (Grechez-Cassaiu et al., 2008). The multifunctional nuclear protein NONO binds to the *p16* promoter and drives its circadian transcription in a PER dependent manner (Kowalska et al., 2013). In the absence of PER or NONO, the circadian expression of *p16* is abolished. Likewise, expression of the *Wee1* gene (an important G2/M checkpoint kinase) is under circadian control (Matsuo et al., 2003). Oppositely, there is also evidence regarding the molecular influence of the cell cycle on the circadian clock. The cell cycle gene *p53* negatively regulates *Per2* expression, therefore affecting circadian period (Miki et al., 2013).

As a consequence of these complex interconnectivities between the circadian clock and the cell cycle, it is not surprising that loss of circadian control can be considered as a key factor for abnormal cell growth. It has been reported that *Per1/Per2* or *Cry1/Cry2* deficient mice show increased bone mass formation because of an accelerated G1/S transition in osteoblast cells (Fu et al., 2005). This result was attributed to high expression levels of G1 cyclins such as cyclin D1 in PER deficient mice (Fu et al., 2005). In another study, by Destici and co-workers, an accelerated cell cycle progression and high proliferation rate has been reported in primary Cry1$^{-/-}$, Cry2$^{-/-}$ mouse fibroblasts (Destici et al., 2011). Primary hepatocytes from *Bmal1* knockout mice showed a decreased proliferation rate, which was related to the altered expression of tumor suppressor gene P21 (Grechez-Cassaiu et al.,2008). Taken together, all the above data suggest a unique effect of clock genes on the cell cycle progression that impact different cell cycle phases in a specific manner.

The circadian clock, cell cycle, and cancer

Genetic disruption and environmental disturbance of the circadian system have been associated with a range of physiological disorders (Lee et al., 2010). For instance, altered insulin and glucose levels in the *Clock* deficient mice lead to a range of metabolic disorders such as obesity, hyperlipidemia, and hypoinsulinemia (Turek et al., 2005).

Epidemiological studies have shown that human night shift work is linked to increased risk of breast, colon, lung, prostate, and non-Hodgkin's cancer (Stevens et al., 2009; schernhammer et al., 2003; Kloog et al., 2009; Lahti et al., 2008). Night shift work is considered as a carcinogenic factor, as the risk of cancer development is increased by the number of the years an individual spends working at night (Schernhammer et al., 2003; Lee et al., 2010). Several studies have shown that loss of circadian homeostasis in mice leads to accelerated mammary tumor growth. For instance, breast cancer prone *p53* mutant mice show accelerated tumor development under a jetlag protocol (Van Dycke et al., 2015). In addition, ablation of the SCN in mice increases the growth rate of implanted tumors (Filipski et al., 2002; Filipski et al., 2009).

Many of the genes that are mutated in human cancers are directly involved in the regulation

of cell division. Likewise, altered expression of circadian clock genes that are involved in the regulation of different cell cycle check points has been reported by various studies (Fu et al., 2002; Kondratov et al., 2006; Lee et al., 2010). For instance, mutations in the *Per1* and *Per2* genes were detected in breast and colon cancer patients (Sjoblom et al., 2006). It has been shown that PER1 participates in the ATM-CHK2 DNA damage signaling pathway, which is activated upon DNA double strand breaks caused by ionizing radiation (Sancar et al., 2010). PER1 interacts with both ATM and CHK2 proteins for an efficient activation of the signaling cascade, which results in cell cycle arrest or activation of repairing pathways (Sancar et al., 2010). Exposure of cancer cell lines over-expressing *Per1* to ionizing radiation (IR) revealed an increased apoptosis sensitivity. In contrast, suppression of *Per1 expression* by siRNA in IR exposed cancer cell lines results in a reduction of the apoptotic rate (Grey et al.,2006). Furthermore, *Per2* mutant mice showed increased tumor development upon exposure to ionizing radiation (Fu et al.,2002; Lee et al.,2006). Altered expression of cell cycle related genes such as *p53* and *c-Myc* is proposed as an underlying mechanism. In addition, down regulation of the *Per2* gene in breast cancer cells accelerates the proliferation rate by increasing Cyclin D and Cyclin E levels in vitro (Yang et al., 2009). All above data suggest that *Per1* and *Per2* are tumor-suppressor genes. Therefore, mutations in circadian clock components can predispose the mice to cancer by increasing the cell growth and cell proliferation rate through general cell cycle dis-regulation.

ATR/CHK1 is another DNA damage signaling cascade that is activated in response to UV DNA damage (Sancar et al., 2010). It has been shown that CRYs are also involved in this DNA damage signaling cascade via the Timeless (TIM) circadian clock protein (Unsal-Kacmaz et al., 2005). TIM simultaneously binds to cryptochromes and ATR/CHK1 proteins, activating ATR/CHK1 DNA damage pathway (Unsal-Kacmaz et al., 2005; Kang et al., 2014). Downregulation of *Tim* disrupts both the circadian oscillation and ATR/CHK1 signaling pathway (Sancar et al., 2010).

Scope of the thesis

The circadian system regulates proper synchronization of several processes within an organism, as well as between an organism and its environment. Importantly, genetic variation in clock genes and environmental circadian disturbance have been linked to metabolic disease, sleep disorders, depression and endocrine imbalance, and abnormal cell growth (Lee et al., 2010). Abnormal cell growth is characterized by impaired cell cycle progression. The circadian clock and the cell cycle have been considered as two independent oscillators for a long time. Increasing evidence has challenged this speculation by showing that there is a strong bi-directional link between these two oscillatory systems (Feillet et al., 2014 and 2015). Importantly, recent molecular studies provided reliable evidence showing the involvement of the clock genes in the regulation of important cell cycle check points, and vice versa. Although our knowledge is steadily increasing, still many questions remain to be answered:

(1) In the context of the bi-directional link between these two oscillatory systems, how do alterations in one of the cycles affect the other?

(2) What are the candidate molecules playing a key role in the coupling between these two systems, and how can use we these newly identified molecules for therapeutic purposes?

(3) Since a hallmark of cancer is cell cycle dysregulation, and almost all cancer cell lines show abnormal cell proliferation and abnormal circadian gene expression, what is the status of the coupling between the circadian clock and the cell cycle in cancer cells?

Here, we investigated the role of positive and negative circadian elements on cell cycle progression of a mouse fibroblast cell line simultaneously expressing a circadian clock (Rev-Erbα) and cell cycle markers (Fucci reporter system: pFucci-G1 and pFucci-S/G2/M) (Feillet et al., 2014). We determined the kinetics of the cell cycle phases in the absence of individual core circadian clock gene at the single cell level. Furthermore, we elucidated the underlying molecular mechanisms. Moreover, we studied the coupling between the circadian clock and cell cycle systems in cancer cells at the single cell level, using a *p53* mutant mouse breast carcinoma cell line. Finally, we took a combined gene knockdown and transcriptomics approach to analyze the impact of clock gene inactivation on the cancer properties of H1299 human non-small lung carcinoma cells.

References

Arble DM, Ramsey KM, Bass J, Turek FW (2010) Circadian disruption and metabolic disease: findings from animal models. Best Pract Res Clin Endocrinol Metab 24:785-800.

Aton SJ, Herzog ED (2005) Come together, right...now: synchronization of rhythms in a mammalian circadian clock. *Neuron* 48:531-4.

Balsalobre A, Marcacci L, Schibler U (2000) Multiple signaling pathways elicit circadian gene expression in cultured Rat-1 fibroblasts. *Curr Biol* 10:1291-4.

Berson DM, Dunn FA, Takao M (2002) phototransduction by retinal ganglion cells that set the circadian clock. *Science* 295:1070-3.

Bieler J, Cannavo R, Gustafson K, Gobet C, Gatfield D, Naef F (2014) Robust synchronization of coupled circadian and cell cycle oscillators in single mammalian cells. *Mol Syst Biol* 10:739.

Bjarnason GA Jordan RCK, Wood PA, Li Q, Lincoln DW, Sothern RB, Hrushesky WJM, Ben-David Y (2001) Circadian expression of clock genes in human oral mucosa and skin. *Am J Pathol* 158:1793-801.

Bjarnason GA, Jordan RCK, Sothern RB (1999) Circadian variation in the expression of cell cycle proteins in human oral epithelium. *Am J Pathol* 154:613-22.

Boutros R, Lobjois V, Ducommun B (2007) CDC25 phosphatases in cancer cells: key players? Good targets? *Nat Rev Cancer* 7:495-507.

Bunger MK, Wilsbacher LD, Moran SM, Clendenin C, Radcliffe LA, Hogenesch JB, Simon MC, Takahashi JS, Bradfield CA (2000) Mop3 is an essential component of the master circadian pacemaker in mammals. *Cell* 103:1009-17.

Cermakian N, Monaco L, Pando MP, Dierich A, Sassone-Corsi P (2001) Altered behavioral rhythms and clock gene expression in mice with a targeted mutation in the *Period1* gene. *EMBO J* 20:3967-74.

Coverley D, Laman H, Laskey RA (2002) Distinct roles for cyclins E and A during DNA replication complex assembly and activation. *Nat Cell Biol* 4:523-8.

Damiola F, Le Minh N, Preitner N, Kornmann B, Fleury-Olela F, Schibler U (2000) Restricted feeding uncouples circadian oscillators in peripheral tissues from the central pacemaker in the suprachiasmatic nucleus. *Genes Dev* 14:2950-61.

Den Elzen N, Pines j (2001) Cyclin A is destroyed in prometaphase and can delay chromosome alignment and anaphase. *J Cell Biol* 153:121-36.

Destici E, Oklejewicz M, Saito S, van der Horst GT (2011) Mammalian cryptochromes impinge on cell cycle progression in a circadian clock-independent manner. *Cell Cycle* 10:3788-97.

Doi M, Hirayama J, Sassone-Corsi P (2006) Circadian regulator CLOCK is a histone acetyltransferase. *Cell* 125:497-508.

Erlandsson F, Linnman C, Ekholm S, Bengtsson E, Zetterberg A (2000) A detailed analysis of Cyclin A accumulation at the G1/S border in normal and transformed cells. *Exp Cell Res* 295:86-95.

Feillet C, Krusche P, Tamanini F, Janssens RC, Downey MJ, Martin P, Teboul M, Saito S, Lévi FA, Bretschneider T, van der Horst GTJ, Delaunay F, Rand DA (2014) Phase locking and multiple oscillating attractors for the coupled mammalian clock and cell cycle. *Proc Natl Acad Sci USA* 111:9828-33.

Feillet C, van der Horst GT, Levi F, Rand DA, Delaunay F (2015) Coupling between the Circadian Clock and Cell Cycle Oscillators: Implication for Healthy Cells and Malignant Growth. *Front Neurol* 6:96.

Filipski E, Delaunay F, King VM, Wu MW, Claustrat B, Grechez-Cassiau A, Guettier C, Hastings MH, Levi F (2004) Effects of chronic jet lag on tumor progression in mice. *Cancer Res* 64:7879-85.

Filipski E, King VM, Li X, Granda TG, Mormont MC, Liu X, Claustrat B, Hastings MH, F (2002) Host circadian clock as a control point in tumor progression. *J Natl Cancer Inst* 94:690-7.

Filipski E, Levi F (2009) Circadian disruption in experimental cancer processes. *Integr Cancer Ther* 4:298-302.

Fu L, Kettner NM (2013) The circadian clock in cancer development and therapy. *Prog Mol Biol Transl Sci* 119:221-82.

Fu L, Patel MS, Bradley A, Wagner EF, Karsenty G (2005) The molecular clock mediates leptin- regulated bone formation. *Cell* 122:803-15.

Fu L, Pelicano H, Liu J, Huang P, Lee C (2002) The circadian gene period2 plays an important role in tumor suppression and DNA damage response in vivo. *Cell* 111:41-50.

functions in the mammalian cell division cycle. *Cell Div* 7:10.

Gauger MA, Sancar A (2005) Cryptochrome, Circadian Cycle, Cell Cycle Checkpoints, and Cancer. *Cancer Res* 65:6828-34.

Geley S, Kramer E, Gieffers C, Gannon J, Peters JM, Hunt T (2001) Anaphase-Promoting Complex/Cyclosome–Dependent Proteolysis of Human Cyclin a Starts at the Beginning of Mitosis and Is Not Subject to the Spindle Assembly Checkpoint. *J Cell Biol* 153:137-48.

Geng Y, Eaton EN, Picon M, Roberts JM, Lundberg AS, Gifford A, Sardet C, Weinberg RA (1996) Regulation of cyclin E transcription by E2Fs and retinoblastoma protein. *Oncogene* 12:1173-80.

Gery S, Komatsu N, Baldjyan L, Yu A, Koo D, Koeffler HP (2006) The circadian gene per1 plays an important role in cell growth and DNA damage control in human cancer cells. *Mol Cell* 22:375-82.

Giacinti C, Giordano A (2006) RB and cell cycle progression. *Oncogene* 25:5220-7.

Gréchez-Cassiau A, Rayet B, Guillaumond F, Teboul M, Delaunay F (2008) The circadian clock component BMAL1 is a critical regulator of p21WAF1/CIP1 expressionand hepatocyte proliferation. *J Biol Chem* 283:4535-42.

Guillemot L, Levy A, Raymondjean M, Rothhut B (2001) Angiotensin II-induced transcriptional activation of the Cyclin D1 gene is mediated by Egr-1 in CHO-AT_{1A} Cells. *J Biol Chem* 276:39394-403.

Hattar S, Lucas RJ, Mrosovsky N, Thompson S, Douglas RH, Hankins MW, Lem J, Biel M, Hofmann F, Foster RG, Yau KW (2003) Melanopsin and rod-cone photoreceptive systems account for all major accessory visual functions in mice. *Nature* 424:76-81.

Henley SA, Dick FA (2012) The retinoblastoma family of proteins and their regulatory functions in the mammalian cell division cycle. *Cell Div* 7:10.

Hirayama J, Sahar S, Grimaldi B, Tamaru T, Takamatsu K, Nakahata Y, Sassone-Corsi P (2007) CLOCK-mediated acetylation of BMAL1 controls circadian function. *Nature* 450:1086-90.

Holloway SL, Glotzer M, King RW, Murray AW (1993) Anaphase is initiated by proteolysis rather than by the inactivation of maturation-promoting factor. *Cell* 73:1393–402.

Iwasaki H, Kondo T (2000) The current state and problems of circadian clock studies in cyanobacteria. *Plant Cell Physiol* 41:1013-20.

Johnson A, Skotheim JM (2013) Start and the Restriction Point. *Curr Opin Cell Biol* 25:717-23.

Kalaszczynska I, Geng Y, Iino T, Mizuno S, Choi Y, Kondratiuk I, Silver DP, Wolgemuth DJ, Akashi K, Sicinski P (2009) Cyclin A is redundant in fibroblasts but essential in hematopoietic and embryonic stem cells. *Cell* 138:352-65.

Khapre RV, Samsa WE, Kondratov RV (2010) Circadian regulation of cell cycle: Molecular connections between aging and the circadian clock. *Ann Med* 42:404-15.

Kang TH, Leem SH (2014) Modulation of ATR-mediated DNA damage checkpoint response by cryptochrome 1. *Nucleic Acids Res* 42:4427-34.

Kastan MB, Bartek J (2004) Cell-cycle checkpoints and cancer. *Nature* 432:316-23.

King DP, Takahashi JS (2000) Molecular genetics of circadian rhythms in mammals. *Annu Rev Neurosci* 23:713-42.

Kloog I, Haim A, Stevens RG, Portnove BA (2009) Global co-distribution of light at night (LAN) and cancers of prostate, colon, and lung in men. *Chronobiol Int* 26:108-25.

Ko CH, Takahashi JS (2006) Molecular components of the mammalian circadian clock. *Hum Mol Genet* 2:271-7.

Koff A, Giordano A, Desai D, Yamashita K, Harper JW, Elledge S, Nishimoto T, Morgan DO, Franza SR, Roberts JM (1992) Formation and activation of a cyclin E-CDK2 complex during the G1 phase of the human cell cycle. *Science* 257:1689-94.

Kondratov RV, Kondratova AA, Gorbacheva VY, Vykhovanets OV, Antoch MP (2006) Early aging and age-related pathologies in mice deficient in BMAL1, the core component of the circadian clock. *Genes Dev* 20:1868-73.

Kowalska E, Ripperger JA, Hoegger DC, Bruegger P, Buch T, Birchler T, Mueller A, Albrecht U, Contaldo C, Brown SA (2013) NONO couples the circadian clock to the cell cycle. *Proc Natl Acad Sci USA* 110:1592-9.

Kuhlman SJ, Machey SR, Duffy JF (2007) Biological Rhythms Workshop I: introduction to chronobiology. *Gold Spring Harb Symp Quant Biol* 72:1-6.

Kwon I, Lee J, Chang SH, Jung NC, Lee BJ, Son GH, Kim K, Lee KH (2006) BMAL1 shuttling controls transactivation and degradation of the CLOCK/BMAL1 heterodimer. *Mol Cell Biol* 26:7318-30.

Lahti TA, Partonen T, Kyyronen P, Kauppinen T, Pukkala E (2008) Night-time work predisposes to non-Hodgkin lymphoma. *Int J Cancer* 123:2148-51.

Lee C, Etchegaray JP, Cagampang FR, Loudon AS, Reppert SM (2001) Posttranslational mechanisms regulate the mammalian circadian clock. *Cell* 107:855-67.

Lee CC, (2006) Tuor suppression by the mammalian Period genes. *Cancer Causes Control* 17:525-30.

Lee JH, Sancar A (2011) Circadian clock disruption improves the efficacy of chemotherapy through p73-mediated apoptosis. *Proc Natl Acad Sci USA* 108:10668-72.

Lee S, Donehower LA, Herron AJ, Moore DD, Fu L (2010) Disrupting circadian homeostasis of sympathetic signaling promotes tumor development in mice. *PloS One* 5:e10995.

Lindqvist A, Rodriguez-Bravo R, Medema RH (2009) The decision to enter mitosis: feedback and redundancy in the mitotic entry network. *Cell Biol* 185:193-202.

Lowery PL, Takahashi JS (2004) Mammalian circadian biology: elucidating genome-wide levels of temporal organization. *Annu Rev Genomics Hum Genet* 5:407-401.

Magnaghi-Jaulin L, Groisman R, Naguibneva I, Robin P, Lorain S, Le Villain JP, Troalen F, Trouche D, Harel-Bellan A (1998) Retinoblastoma protein represses transcription by recruiting a histone deacetylase. *Nature* 391:601-5.

Matsuo T, Yamaguchi S, Mitsui S, Emi A, Shimoda F, Okamura H. Control Mechanism of the Circadian Clock for Timing of Cell Division in Vivo. *Science*, 2003, 302 (5643):255-9.

Meijer JH, Michel S, Vansteensel MJ (2007) processing of daily and seasonal light information in the mammalian circadian clock. *Gen Comp Endocrinol* 152:159-64.

Miki T, Matsumoto T, Zhao Z, Lee CC (2013) p53 regulates Period2 expression and the circadian clock. *Nat Commun* 4:2444.

Miller BH, McDearmon EL, Panda S, Hayes KR, Zhang J (2007) Circadian and CLOCK-controlled regulation of the mouse transcriptome and cell proliferation. *Proc Natl Acad Sci USA* 104:3342–7.

Mohawk JA, Green CB, Takahashi JS (2012) Central and peripheral circadian clocks in mammals. *Annu Rev Neurosci* 35:445-62.

Mori T, Johnson CH (2000) Circadian control of cell division in unicellular organisms. *Prog Cell Cycle Res* 4:185-92.

Mueller PR, Coleman TR, Kumagai A, Dunphy WG (1995) Myt1: a membrane-associated inhibitory kinase that phosphorylates Cdc2 on both threonine-14 and tyrosine-15. *Science* 270:86-90.

Nagoshi E, Saini C, Bauer C, Laroche T, Naef F, Schibler U (2004) Circadian gene expression in individual fibroblasts: cell-autonomous and self-sustained oscillators pass time to daughter cells. *Cell* 119:693-705.

Nojima H (1997) Cell cycle checkpoints, chromosome stability and the progression of cancer. *Hum Cell* 10:221-30.

Norbury C, Nurse P (1992) Animal cell cycles and their control. *Annu Rev Biochem* 61:441-70.

Oklejewicz M, Destici E, Tamanini F, Hut RA, Janssens R, van der Horst GT (2008) Phase resetting of the mammalian circadian clock by DNA damage. *Curr Biol* 18:286-91.

Panda S, Antoch MP, Miller BH, Su AI, Schook AB, Staume M, Schultz PG, Kay SA, Takahashi JS, Hogenesch JB (2002) Coordinated transcription of key pathways in the mouse by the circadian clock. *Cell* 109:307-20.

Pardee AB (1974) A restriction point for control of normal animal cell proliferation. *Proc Natl Acad Sci USA* 71:1286-90.

Parker LL, Piwnica-Worms H (1992) Inactivation of the p34cdc2-cyclin B complex by the human WEE1 tyrosine kinase. *Science* 257:1955-7.

Pines J (2006) Mitosis: a matter of getting rid of the right protein at the right time. *Trends Cell Biol* 16:55-63.

Pines J, Hunter T (1989) Isolation of a human cyclin cDNA: evidence for cyclin mRNA and protein regulation in the cell cycle and for interaction with p34cdc2. *Cell* 58:833-46.

Pittendrigh CS (1960) Circadian rhythms and the circadian organization of living systems. *Cold Spring Harb Symp Quant Biol* 25:159-84.

Pittendrigh CS (1988) The photoperiodic phenomena: seasonal modulation of the "day within". *J Biol Rhythms* 3:173-88.

Preitner N, Damiola F, Lopez-Molina L, Zakany J, Duboule D, Albrecht U, Schibler U (2002) The orphan nuclear receptor REV-ERBalpha controls circadian transcription within the positive limb of the mammalian circadian oscillator. *Cell* 110:251-60.

Preuss F, Tang Y, Laposky AD, Arble D, Keshavarzian A, Turek FW (2008) Adverse effects of chronic circadian desynchronization in animals in a "challenging" environment. *AM J Physiol Regul Integr Comp Physiol* 295: R2034-40.

Ralph MR, Foster RG, Davis FC, Menaker M (1990) Transplanted suprachiasmatic nucleus determines circadian period. *Science* 247:975-8.

Reppert SM, Weaver DR (2001) Molecular analysis of mammalian circadian rhythms. *Annu Rev Physi-o*l 63:647-76.

Sancar A, Lindsey-Boltz LA, Kang TH, Reardon JT, Lee JH, Ozturk N (2010) Circadian clock control of the cellular response to DNA damage. *FEBS Lett* 584:2618-25.

Schernhammer ES, Laden F, Speizer FE, Willett WC, Hunter DJ, Kawachi I, Fuchs CS, Colditz GA (2003) Night-shift work and risk of colorectal cancer in the nurses' health study. *J Natl Cancer Inst* 95:825-8.

Scheving LE, Tsai TH, Scheving LA (1983) Chronobiology of the intestinal tract of the mouse. *Am J Anat* 168:433-65.

Scheving LE (1959) Mitotic activity in the human epidermis. *Anat* Rec 135:7-19.

Burns ER, Scheving LE, Pauly JE, Tsai T (1976) Effect of altered lighting regimens, time-limited feeding, and presence of Ehrlich ascites carcinoma on the circadian rhythm in DNA synthesis

of mouse spleen. *Cancer Res* 36:1538-44.

Shearman LP, Sriram S, Weaver DR, Maywood ES, Chaves I, Zheng B, Kume K, Lee CC, van der Horst GT, Hastings MH, Reppert SM (2000) Interacting molecular loops in the mammalian circadian clock. *Science* 288:1013-9.

Sharma VK (2003) Adaptive significance of circadian clocks. *Chronobiol Int* 20:901-19.

Sjoblom T, Jones S, Wood LD, Parsons DW, Lin J, Barber TD, Mandelker D, Leary RJ, Ptak J, Silliman N, Szabo S, Buckhaults P, Farrell C, Meeh P, Markowitz SD, Willis J, Dawson D, Willson Jk, Gazdar AF, Hartigan J, Wu L, Liu C, Parmigiani G, Park BH, Bachman KE, Papadopoulos N, Vogelstein B, Kinzler KW, Velculescu VE (2006) The consensus coding sequences of human breast and colorectal cancers. *Science* 314:268-74.

Stark GR, Taylor WR (2004) Analyzing the G2/M checkpoint. *Methods Mol Biol* 280:51-82.

Stephan FK, Zucker I, (1972) Circadian rhythms in drinking behavior and locomotor activity of rats are eliminated by hypothalamic lesions. *Proc Natl Acad Sci USA* 69:1583-6.

Stevens RG (2009) Light-at-night, circadian disruption and breast cancer: assessment of existing evidence. *Int J Epidemiol* 38:963-70.

Stokkan KA, Yamazaki S, Tei H, Sakaki Y, Menaker M (2001) Entrainment of the circadian clock in the liver by feeding. *Science* 291:490-3.

Stratmann M, Schibler U (2006) Properties, entrainment, and physiological functions of mammalian peripheral oscillators. *J Biol Rhythms* 21:494-506.

Takahashi JS, Hong H.K, Ko C.H, McDearmon E.L (2008) The genetics of mammalian circadian order and disorder: implications for physiology and disease. *Nature* 9:764-75.

Tamaru T, Hirayama J, Isojima Y, Nagai K, Norioka S, Takamatsu K, Sassone-Corsi P (2009) CK2alpha phosphorylates BMAL1 to regulate the mammalian clock. *Nat Struct Mol Biol* 16:446-8.

Turek FW, Joshu C, Kohsaka A, Lin E, Ivanova G, McDearmon E, Laposky A, Losee-Olson S, Easton A, Jensen DR, Eckel RH, Takahashi JS, Bass J (2005) Obesity and metabolic syndrome in circadian Clock mutant mice. *Science* 308:1043-5.

Tyson JJ, Novak B (2008) Temporal Organization of the Cell Cycle. *Curr Biol* 18:759-68.

Unsal-Kacmaz K, Mullen TE, Kaufmann WK, Sancer A (2005) Coupling of human circadian and cell cycles by the timeless protein. *Mol Cell Biol* 25:3109-16.

Van der Horst GT, Muijtjens M, Kobayashi K, Takano R, Kanno S, Takao M, de Wit J, Verkerk A, Eke AP, van Leenen D, Buijs R, Bootsma D, Hoeijmakers JH, Yasui A (1999) Mammalian Cry1 and Cry2 are essential for maintenance of circadian rhythms. *Nature* 398:627-30.

Van Dycke KC, Rodenburg W, van Oostrom CT, van Kerkhof LW, Pennings JL, Roenneberg T, van Steeg H, van der Horst GT (2015) Chronically Alternating Light Cycles Increase Breast Cancer Risk in Mice. *Curr Biol* 25:1932-7.

Vitaterna MH, King DP, Chang AM, Kornhauser JM, Lowrey PL, MCDonald JD, Dove WF, Pinto LH, Turek FW, Takahashi JS (1994) Mutagenesis and mapping of a mouse gene, Clock, essential for

circadian behavior. *Science* 264:719-25.

Welsh DK, Yoo SH, Liu AC, Takahashi JS, Kay SA (2004) Bioluminescence imaging of individual fibroblasts reveals persistent, independently phased circadian rhythms of clock gene expression. *Curr Biol* 14:2289-95.

Welsh DK, Logothetis DE, Meister M, Reppert SM (1995) Individual neurons dissociated from rat suprachiasmatic nucleus express independently phased circadian firing rhythms. *Neuron* 14:697–706.

Welsh DK, Takahashi JS, Kay SA (2010) Suprachiasmatic nucleus: cell autonomy and network properties. *Annu Rev Physiol* 72:551-7.

Wever RA (1986) Characteristics of circadian rhythms in human functions. *J Neural Transm Suppl* 21:323-73.

Yamazaki S, Numano R, Abe M, Hida A, Takahashi R, Ueda M, Block GD, Sakaki Y, Menaker M, Tei H (2000) Resetting central and peripheral circadian oscillators in transgenic rats. *Science* 288:682-5.

Yagita K, Tamanini F, van Der Horst GT, Okamura H (2001) Molecular mechanisms of the biological clock in cultured fibroblasts. *Science* 292:278-81.

Yagita K, Tamanini F, Yasuda M, Hoeijmakers JH, van der Horst GT, Okamura H (2002) Nucleocytoplasmic shuttling and mCRY-dependent inhibition of ubiquitylation of the mPER2 clock protein. *EMBO J* 21:1301-14.

Yang X, Wood PA, Oh EY, Du-Quiton J, Ansell CM, Hrushesky WJ (2009) Down regulation of circadian clock gene Period 2 accelerates breast cancer growth by altering its daily growth rhythm. *Breast Cancer Res Treat* 117: 423-31.

Zheng B, Albrecht U, Kaasik K, Sage M, Lu W, Vaishnav S, Li Q, Sun ZS, Eichele G, Bradley A, Lee CC (2001) Nonredundant roles of the mPer1 and mPer2 genes in the mammalian circadian clock. *Cell* 105:683-94.

Zheng B, Larkin DW, Albrecht U, Sun ZS, Sage M, Eichele G, Lee CC, Bradley A (1999) The mPer2 gene encodes a functional component of the mammalian circadian clock. *Nature* 400:169-73.

CHAPTER 2

The positive circadian regulators CLOCK and BMAL1 heterodimer control G2/M cell cycle transition through Cyclin B1

Names: Elham Farshadi, Jie Yan, Pierre Leclere, Albert Goldbeter, Inês Chaves, Gijsbertus T.J. van der Horst

Key words: circadian clock, cell cycle, CLOCK/BMAL1, Cyclin B1, G2/M transition

Abstract

We previously identified a tight bidirectional phase coupling between the circadian clock and the cell cycle. To understand the role of the CLOCK/BMAL1 complex, representing the main positive regulator of the circadian oscillator, we knocked down Bmal1 or Clock in NIH3T33C mouse fibroblasts (carrying fluorescent reporters for clock and cell cycle phase) and analyzed timing of cell division in individual cells and cell populations. Inactivation of Bmal1 resulted in a loss of circadian rhythmicity and a lengthening of the cell cycle, originating from delayed G2/M transition. Subsequent molecular analysis revealed reduced levels of Cyclin B1, an important G2/M regulator, upon suppression of Bmal1 gene expression. In complete agreement with these experimental observations, simulation of Bmal1 knockdown in a computational model for coupled mammalian circadian clock and cell cycle oscillators (now incorporating Cyclin B1 induction by BMAL1) revealed a lengthening of the cell cycle. Similar data were obtained upon knockdown of Clock gene expression. In conclusion, the CLOCK/BMAL1 complex controls cell cycle progression at the level of G2/M transition through direct regulation of Cyclin B1 expression.

Introduction

The circadian clock and the cell cycle are two fundamental, highly dynamic, and evolutionary well conserved biological oscillators that employ cyclic gene expression and protein degradation to impose diurnal rhythmicity on behavior, physiology and metabolism, and to drive cell division, respectively.

The mammalian circadian clock consists of a light-entrainable central clock located in the hypothalamic suprachiasmatic nucleus (SCN) of the brain, and peripheral clocks situated in the individual cells of almost all other tissues (Takahashi et al., 2008). At the molecular level, the circadian clock is based on intertwined positive and negative transcriptional-translational feedback loops (Mohawk et al., 2012). In short, the positive elements of the circadian clock, encoded by the *Brain* and *Muscle Arnt-like protein-1 (Bmal1*) and the *Clock* genes, form a heterodimer that activates transcription of E-box promoter element containing genes, including the core clock genes *Period* (*Per1* and *Per2*), *Cryptochrome (Cry1 and Cry2),* and nuclear hormone receptor *Rev-Erbα*. Once formed, PER and CRY proteins heterodimerize and translocate to the nucleus where they inhibit CLOCK/BMAL1-mediated transcription of E-box genes, including their own (Mohawk et al., 2012). Post-translational modification events, including phosphorylation and ubiquitination, target the PER and CRY proteins for degradation by the 26S proteasome complex, which in turn allows reactivation of CLOCK/BMAL1-mediated transcription and initiation of a new circadian cycle (Gallego et al., 2007; Stojkovic et al., 2014). In addition, CLOCK/BMAL1-driven cyclic expression of the *Rev-Erbα* gene (encoding an inhibitor of ROR-driven *Bmal1* expression) causes *Bmal1* expression to oscillate, which confers robustness to the circadian core oscillator. BMAL1 and CLOCK are also responsible for the cyclic transcription of E-box-containing clock-controlled genes (CCG) that couple the circadian oscillator to a wide variety of physiological pathways.

Similar to the circadian clock, the cell cycle behaves as an oscillator in which cyclic expression of key cell cycle molecules (i.e. cyclins) regulates cell cycle progression in a sequential and unidirectional manner (Tyson & Novak, 2008; Gérard & Goldbeter, 2009). Cyclins are produced at specific stages of the cell cycle and associate with their respective constitutively expressed Cyclin-Dependent Kinase (CDK) partner. The kinase activity of the cyclin-CDK complexes triggers various events at specific times during the cell cycle. In short, mitogenic signals prompt the expression of Cyclin D, which binds to CDK4 and CDK6 and irreversibly drives the cell through G1 phase and prepares it for replication. The underlying signalling cascade includes activation of the *Ccne1* and *Ccna2* cyclin genes (Henley & Dick, 2012). Cyclin E protein levels peak at late G1, resulting in the formation of Cyclin E/CDK2 complexes that initiate G1/S transition and subsequent DNA replication (Koff et al., 1992; Jackson et al., 1995). Cyclin A2 starts to appear during S phase and, along with its catalytic subunit CDK2, is essential for DNA replication and S phase progression (Erlandsson et al., 2000; Coverley et al., 2002; Kalaszczynska et al., 2009). Ablation of Cyclin A2 in cultured cells blocks DNA synthesis and delays S phase progression (Girard et al., 1991; Pagano et al., 1992). Mitotic entry is triggered by Cyclin B1/CDK1 (Gavet & Pines, 2010). Transcription of the Cyclin B1

gene *CcnB1* starts in S phase with Cyclin B1 protein levels and Cyclin B1/CDK1 complex formation peaking at late G2 (Lindqvist et al., 2009, Fung et al., 2005). However, Cyclin B1/CDK1 complexes are initially kept in an inactive state by WEE1 and MYT1 kinase-mediated phosphorylation of specific CDK1 residues to avoid premature mitosis (Mueller et al., 1995; Parker & Piwnica-Worms, 1992; Fung et al., 2005). Once protein levels are sufficiently high, Cyclin B1 triggers the de-phosphorylation of CDK1, thereby activating its own (i.e. Cyclin B1/CDK1) complex and promotes entry into mitosis (Lindqvist et al., 2009). In conclusion, oscillations in the amount and activity of the various Cyclin/CDK complexes are crucial for cell cycle progression.

Multiple studies have provided evidence for a strong connection between the circadian clock and cell cycle in proliferating cells. Bjarnason and coworkers have shown circadian variation in the abundance of cell cycle proteins in human oral mucosa (Bjarnason et al., 1999). Moreover, expression of clock genes in human oral mucosa and skin was associated with specific cell cycle phases. Notably, peak expression of the Cyclin B1 gene *Cnnb1* coincides with that of the *Bmal1* clock gene, while *Per1* transcription coincides with the peak of *p53* mRNA levels in late G1 (Bjarnason et al., 2001). Studies addressing the molecular link between the circadian and cell cycle oscillator have shown that the circadian clock can affect the cell cycle at different levels. For instance, expression of the G2/M inhibitor WEE1 is under circadian control via CLOCK/BMAL1 responsive E-box elements in the *Wee1* gene promoter (Matsuo et al., 2003). Likewise, G1 to S transition has been reported to be under circadian control through CLOCK/BMAL1-mediated cyclic transcription of the cell cycle inhibitor gene *p21WAF1/CIP1* (Gréchez-Cassiau et al., 2008). Furthermore, the multifunctional nuclear protein NONO was found to bind to the promoter of the p16-Ink4A cell cycle checkpoint gene and drive circadian expression in a PER-dependent manner (Kowalska et al., 2013). Oppositely, the cell cycle regulator protein CDK1 has been suggested to control the circadian clock through phosphorylation of REV-ERBα, which targets the latter protein for FBXW7α-mediated degradation (Zhao et al., 2016).

Besides those molecular links, initial studies with NIH3T3 cells containing a fluorescent clock reporter that allows time lapse imaging of the circadian clock in individual proliferating cells revealed that mitosis occurred at specific time windows, suggesting that cell division is gated by the circadian clock (Nagoshi et al., 2004). Recently, we and others used aforementioned NIH3T3 cells to address the dynamic coupling between the clock and cell cycle in more detail by simultaneous single cell time lapse imaging of circadian clock performance and cell cycle progression, the latter visualized through mitotic events (Bieler at al., 2014) or fluorescent cell cycle reporters (Feillet et al., 2014). Interestingly, in the absence of external resetting cues, the cell cycle and circadian clock were shown to be phase locked in a 1:1 ratio, with the clock reporter reproducibly peaking 5 h after mitosis (Feillet et al., 2014; Bieler et al., 2014). Notably, the length of the circadian cycle in proliferating cells adjusted to that of the cell cycle. On the other hand, synchronization of the circadian clock by physiological cues (such as dexamethasone) causes clustering of cell divisions, indicating that the cell cycle is synchronized via the circadian clock and that, accordingly, the coupling between these two oscillators is bidirectional (Feillet et al., 2014). The molecular nature of the coupling of the circadian clock to the cell cycle nevertheless remains to be determined. Mathematical models for the circadian clock (Leloup & Goldbeter, 2003, 2004) and the cell cycle (Gérard

& Goldbeter, 2009, 2014) have been integrated into a comprehensive computational model (Gérard & Goldbeter 2012) that enables the in silico analysis of the connection between the circadian clock and the cell cycle based on the molecular information provided in literature. This approach has provided new insight into the interaction of these oscillating systems and the conditions under which the cell cycle can be entrained by the circadian clock as a function of both the strength of coupling to the circadian clock and the duration of the cell cycle prior to such coupling (Gérard & Goldbeter 2012).

Although our knowledge on the coupling of the circadian clock and cell cycle is steadily increasing, relatively little is known on how genetic clock defects affect the interaction between these two oscillatory machineries. In the current study, we used our NIH3T3^{3C} mouse fibroblast line with fluorescent reporter genes for the circadian clock and cell cycle phase (Feillet et al., 2014) to investigate the role of the BMAL1 and CLOCK proteins in cell cycle progression. We show that cell cycle duration is prolonged after siRNA mediated silencing of either *Bmal1* or *Clock* expression, and provide insight into the mechanism underlying this effect. Moreover, we used the biological data to probe and reinforce the computational model for the coupled mammalian circadian clock and cell cycle oscillators.

Materials & Methods

Cell culture and gene knockdown

NIH3T3 and NIH3T3^{3C} cells, the latter containing *Rev-Erbα-VNP* clock reporter and FUCCI *hCdt1-mKOrange* and *hGeminin-CFP* FUCCI cell cycle reporter genes; Feillet et al., 2014) were cultured in Dulbecco's Modified Eagle's Medium (DMEM)/F10 (Lonza) containing 10% Fetal Bovine Serum (FBS) (Gibco), 100 U/ml Penicillin and 100 µg/ml Streptomycin in a standard humidified incubator at 37°C and 5% CO_2 (pH7.7).

To knockdown *Bmal1* or *Clock* expression, we used Silencer® Select Pre-designed siRNA for *Arntl* (ThermoFisher Scientific; catalog number 4390771) and Clock (ThermoFisher Scientific; catalog number 4390771). As a negative control, we used Silencer® Select Negative Control No. 1 siRNA (ThermoFisher Scientific; catalog number 4390843). Reverse transfection was performed in 6 well plates (population studies) or in 4 well poly-L-lysine coated glass bottom dishes (D141410, Matsunami Glass Ind.), using the Lipofectamine® RNAiMAX method (Invitrogen) as described by the manufacturer, except that Opti-MEM was replaced by (serum-free) DMEM/F10. After 24 hours, transfection medium was replaced by regular culture medium. Cells were harvested at the indicated time points and processed for further analysis.

In a subset of experiments, the cell cycle of proliferating cells was synchronized by treatment of cell cultures with 2.5 mM thymidine (Sigma), starting 48 hours after RNAi transfection. After 24 hours, cells were released from thymidine block by washing 3 times with PBS and harvested at the indicated time points.

Time-lapse fluorescence microscopy

For time-lapse recording of circadian clock and cell cycle progression, cells (transfected and grown on glass bottom dishes) were placed in the temperature (37°C), CO_2 (5%) and humidity controlled chamber of a live cell imaging Zeiss LSM510/Axiovert 200M confocal microscope, equipped with a 10x Ph objective. Images were recorded every 30 min for 72 hours or more using a Coolsnap HQ/Andor Neo sCMOS camera. Live cell imaging was conducted using the following parameters (as set up in Zeiss 200 software): Venus (green): 1000 ms (filter cube: Ex= 475/40 nm, DM= 500 nm, Em= 530/50 nm); mKO2 (red): 300 ms (filter cube: Ex= 534/20 nm, DM=552 nm, Em: 572/38 nm); CFP (blue): 300 ms (filter cube: Ex= 458/17 nm, DM=450 nm, Em: 479/40 nm). Acquired images were concatenated and merged into a single file to generate a movie which was used for further analysis as described in detail by Feillet and coworkers (Feillet et al., 2014). In short, single cell numerical time series for each of the fluorescent markers were generated using the LineageTracker plugin for ImageJ (https://github.com/pkrusche/lineagetracker.jsonexport). Time series were analyzed for circadian cycle length, cell cycle length and G1 and S/G2/M cell cycle phase length. The G1 phase is defined as the interval between the peaks of hGeminin-CFP and hCDT1-mKOrange expression. Oppositely, the S/G2/M phase is defined as the interval between the peaks of hCDT1-mKOrange and hGeminin-CFP expression.

mRNA and protein analysis

Gene expression levels were determined by quantitative RT-PCR. Total RNA was isolated from cultured cells in triplicate using TRIzol (Invitrogen) following manufacturer's instructions. First-strand cDNA was synthesized from 1 µg of total RNA using oligo (dT) primers and SuperScript reverse transcriptase (Invitrogen) according to the manufacturer's protocol. Quantitative PCR amplification was performed using the iCycler iQ™ Real-Time PCR Detection System (BioRad), with SYBR-green and primer sets generating intron-spanning products of 150-300 bp. The following forward and reverse primers were used: *Bmal1:* Fwd 5'-AAG CTT CTG CAC AAT CCA CAG CAC-3' and Rev 5'-TGT CTG GCT CAT TGT CTT CGT CCA-3'; *Clock:* Fwd 5'-CTT CCT GGT AAC GCG AGA AAG -3' and Rev 5'-GTC GAA TCT CAC TAG CAT CTG AC -3'; *B2M*: Fwd 5'-CCG GCC TGT ATC CAG AAA-3' and Rev 5'-AAT TCA ATG TGA GGC GGG TGG AAC-3'.

Protein expression levels were determined by Western blot analysis. Cells were lysed in RIPA lysis buffer, composed of 2 mM Tris-HCl PH8.0, 1% TX-100, 0.5% NaDOC, 0.1% SDS, 5.15 mM NaCl, 5 mM NaF, 1.25 mM $NaVO_3$, 10 mM EDTA supplemented with a PhosSTOP phosphatase inhibitor tablet (Roche) and a Pierce Protease Inhibitor tablet (ThermoFisher). Lysates were cleared by centrifugation at 13,000 g for 10 minutes at 4°C. Protein concentration was determined using the BCA Protein Assay Reagent (Pierce®, Thermo Scientific). Absorbance was measured at 560 nm using a GloMax-Multi+ Microplate Multimode Reader (Promega). Proteins were loaded on Bis-Tris Plus 4-12% polyacrylamide gel (Novex®, Life technologies), size separated and transferred to a Polyvinylidene fluoride

(PVDF) membrane. After blocking with 4% skim milk, membranes were incubated with primary antibodies (listed below) overnight at 4°C. After washing, membranes were incubated with the secondary antibodies (1:2000 dilution) for 1 hour at 4°C. Protein bands were visualized using Western Lightning™ Chemiluminescence Reagent Plus (PerkinElmer) and autoradiography. Bands were quantified by Fiji® software and normalized against to β-actin protein levels.

Antibodies used: Primary antibodies: Santa Cruze: Actin C-2 (sc8432), BMAL1 (sc48790), CLOCK (sc25361), Cyclin B1 (sc245), Cyclin A (sc751), WEE1 (sc325); Abcam: Cyclin E (ab7959), Cyclin D (ab134175),. Secondary antibodies: goat anti-rabbit IgG (H+L)-HRP conjugate or goat anti-mouse IgG (H+L)-HRP conjugate.

Flow cytometry

To analyze cell cycle status by quantification of DNA content, cells were harvested 48 hours after siRNA transfection, washed with PBS, and fixed overnight at 4°C with cold 70% ethanol. Next, fixed cells were washed with PBS, treated for 15 min at 37°C with PBS containing 100 μg/ml bovine pancreas RNase (Calbiochem), and left overnight at 4°C in PBS with 40 μg/ml propidium iodide (PI; Life Technologies). Alternatively, to specifically detect mitotic cells, fixed cells were stained for the presence of the MPM-2 phospho-epitope on DNA topoisomerase IIα, using mouse anti-MPM2 primary antibodies (Merck-Millipore; dilution 1:200; 1 h on ice) and goat-anti mouse FITC secondary antibodies (Jackson ImmunoResearch; dilution 1:50; 30 min on ice). Cells were analyzed by a Becton Dickinson LSRFortessa™ Cell Analyzer (BD Biosiences). PI and FITC fluorescence intensities were measured at 610 nm and 530 nm, respectively. For each condition, at least 20000 cells were counted. Frequency histograms were made using BD FACSDiva™ software (BD Biosciences).

DNA synthesis assay

DNA synthesis was determined using the Click-iT® EdU Alexa Fluor® 594 Imaging Kit (Invitrogen). Cells were pulse labelled with 5-ethynyl-2'-deoxyuridine (EdU) for 1 hour, fixed with 3.7% formaldehyde, and incubated with Alexa Fluor® 594 *according* to the *manufacturer's instructions*. Images were generated using a Zeiss Axiovert 200M microscope and processed using ImageJ software. For each image, total intensity was normalized to the number of cells.

Mathematical modeling

To study the interaction between the circadian clock and the cell cycle we used two computational models previously proposed for the mammalian circadian clock and for the mammalian cell cycle, respectively. The model for the mammalian circadian clock incorporates the positive and negative regulations involving the PER, CRY, CLOCK, BMAL1 and REV-ER-

Bα proteins (Leloup & Goldbeter, 2003, 2004). This model (in which, for simplicity, PER1 and PER2, as well as CRY1 and CRY2 are treated as single entities) accounts for the occurrence of spontaneous circadian oscillations of the above-mentioned proteins and their mRNAs in a variety of experimental conditions.

The model for the mammalian cell cycle is based on the regulatory properties of the CDK network that drives the transitions between the successive phases of the cell cycle (Gérard & Goldbeter, 2009, 2014). The model contains four CDK modules, each of which controls the transition to a particular cell cycle phase. Thus, Cyclin D/CDK4-6 and Cyclin E/CDK2 promote progression in G1 and elicit the G1/S transition; the activation of Cyclin A/CDK2 ensures progression in S and G2, while the peak of Cyclin B/CDK1 activity brings about progression into mitosis. Exit from the quiescent state is triggered above a critical level of growth factor by the synthesis of Cyclin D, which allows cells to enter the G1 phase. Synthesis of the various cyclins is regulated through the balance between the antagonistic effects exerted by the transcription factor E2F and the tumor suppressor pRB, which respectively promote and inhibit cell cycle progression. Additional regulations in this model for the CDK network bear on the control exerted by the proteins SKP2, CDH1, or CDC20 on the degradation of cyclins E, A, and B at the G1/S or G2/M transitions, respectively. Moreover, the activity of each cyclin/CDK complex can itself be regulated through CDK phosphorylation-dephosphorylation. At suprathreshold levels of growth factor sustained oscillations spontaneously occur in the CDK network, which may be associated with cellular proliferation since they correspond to the repetitive, sequential activation of the various cyclin-CDK complexes responsible for the ordered progression along the successive phases of the cell cycle (Gérard & Goldbeter, 2009, 2014).

The cell cycle is coupled to the circadian clock through several molecular processes (see above), such as the induction of *Wee1* expression by CLOCK/BMAL1. Such coupling may lead to entrainment of the cell cycle by the circadian clock (Gérard & Goldbeter, 2012). The equations governing the models for the coupled circadian clock and cell cycle models are given in the Supporting Information section. Here we focus on the case where the cell cycle is coupled to the circadian control via the induction of *Wee1* gene expression by CLOCK/BMAL1. We also introduce coupling via the induction of *Cnnb1* (*Cyclin B1*) gene expression by CLOCK/BMAL1, as suggested by the experiments reported in the present study. To model the impact of knockdown of *Bmal1* gene expression, we reduce the rate of *Bmal1* mRNA synthesis (measured by parameter v_{sB}) in the model for the circadian clock.

Statistical analysis

All statistical analyses were carried out with GraphPad software. For single cell studies, after performing the normality test, the two-tailed Mann-Whitney U-test was used to analyze the period of the circadian and cell cycle clocks (including G1, S/G2/M phase length). For Western blot, flow cytometry, and immunofluorescence experiments, the two-tailed Student's t-test was applied.

Results

Suppression of *Bmal1* expression lengthens the cell cycle

To study the role of BMAL1 in cell cycle progression, we used NIH3T3^{3C} cells, expressing fluorescent markers for the circadian clock (Rev-Erbα-VNP fusion protein; yellow), as well as G1 phase (hCdt1-mKOrange fusion protein; red) and combined S, G2, and M (hereafter referred to as S/G2/M) phase (hGeminin-CFP fusion protein; blue) of the cell cycle (Feillet et al., 2014). NIH3T3^{3C} cells were transiently transfected with a siRNA targeting *Bmal1* mRNA or with a non-targeting siRNA (used as a negative control) and are hereafter referred to as *siBmal1* and *siCtrl* cells, respectively. Analysis of *Bmal1* mRNA and BMAL1 protein levels in proliferating *siBmal1* cells 72 hours after transfection, revealed 74% down regulation of *Bmal1* gene expression in *siBmal1* cell cultures (Fig S1A), resulting in a 71% reduction in BMAL1 protein (Fig S1B) levels.

We first analysed clock performance and cell cycle progression in *siBmal1* and *siCtrl* cells (n=50 individual cells per condition) over a period of 72 hours using live cell imaging confocal microscopy (see Fig 1A for a representative example of time lapse images of a *siCtrl* cell, spanning a complete G1/S/G2/M cycle). In line with our previous data (Feillet et al., 2014), proliferating *siCtrl* cells show robust rhythmic expression of the clock marker and a tight phase coupling of the circadian clock and cell cycle (Fig 1B; upper panel). The period of the cell cycle, as calculated from the interval between two peaks of hCdt1-mKOrange expression, is 17.1 ± 0.3 h (mean ± SE; Fig 1C). In marked contrast, we observed a complete suppression of circadian oscillations and robust down regulation of Rev-Erbα-VNP protein levels in proliferating *siBmal1* cells, indicative for efficient knockdown of *Bmal1* expression (Fig 1B, lower panel). Moreover, knockdown of *Bmal1* expression significantly ($p<0.001$) increased cell cycle length from 17.1 ± 0.3 h to 21.4 ± 0.5 h (mean ± SE; Fig 1C).

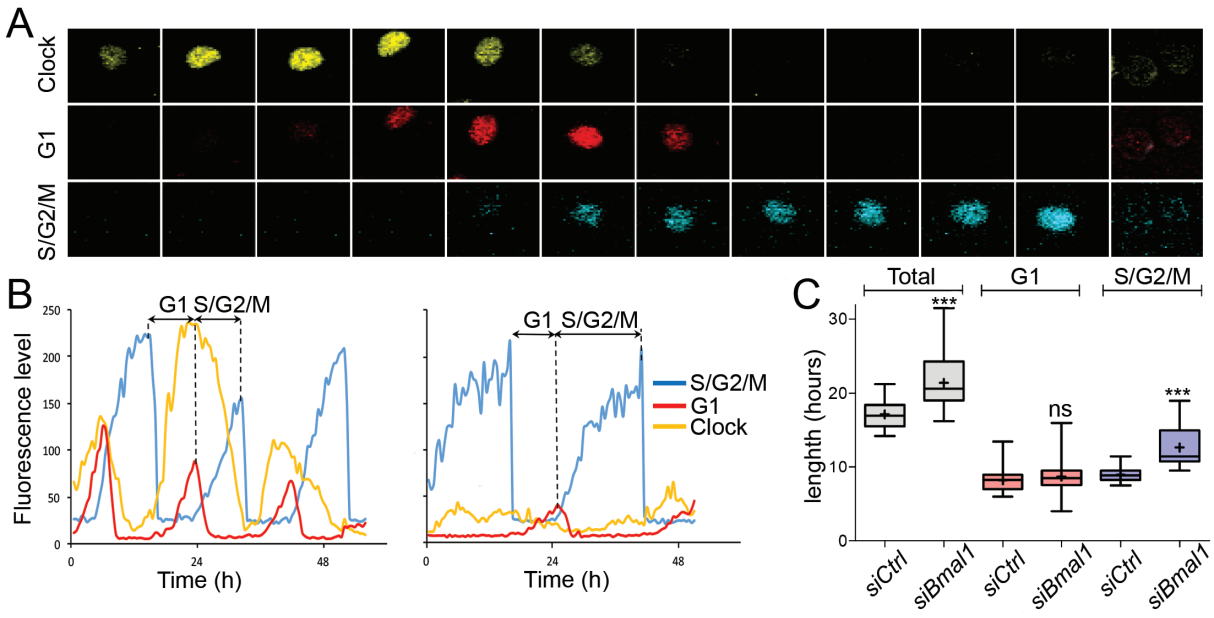

Figure 1. Cell cycle dynamics in *siCtrl* and *siBmal1* cells. (A) Representative example of time series images of the nucleus of a proliferating *siCtrl* (NIH3T3^{3C}) cell, stably expressing circadian clock (Rev-Erbα-VNP; yellow), as well as G1 (hCdt1-mKOrange; red) and S/G2/M (hGeminin-CFP; blue) cell cycle markers. Shown are pictures at 1.5 hour time intervals over a 18 h period, spanning one cell cycle. (B) Circadian clock performance and cell cycle progression in a *siCtrl* (left panel) and a *siBmal1* cell (right panel). Plotted are fluorescence intensities of each of the markers over a 48 hour period. The G1 phase is defined as the interval between the peaks of hGeminin-CFP and hCDT1-mKOrange expression. Oppositely, the S/G2/M phase is defined as the interval between the peaks of hCDT1-mKOrange and hGeminin-CFP expression. (C) Box plot showing the cell cycle period and G1 and S/G2/M cell cycle phase length in *siCtrl* and *siBmal1* cells (n=50 cells per condition). Lowest and highest boundaries of the box indicate the 25th and 75th percentiles, respectively. The whiskers above and below the box designate the 95th and 5th percentiles, respectively. The solid line and cross within the box represent the median and mean value, respectively. *** $p<0.001$ (Mann Whitney test).

Next, we quantified the length of G1 and S/G2/M phase in *siCtrl* and *siBmal1* cells. For simplicity, as the FUCCI markers are indicators for either G1 or S/G2/M phase rather than exact predictors of the start and end of these cell cycle phases, we defined the G1 phase as the interval between the peaks of hGeminin-CFP and hCDT1-mKOrange expression, and the S/G2/M phase as the interval between the peaks of hCDT1-mKOrange and hGeminin-CFP expression. As shown in Fig 1C, the mean length of the G1 phase in *siCtrl* cells (8.2 ± 0.2 h) does not significantly differ ($p=0.2$) from that in *siBmal1* cells (8.7 ± 0.3 h). Interestingly, the average length of the S/G2/M phase significantly ($p<0.001$) increased from 9.0 ± 0.8 h in *siCtrl* cells to 13.0 ± 0.3 h in *siBmal1* cells (Fig 1C).

Taken together, these results show that the BMAL1 protein acts as a cell cycle period modulator.

Suppression of *Bmal1* expression specifically affects the G2 phase

The single cell experiments show that silencing *Bmal1* expression lengthens the S/G2/M phase of the cell cycle, but do not allow to discriminate between the three phases. To investigate which specific cell cycle phase is prolonged, we compared the cell cycle distribution of proliferating *siCtrl* and *siBmal1* cells by flow cytometry of propidium iodide stained cells (Fig 2A) and quantified the cell cycle phase distribution (Fig 2B). In line with the single cell experiments, we did not observe significant changes in the percentage of G1 and S phase cells after knockdown of *Bmal1* expression (G1 phase: 53.5 ± 1.2 % and 52.7 ± 0.5 % ; S phase: 31.4 ± 1.0% and 28.5 ± 0.3 for *siCtrl* and *siBmal1* cells respectively; mean ± SEM). On the other hand, the percentage of G2/M cells significantly ($p=0.01$) increased from 13.4 ± 0.5 % in *siCtrl* cells to 17.1 ± 0.3 % in *siBmal1* cells (Fig 2B). In order to discriminate between G2 and M phase, we also stained the cells with an antibody against the mitosis-specific MPM-2 phosphoepitope on DNA topoisomerase IIα. As shown in Fig 2C, the percentage of MPM2-positive cells is comparable for proliferating *siCtrl* and *siBmal1* cell cultures. From these data, we conclude that the observed lengthening of the S/G2/M phase after knockdown of *Bmal1* is solely due to an increased duration of the G2 phase.

Suppression of *Bmal1* expression specifically affects Cyclin B1 expression

The observed lengthening of the combined S/G2/M phase in *siBmal1* cells (single cell analysis) and increased number of *siBmal1* cells in the G2 phase (flow-cytometry analysis) clearly point to a regulatory role of BMAL1 in the kinetics of the cell cycle. We therefore next examined the expression levels of the various cyclins in proliferating *siCtrl* and *siBmal1* cells by western blot analysis (Fig 2D). Following quantification (Fig 2E), the expression levels of Cyclin D1, Cyclin E, and Cyclin A (important regulators of G1 phase, G1/S transition and S phase, respectively) in *siBmal1* cells did not significantly differ from those in *siCtrl* cells. However, the Cyclin B1 (a driver of G2/M transition) protein level is significantly ($p=0.03$) reduced in *siBmal1* cells. This suggests that the accumulation of *siBmal1* cells in G2 phase, and the delay in G2/M transition, are caused by low levels of Cyclin B1.

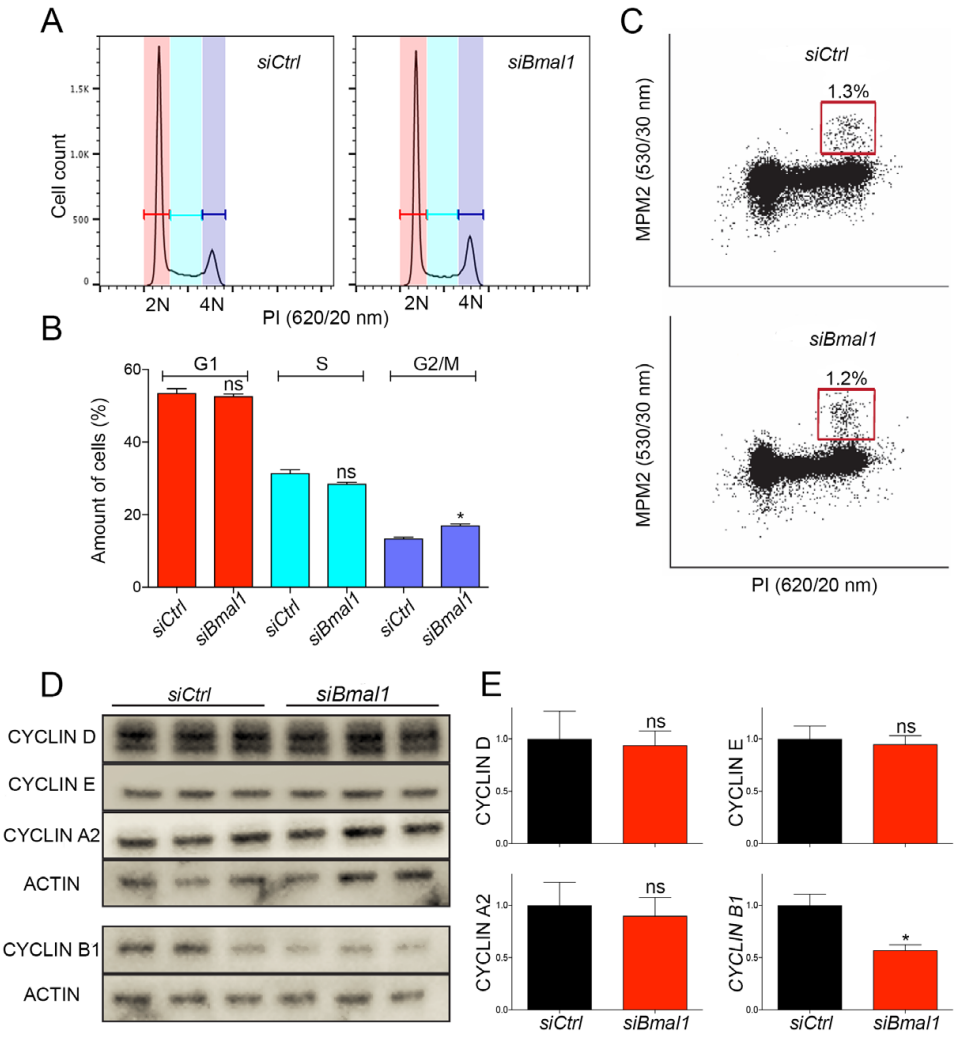

Figure 2. Cell cycle phase distribution of *siCtrl* and *siBmal1* cells. (A) Flow cytometric analysis of cell cycle phases in *siCtrl* and *siBmal1* cells. Shown are representative examples of propidium iodide (PI) stained *siCtrl* and *siBmal1* cells, analysed for DNA content. The vertical axis indicates the relative number of cells and the horizontal axis indicates the relative PI fluorescence. The 2N and 4N peaks and intermediate region correspond to G1, G2/M and S phase, respectively. (B) Quantification of cell cycle phase distribution of proliferating *siCtrl* and *siBmal1* cells. Shown are the average cell numbers of the 3 independent experiments (each performed in triplicate; 20000 cell counts per triplicate). The data were compared using the two-tailed unpaired Student's t-test. Error bars indicate SE. * p=0.01. (C) Flow cytometry analysis of the number of mitotic cells. The bivariate dot plots show DNA content (PI) and mitotic phosphoproteins content (MPM2 stain) on the X and Y axis, respectively. The box marks cells stained positive for MPM2. (D) Western blot analysis of whole cell extracts from proliferating *siCtrl* and *siBmal1* cells for Cyclin D, Cyclin E, Cyclin A2, and Cyclin B1 proteins. Shown are representative examples of n=3 biological replicates. Actin was used as a loading control. (E) Average cyclin protein levels in proliferating *siCtrl* and *siBmal1* cells. Cyclin expression levels were normalized against actin. Cyclin expression levels in control cells were set as 1. Error bars indicate SD (n=3 experiments).

Suppression of *Bmal1* expression causes an overall reduction of Cyclin B1 expression

Obviously, aforementioned experiments with asynchronously proliferating cells do not discriminate between the various cell cycle phases. We therefore set out to further investigate the expression and kinetics of accumulation of the various cyclins in cell cycle synchronized *siCtrl* and *siBmal1* cells. To this end, we used a single 24 hour thymidine block, which causes cells to accumulate at G1/S boundary. Pulse-labeling of *siCtrl* and *siBmal1* cells with 5-ethynyl-2′-deoxyuridine (EdU) for one hour at 1 h intervals after release from the thymidine block (Fig 3A) revealed that DNA synthesis (as detected by immunofluorescent labeling) in *siCtrl* and *siBmal1* cells follows similar kinetics, peaking 3 hours after thymidine block release (Fig 3B). Assuming that the peak in DNA synthesis represents mid-S phase, S phase in *siCtrl* and *siBmal1* cells is estimated to span 5 to 6 hours, which is in good agreement with the flow cytometry data (30% S-phase cells at a cell cycle length of 18 hours = 5.4 h). Next, we determined Cyclin E (G1/S marker) and Cyclin A2 (S phase marker) protein levels by western blot analysis in *siCtrl* and *siBmal1* cells harvested 0, 2, 4, 6, 8, and 10 hours after release from thymidine (Fig 3C). Quantification of the cyclin levels (Fig 3D and E) revealed that kinetics of Cyclin E and Cyclin A2 were comparable to *siCtrl* cells, which is in complete agreement with our observation that *siBmal1* cells show normal G1 and S phase progression.

Next, we determined Cyclin B1 protein levels in *siCtrl* and *siBmal1* cells after release from the thymidine block. As shown in Fig 3F and G, *Cyclin* B1 protein levels gradually increased in *siCtrl* cells, reaching a maximum 6 h after thymidine release at the moment when cells are in G2 phase. In line with our earlier observation in asynchronously dividing cells (Fig 2D and F), *siBmal1* cells express the Cyclin B1 protein at lower levels. Moreover, *siBmal1* cells display impaired induction of Cyclin B1 during G2 phase, which may explain the delay in G2/M transition.

Last but not least, as WEE1 is an inhibitor of Cyclin B/CDK1 activity and *Wee1* expression is under circadian control (Matsuo et al., 2003), we also analyzed aforementioned protein samples for WEE1 expression (Fig 3H). As expected, in the absence of the CLOCK/BMAL1 transcription activator, *siBmal1* cells express WEE1 protein at markedly reduced level (Fig 3I). However, as reduced expression of this negative regulator is expected to accelerate, rather than delay G2 to M transition, the lower WEE1 protein levels in *siBmal1* cells do not explain the delayed G2/M transition. Instead, our data demonstrate that the circadian clock protein BMAL1 is a modulator of cell cycle period that promotes G2 to M transition through induction of Cyclin B1 expression.

Suppression of *Clock* expression lengthens the cell cycle and dampens Cyclin B1 expression

The question arises to what extent the observed modulation of G2/M transition is a specific function of the individual BMAL1 protein, or whether this requires CLOCK/BMAL1

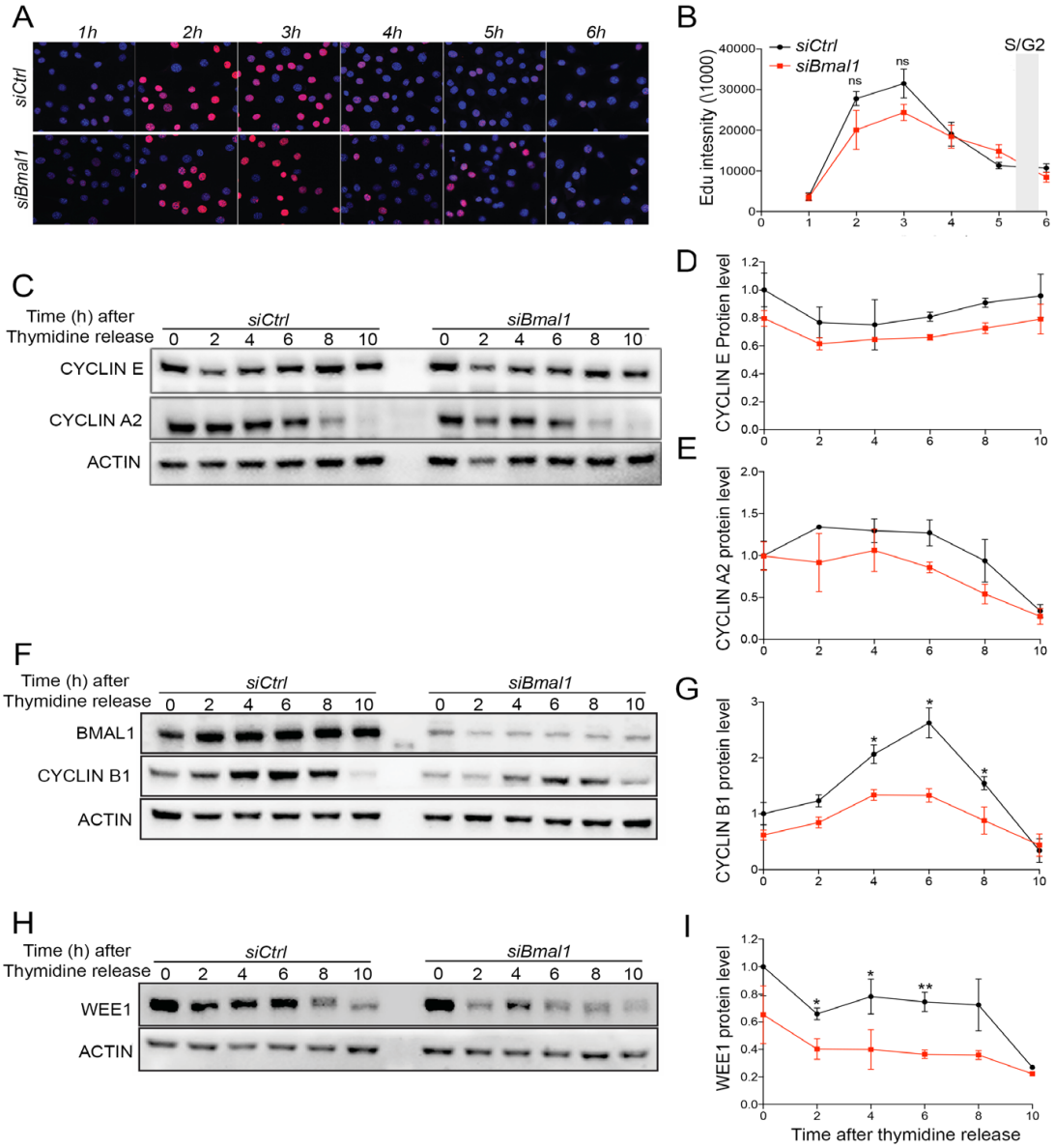

Figure 3. Cell cycle protein expression in *siCtrl* and *siBmal1* cells. (A) Cytochemical analysis of DNA synthesis in cell cycle synchronized *siCtrl* and *siBmal1* cells after release from a 24 h thymidine block. Cells were harvested at 1 h intervals. Prior to harvesting, cells were exposed to a 1 h pulse labelling with EdU. (B) S phase kinetics. Quantification of Edu incorporation by *siCtrl* and *Bmal1* cells during the 1 h pulse labelling interval, preceding cell harvesting. The Y axis indicates the mean fluorescence intensity, corrected for the number of cells. The X axis indicates time of harvesting after thymidine release. Error bars indicate SE (n=3 experiments). The grey bar indicates the estimated time of S/G2 transition. (C, F and H) Western blot analysis of Cyclin E and Cyclin A2 (C), Cyclin B1 (F) and WEE1 (H) protein levels in *siCtrl* and *siBmal1* cells after release from a thymidine block. Shown are representative examples of n=3 independent experiments. Actin was used as a loading control. (D, E, G and I) Kinetics of Cyclin E (D), Cyclin A2 (E), Cyclin B1 (G) and WEE1 (I) expression after release from a thymidine block. Expression levels were normalized against actin. Expression levels in *siCtrl* cells at t=0 were set as 1. Error bars indicate SE.

heterodimerization. We therefore transiently transfected NIH3T3^{3c} cells with a siRNA targeting the *Clock* gene or with a non-targeting control siRNA to obtain *siClock* cells. Analysis of *Clock* mRNA and CLOCK protein levels in proliferating *siClock* and *siCtrl* cells 72 hours after transfection, revealed 63% down regulation of *Clock* gene expression in *siClock* cell cultures (Fig S1C), resulting in a 88% reduction in CLOCK protein levels (Fig S1D). We next analysed clock performance and cell cycle progression in *siClock* and *siCtrl* cells (n=40 individual cells per condition) over a period of 72 hours using time laps confocal microscopy (for a representative example, see Fig 4A). Like *siBmal1* cells, *siClock* cells are arrhythmic, as evident from the loss of cyclic expression of the REV-ERBα clock reporter, and proliferate significantly slower (p=0.03) than *siCtrl* cells (19.7 ± 0.3 h vs 18.7 ± 0.3 h per cycle; mean ± SEM). As shown in Fig 4B, the G1 phase was not significantly affected in *Clock* knock down cells, as compared to *siCtrl* cells (9.2 ± 0.2 h vs 8.5 ± 0.3 h; mean ± SEM p=0.07). Instead, the increased cell cycle period in *siClock* cells originates from a lengthened S/G2/M phase (9.4 ± 0.1 h in *siCtrl* and 11.0 ± 0.2 h in *siClock* cells; p<0.001). Subsequent analysis of the cell cycle distribution of proliferating *siCtrl* and *siClock* cells by flow cytometry revealed a significant increase in the percentage of G2/M cells (14.3 ± 0.1 in *siCtrl* and 20.1 ± 1.2 in *siClock* cells; mean ± SEM; p=0.03), and relatively less S phase cells in proliferating *siClock* cell cultures (27.1 ± 0.6 in *siCtrl* and 21.3 ± 1.0 in *siClock* cells; p=0.01) (Fig.4D). These findings indicate that proliferating *siClock* cells markedly resemble *siBmal1* cells in that the cell cycle period is increased due to slower G2/M cell cycle progression.

We therefore next analyzed the kinetics of Cyclin B1 accumulation in *siClock* and *siCtrl* cells after release from a 24 hour thymidine block (Fig 4D). As expected, Cyclin B1 protein levels gradually increased in *siCtrl* cells peaking 6 hours after thymidine release (Fig 4E, see also Fig 3G). In contrast, *siClock* cells show markedly reduced Cyclin B1 protein levels peaking some 7 hours after thymidine release (Fig 4E). Taken together, these data indicate that modulation of G2/M transition through induction of Cyclin B1 is a characteristic of the CLOCK/BMAL1 heterodimer, rather than the BMAL1 protein alone.

Mathematical modeling of CLOCK/BMAL1-controlled cell cycle progression

The biological data on the modulating effect of CLOCK/BMAL1 on cell cycle progression serve as an ideal tool to probe and reinforce the computational model for coupled mammalian circadian clock and cell cycle oscillators, as defined by Goldbeter and coworkers (Leloup & Goldbeter, 2003, 2004; Gérard & Goldbeter, 2009, 2012). We therefore set out to test whether the computational model would also respond with a delay in G2/M transition after simulating a reduction in *Bmal1* or *Clock* expression levels. The coupling between the circadian clock and the cell cycle is mediated by several cell cycle proteins such as WEE1 (Matsuo et al, 2003), p21 (Gréchez-Cassiau et al., 2008), NONO (Kowalska et al., 2013), and, as shown here, Cyclin B1. Oppositely, there are indications that the cell cycle may have an effect on the circadian clock, but the mechanism of such a coupling remains unclear (Traynard et al, 2016; Paijmans et al, 2016), although a recent study points to the enhancement of REV-ERBα

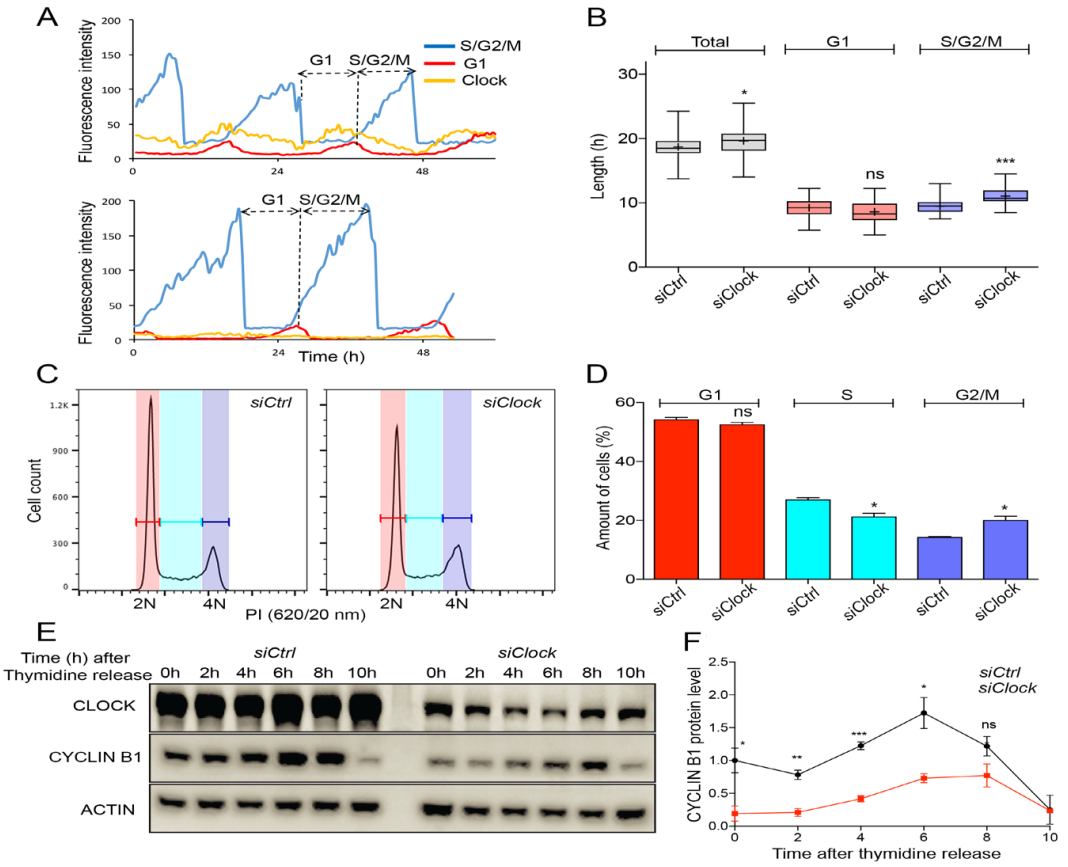

Figure 4. Cell cycle dynamics and Cyclin B1 protein expression in *siCtrl* and *siClock* cells. (A) Circadian clock performance and cell cycle progression in a *siCtrl* (left panel) and a *siClock* cell (right panel). Plotted are fluorescence intensities of each of the markers over a 60 hour period. (B) Box plot showing the total cell cycle period and G1 and S/G2/M cell cycle phase length in *siCtrl* and *siClock* cells (n=40 cells per condition). Lowest and highest boundaries of the box indicate the 25th and 75th percentiles, respectively. The whiskers above and below the box designate the 95th and 5th percentiles, respectively. The solid line and cross within the box represent the median and mean value, respectively. *** $p<0.001$ (Mann Whitney test). (C) Flow cytometric analysis of cell cycle phases in *siCtrl* and *siClock* cells. Shown are representative examples of propidium iodide (PI) stained *siCtrl* and *siBmal1* cells, analysed for DNA content. The vertical axis indicates the relative number of cells and the horizontal axis indicates the relative PI fluorescence. The 2N and 4N peaks and intermediate region correspond to G1, G2/M and S phase, respectively. (D) Quantification of cell cycle phase distribution of proliferating *siCtrl* and *siClock* cells. Shown are the average cell numbers of the 3 independent experiments (each performed in triplicate; 20000 cell counts per triplicate). The data were compared using the two-tailed unpaired Student's t-test. Error bars indicate SE. * $p=0.01$ and $p=0.3$. (E) Western blot analysis of Cyclin B1 protein levels in *siCtrl* and *siClock* cells after release from a thymidine block. Shown are representative examples of n=3 independent experiments. Actin was used as a loading control. (F) Kinetics of Cyclin B1 expression after release from a thymidine block. Cyclin B1 expression levels were normalized against actin. The Cyclin B expression level in *siCtrl* cells at t=0 was set as 1. Error bars indicate SE (n=3 independent experiments).

degradation through phosphorylation by CDK1 (Zhao et al., 2016). Therefore, despite recent evidence for bidirectional coupling between the cell cycle and the circadian clock (Feillet et al., 2015; Bieler et al, 2014), we decided to focus on the situation where the cell cycle is unidirectionally coupled to the circadian clock via CLOCK/BMAL1-mediated induction of *Wee1* and *Cnnb1* expression. Below, we first model the impact of *Bmal1* inactivation on cell cycle progression, and subsequently address the effect of in silico knockdown of *Clock* gene expression.

We consider that in proliferating cells the circadian clock has an overall length of 18 hours (close to the value of 17.1 h observed experimentally in proliferating *siCtrl* cells; Fig 1B and 1C). We select an autonomous period of the cell cycle of 21.1 h, which is close to the cell cycle length observed in *siBmal1* cells in the absence of the circadian clock (Fig 1B). In line with the experimental data (Fig 1B), the time evolution of *Bmal1* and *Rev-Erbα* mRNA levels in our computational model shows that under control conditions the circadian clock oscillates with a cycle length of 18h (Fig 5A), while all four Cyclin/CDK protein complexes (Fig 5C), as well as the WEE1 protein (Fig 5E) display sustained oscillations with the same period. These results represent entrainment of the cell cycle by the circadian clock via BMAL1-mediated induction of *Wee1* and *CcnB1 (Cyclin B1)* gene expression. This circadian control comes on top of a basal expression of the two genes, as suggested by the observation of low levels of Cyclin B1 and WEE1 protein in *siBmal1* cells (Fig 3G and 3I).

When *Bmal1* gene expression is suppressed in silico by reducing the *Bmal1* mRNA synthesis rate (v_{sB}) by 70%, computational time series analysis reveals that *Bmal1* mRNA levels are no longer oscillating and that BMAL1 protein levels are constitutively low (Fig 5B). As a consequence, *Rev-Erbα* mRNA levels are also constitutively low (Fig 5B). These data are in full agreement with the experimental data obtained with *siBmal1* cells (Fig 1B; Figs S1A and S1B) and show that the circadian clock is arrested when *Bmal1* expression is knocked down. Interestingly, and also in full agreement with the experimental data, the cell cycle length is prolonged from 18h to 21.1 h after in silico reduction of *Bmal1* expression levels (compare Fig 5C and 5D). Notably, the width of the activity peak of Cyclin B/CDK1 is significantly increased upon suppression of *Bmal1* expression, while that of other Cyclins appears unaffected (Fig 5C and 5D). In addition, the WEE1 protein concentration decreases in the model after in silico *Bmal1* knockdown due to the lack of CLOCK/BMAL1-mediated induction of *Wee1* gene expression (Fig 5Eand 5F).

Next, we examined in more detail how suppression of *Bmal1* expression in our mathematical model affects the duration of the G1 and S/G2/M cell cycle phases. To this end, we defined the G1 phase as the time from mid-decrease of Cyclin B/CDK1 to 30%-decrease of Cyclin D/CDK4-6 levels and the S/G2/M phase as the time from 30%-decrease of Cyclin D/CDK4-6 to mid-decrease of Cyclin B/CDK1 levels (see Fig 6A and 6B). Analysis of the computed time series reveals that under normal conditions, the G1 and S/G2/M phases span 5.84 h and 12.19h, respectively (Fig 6A), while in silico reduction of *Bmal1* mRNA synthesis by 70% results in G1 and S/G2/M cell cycle phase lengths of 6.41 h and 14.74 h, respectively (Fig 6B). Thus, in line with the experimental data (Figs 1B and 1C), elongation of the cell

cycle period upon suppression of *Bmal1* expression is predominantly caused by lengthening of the S/G2/M phase.

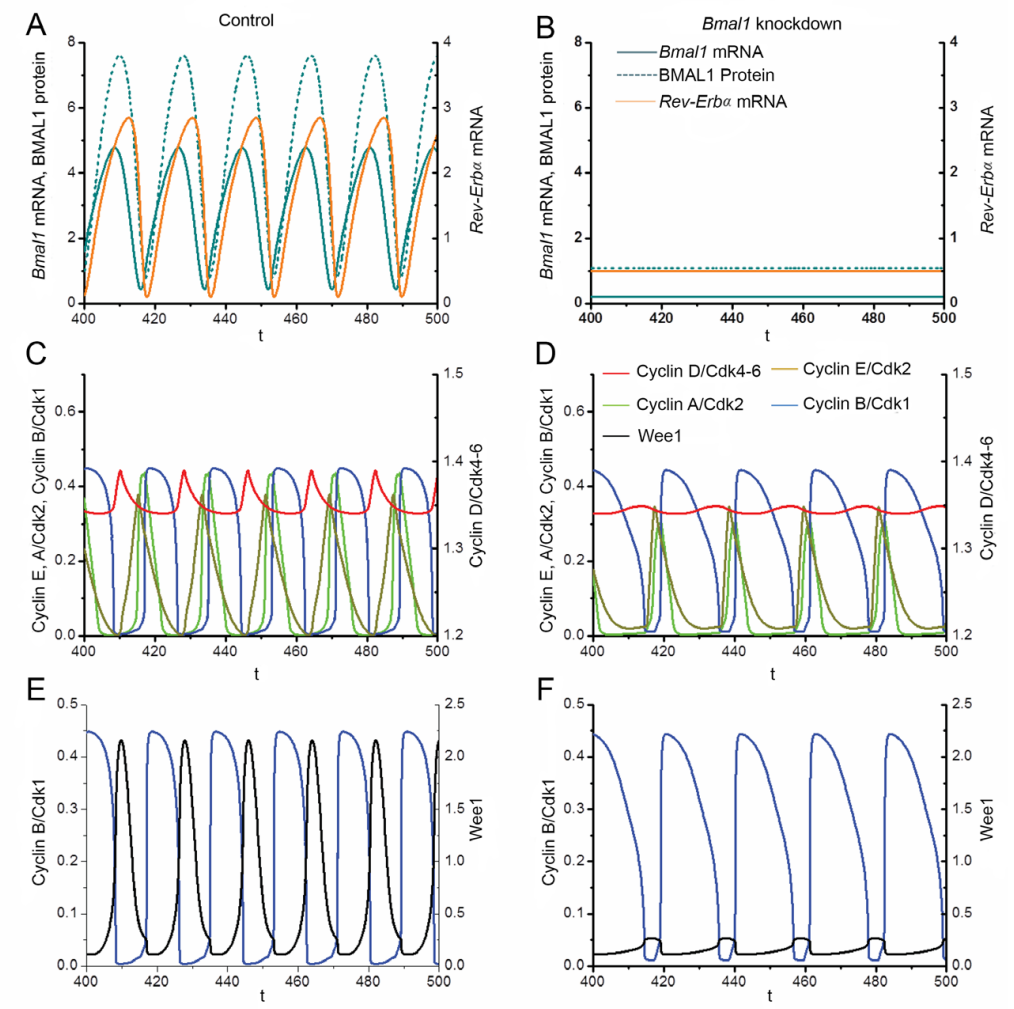

Figure 5. Computational modeling of the impact of *Bmal1* knockdown on Cyclin/CDK levels. Analysis of the effect of silencing of *Bmal1* expression in the computational model for coupled mammalian circadian clock and cell cycle oscillators. The time series in the upper panels show the evolutions of *Bmal1* mRNA (dark cyan, solid line), total BMAL1 protein (dark cyan, dashed line) and *Rev-Erbα* mRNA (orange) under normal conditions (A) or when the synthesis rate of *Bmal1* mRNA is reduced by 70% (B). The period of the circadian clock is 18h in control conditions. However, the oscillations in (B) disappear upon decreasing *Bmal1* mRNA synthesis. The time series in the middle panels show the time evolutions of Cyclin A/CDK2 (light green), Cyclin E/CDK2 (mustard green), Cyclin B/CDK1 (blue) and CyclinD/CDK4-6 (red) in control conditions, when the cell cycle is synchronized to the circadian clock (C), or when *Bmal1* is knocked down (D). The period of the cell cycle increases from 18h in (C) to 21.1 h in (D). Also, the width of the activity peak of Cyclin B/CDK1 (blue) is significantly increased. The time series in the bottom panels show the evolutions of Cyclin B/CDK1 (blue) and WEE1 (black) when cells are in control conditions (C) or when *Bmal1* gene expression is knocked down (D). The concentration of WEE1 decreases in (D) due to the lack of induction *Wee1* transcription by BMAL1. Parameter values used for numerical simulations are listed in the SI appendix.

The mathematical simulations, as shown above, reveal a normal amplitude oscillation of Cyclin B1/CDK1 levels after 70% reduction of the *Bmal1* mRNA synthesis, which appears to contrast somewhat with the experimental data, showing a 20-25% reduction in Cyclin B1 protein levels. We therefore also determined the time evolution of the total Cyclin B1 protein level (free and complexed with CDK1) under control conditions (Fig 6C) and upon reduced *Bmal1* gene expression (Fig 6D). The results indicate that, as in the experimental observations (see Fig 2D), total Cyclin B1 levels decrease upon knocking down *Bmal1*, which holds with the view that BMAL1 induces *CcnB1* gene expression, as reported above.

Similar results were obtained upon knocking down *Clock* instead of *Bmal1* in the computational model for coupled mammalian circadian clock and cell cycle oscillators (data not shown), which may not come as a surprise as CLOCK and BMAL1 act as a heterodimeric complex.

In conclusion, the performance of the computational model for coupled mammalian circadian clock and cell cycle oscillators after simulation of *Bmal1* or *Clock* silencing is in full agreement with the experimental observations in proliferating *siCtrl, siBmal1* and *siClock* cells.

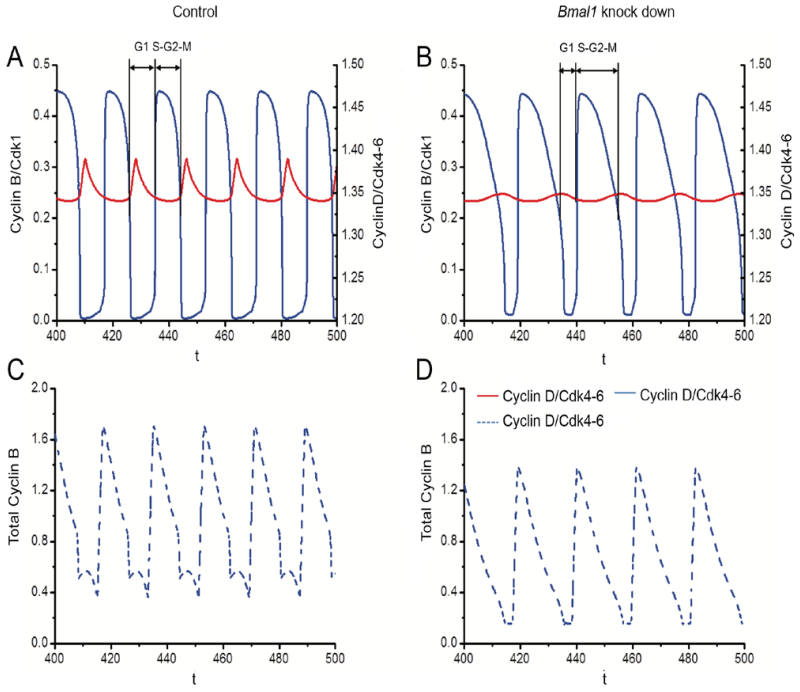

Figure 6. Computational modeling of the impact of *Bmal1* knockdown on cell cycle phase length. The time series in the upper panels show the evolutions of Cylin D/CDK4-6 (red) and Cyclin B/CDK1 (blue) when the circadian clock is in control conditions (A) or when *Bmal1* expression is reduced by 70% (B). As in the corresponding Figure 4, the period of the cell cycle increases from 18 h in (A) up to 21.1 h when *Bmal1* expression is supressed (B). The black bars indicate the G1 phase (from mid-decrease of Cyclin B/CDK1 to 30%-decrease in Cyclin D/CDK4-6) and S/G2/M phase (from 30%-decrease in Cyclin D/CDK4-6 to mid-decrease of cyclin B/CDK1). The durations of G1 and S/G2/M in (A) are 5.84 h and 12.19 h, respectively. The durations of G1 and S/G2/M in (B) are 6.41 h and 14.74 h, respectively. Thus, the S/G2/M phase contributes most to the prolongation of cell cycle duration upon knocking down BMAL1. The time series in the lower panels show the evolutions of total Cyclin B (dashed blue line) in control conditions (C) or upon suppression of *Bmal1* RNA synthesis (D). The total amount of Cyclin B (free + complexed with the kinase CDK1 and its inhibitor p21) decreases when *Bmal1* expression is reduced.

Discussion

Previously, we have reported the existence of a bi-directional link between the circadian clock and the cell cycle (Feillet et al., 2014). Indeed, synchronization and resetting of the circadian clock by external cues (such as dexamethasone) can synchronize cell cycle progression. Oppositely, a clear shortening of the circadian cycle occurred in dividing cells as compared to non-dividing cells, suggesting that the cell cycle can reset the circadian clock. In the present study, we have taken a combined cell and molecular biological approach to investigate the impact of the circadian clock on cell cycle progression by genetic disruption of the molecular circadian oscillator. We show that disruption of the positive limb of the circadian transcription-translation feedback loop-based molecular oscillator through knock-down of the circadian clock genes *Bmal1* or *Clock* prolonged the cell cycle of cultured fibroblasts. Our results show that this slowdown in cell cycle progression results from a delay in the G2/M transition. Since inactivation of *Bmal1* or *Clock* triggers a highly comparable cell cycle phenotype, G2/M checkpoint control appears a function of the CLOCK/BMAL1 heterodimer, rather than the individual proteins.

To investigate the molecular mechanism underlying the observed delay in cell cycle progression in the absence of BMAL1 or CLOCK, we zoomed in on cell cycle protein expression during G2 phase and G2/M transition using cell cycle synchronized *siBmal1* and *siClock* cells. Interestingly, whereas the kinetics of S phase progression remained unaffected, knockdown of *Bmal1* or *Clock* expression resulted in overall lower Cyclin B1 protein levels, as well as a reduction of the Cyclin B1 peak at G2 phase. Since a high Cyclin B1 protein level is essential for G2 progression and mitotic entry, the impaired induction of Cyclin B1 protein levels well explains the delayed cell cycle progression in G2 phase. This view is consistent with the study by Matsuo and coworkers (2003) focussing on cell cycle re-entry of remaining mouse hepatocytes after partial hepatectomy at ZT0 or ZT8 (ZT, Zeitgeber time in a 12 hour light–12 hour dark cycle; ZT0 represents lights on and ZT12, lights off). Whereas S phase kinetics was independent of the time of surgery, *CcnB1* mRNA and Cyclin B1 protein levels, as well as Cyclin B1/CDK1 peak activity, were delayed by about 8 to 12 hours when partial hepatectomy was performed at ZT0 as compared to ZT8 (Matsuo et al., 2003), demonstrating that clock-controlled timing of Cyclin B1 expression and activity is determining G2/M transition.

It has been well established that expression of the *Wee1* gene, encoding an important kinase regulating the G2/M checkpoint, is under direct control of the CLOCK/BMAL1 complex (Matsuo et al., 2003). As WEE1 acts as an inhibitor of CDK1 to prevent premature mitotic entry, one would expect inhibition of *Bmal1* expression to accelerate cell cycle progression due to a reduction of WEE1 protein level and kinase activity. On the contrary, however, we observed a delay in G2/M transition of proliferating *siBmal1* and *siClock* cells, accompanied by a reduction in Cyclin B1 protein levels. It appears, therefore, that the CLOCK/BMAL1 complex regulates at the same time the expression of an inhibitor (WEE1) and an activator (Cyclin B1) of G2/M transition. Regardless of this dual role of the CLOCK/BMAL1 complex

in controlling the G2/M checkpoint, the increased cell cycle length of *siBmal1* and *siClock* cells suggests that the dominant effect of CLOCK/BMAL1 is to induce expression of the Cyclin B1 encoding gene *Cnnb1*. The induction of *Wee1* by CLOCK/BMAL1 could nevertheless contribute to further extending the duration of the G2/M phase by enlarging the width of the peak in CyclinB1/CDK1 in the absence of its inhibitor WEE1 in *siBmal1* cells. Such a counter-intuitive effect is suggested by numerical simulations of the mathemathical model for coupled clock - cell cycle oscillators, which showed that induction of *Wee1* by CLOCK/BMAL1 can shorten the duration of the cell cycle by reducing the half-width of the peaks in Cyclin B1/CDK1 (Gérard & Goldbeter, 2012).

Understanding how transcription of the Cyclin B1 gene *CcnB1* is regulated during the cell cycle would help us to understand how BMAL1 can modulate cell cycle progression. Promoter analysis of the *CcnB1* gene uncovered four E-box elements (CANNTG), one of which showing consensus for the *Upstream Stimulatory Factor* (USF) and acting as a G2-specific regulator of *Cyclin B1* expression (Cogswell et al., 1995). Since the USF E-box sequence CACGTG matches that of the E-box elements recognized by CLOCK/BMAL1, our results suggest a direct role for BMAL1 in the G2-specific induction of *CyclinB1*. We do not exclude the possibility that BMAL1 may also indirectly influence Cyclin B1 protein levels through (cyclic) expression of other clock genes or clock-controlled genes. For instance, BMAL has been shown to control expression of the tumor suppressor gene p53 (Mullenders et al., 2009; Jiang et al., 2016). The p53 protein, in turn, has been suggested to prevent G2/M transition by attenuating *CcnB1* promoter activity and reducing Cyclin B1 protein levels (Innocente et al., 1999). Adding to the level of complexity of circadian control of G2/M transition, the circadian clock protein PER2 (expression of which is under control of CLOCK/BMAL1) can stabilize the p53 protein and influence its subcellular localization, i.e. cytoplasmic vs nuclear (Gotoh et al., 2016). The latter scenario, however, appears less likely as, in contrast with our experimental data, suppression of BMAL1 should result in enhanced Cyclin B1 levels and accelerated mitotic entry. To discriminate between direct and indirect control of CLOCK and BMAL1 over G2/M transition, it will be of prime importance to generate a NIH3T3^{3C} cell line with (endogenous) fluorescent protein tagged *CcnB1* genes to study the kinetics of Cyclin B1 expression in the presence/absence of proteins like WEE1, p53, and PER2.

The availability of a model for the coupling of the cell cycle to the circadian clock in mammalian cells allows us to probe, by means of computer simulations, the effect of knocking down *Bmal1* or *Clock* on the dynamics of the cell cycle. Previous theoretical investigations of this coupling (Gérard & Goldbeter, 2012) were based on the circadian control of several components of the cell cycle machinery, such as the kinase WEE1, the CDK inhibitor p21, and Cyclin E. Here, the experimental study confirmed that WEE1, a kinase that inhibits CDK1, is under control of the circadian clock via the induction of *Wee1* expression by CLOCK/BMAL1. The experiments uncovered an additional mode of coupling due to the induction of *CcnB1* expression by CLOCK/BMAL1. We therefore incorporated these two modes of coupling into the combined model for the cell cycle and circadian clock in mammalian cells.

The model indicates that the induction of *Ccnb1* and *Wee1* expression by CLOCK/BMAL1

allows the cell cycle to synchronize with to the circadian clock at a period in the order of 18h. Upon suppression of BMAL1 expression by reducing the *Bmal1* mRNA synthesis rate by 70%, the circadian clock stops ticking and the cell cycle recovers its autonomous period of oscillation, close to 21h. The lengthening of the period in our mathematical model is largely due to an increase of a few hours in the duration of the S/G2/M phase, which is in good agreement with the experimental data. The simulations suggest that this increase can be related to an increase in the half-width of the peak in CDK1. The larger duration of the peak in CDK1 is due to the decreased inhibition of the enzymatic activity by WEE1, given that the level of this inhibitory kinase drops when knocking down its inducer BMAL1. In this respect, it is interesting to note that inactivation of BMAL1 in hippocampal neurons both experimentally and in silico causes a cell cycle effect, i.e. delayed cell cycle exit (Bouchard-Cannon et al., 2013).

Disruption of the circadian clock (genetically or environmentally) results in altered cell proliferation, and in some cases cancer predisposition. However, only few studies have been performed to detect the intracellular pathways or the key molecules responsible for the altered proliferation capacity. Our study addressed the role of BMAL1 and CLOCK in the expression of Cyclin B1, one of the key molecules for G2 phase and G2/M transition. The question arises whether the reduced Cyclin B1 protein levels in the absence of CLOCK/BMAL1 are the result of (i) the inactivation of the positive limb of the circadian transcription translation feedback loop, or (ii) a complete/overall loss of the clock. Future experiments with circadian clock deficient *Cry1/Cry2* knockdown NIH3T3^{3C} cells should provide an answer to this question.

Finally, stable gene silencing of Cyclin B1 has been reported to inhibit proliferation, and sensitizes breast cancer cells to taxol treatment (Androic et al., 2008). Downregulation of Cyclin B1 via knock-down of *Bmal1* could be an attractive strategy for anti-proliferative therapy. This might ultimately delay tumor progression. However, the state of circadian clock and cell cycle coupling in cancer cells still remains to be studied.

Acknowledgements

This work was supported by grants from the Netherlands Organization for Scientific Research (ZonMW/EraSysBio+ grant nr. 90.201.127, “Circadian and cell cycle clock systems in cancer: C5Sys”), the Netherlands Genomics Initiative (grant nr. 050-060-510, “Netherlands Toxicogenomics Center”) and an Erasmus University Medical Center Mrace PhD grant (“The relation between the circadian clock, cell cycle, and cancer”) to GTJvdH. Work by AG was supported by FRS-FNRS (CDR grant nr. 26027580, «Auto-organisation in cell signalling»). The research stay of JY at ULB (Brussels) was supported by the Chinese Scholar Council. Her subsequent work in Suzhou receives financial support from the National Science Foundation of China (grant nr. 61271358). We are grateful to the members of the C5Sys project for many useful discussions.

References

Androic I, Krämer A, Yan R, Rödel F, Gätje R, Kaufmann M, Strebhardt K, Yuan J (2008) Targeting cyclin B1 inhibits proliferation and sensitizes breast cancer cells to taxol. *BMC Cancer* 8:391.

Bieler J, Cannavo R, Gustafson K, Gobet C, Gatfield D, Naef F (2014) Robust synchronization of coupled circadian and cell cycle oscillators in single mammalian cells. *Mol Syst Biol* 10:739.

Bjarnason GA, Jordan RCK, Sothern RB (1999). Circadian variation in the expression of cell-cycle proteins in human oral epithelium. *Am J Pathol* 154:613-622.

Bjarnason GA Jordan RCK, Wood PA Li Q, Lincoln DW, Sothern RB, Hrushesky WJM, Ben-David Y (2001) Circadian expression of clock genes in human oral mucosa and skin. *Am J Pathol* 158:1793-1801.

Bouchard-Cannon P, Mendoza-Viveros L, Yuen A, Kærn M, Cheng HY (2013) The circadian molecular clock regulates adult hippocampal neurogenesis by controlling the timing of cell-cycle entry and exit. *Cell Rep* 5:961-973.

Cogswell JP, Godlevski MM, Bonham M, Bisi J, Babiss L (1995) Upstream stimulatory factor regulates expression of the cell cycle-dependent cyclin B1 gene promoter. *Mol Cell Biol* 15:2782-2790.

Coverley D, Laman H, Laskey RA (2002). Distinct roles for cyclins E and A during DNA replication complex assembly and activation. *Nat Cell Biol* 4:523-528.

Erlandsson F, Linnman C, Ekholm S, Bengtsson E, Zetterberg A (2000) A detailed analysis of Cyclin A accumulation at the G1/S border in normal and transformed cells. *Exp Cell Res* 295:86-95.

Feillet C, Krusche P, Tamanini F, Janssens RC, Downey MJ, Martin P, Teboul M, Saito S, Lévi FA, Bretschneider T, van der Horst GTJ, Delaunay F, Rand DA (2014) Phase locking and multiple oscillating attractors for the coupled mammalian clock and cell cycle. *Proc Natl Acad Sci USA* 111:9828-9833.

Fung TK, Poon RYC (2005) A roller coaster ride with the mitotic cyclins. *Sem Cell Dev Biol* 16:335-342.

Gallego M, Virshup DM (2007) Post-translational modifications regulate the ticking of the circadian clock. *Nat Rev Mol Cell Biol* 8:139-148.

Gavet O, Pines J (2010) Progressive activation of CyclinB1-Cdk1 coordinates entry to mitosis. *Dev Cell* 18:533-543.

Gérard C, Goldbeter A (2009) Temporal self-organization of the cyclin/Cdk network driving the mammalian cell cycle. *Proc Natl Acad Sci USA* 106:21643-21648.

Gérard C, Goldbeter A (2012) Entrainment of the mammalian cell cycle by the circadian clock: Modeling two coupled cellular rhythms. *PLoS Comput Biol* 8:e1002516.

Gérard C, Goldbeter A (2014) The balance between cell cycle arrest and cell proliferation: control by the extracellular matrix and by contact inhibition. *Interface Focus* 4:20130075.

Girard F, Strausfeld U, Fernandez A, Lamb NJ (1991) Cyclin A is required for the onset of DNA replication in mammalian fibroblasts. *Cell* 67:1169-1179.

Gotoh T, Kim JK, Liu J, Vila-Caballer M, Stauffer PE, Tyson JJ, Finkielstein CV (2016) Model-driven experimental approach reveals the complex regulatory distribution of p53 by the circadian factor Period 2. *Proc Natl Acad Sci USA* 113:13516-13521.

Gréchez-Cassiau A, Rayet B, Guillaumond F, Teboul M, Delaunay F (2008) The circadian clock component BMAL1 is a critical regulator of p21WAF1/CIP1 expression and hepatocyte proliferation. J Biol Chem 283:4535-4542.

Henley SA, Dick FA (2012) The retinoblastoma family of proteins and their regulatory functions in the mammalian cell division cycle. *Cell Div*. 7:10.

Hunt T, Sassone-Corsi P (2007) Riding tandem: Circadian clocks and the cell cycle. *Cell* 129:461-464.

Innocente SA, Abrahamson JLA, Cogswell JP, Lee JM (1999) p53 regulates a G2 checkpoint through Cyclin B1. *Proc Natl Acad Sci USA* 96:2147-2152.

Jackson PK, Chevalier S, Philippe M, Kirschner MW (1995) Early events in DNA replication require cyclin E and are blocked by p21CIP1. *J Cell Biol* 130:755–769.

Jiang W, Zhao S, Jiang X, Zhang E, Hu G, Hu B, Zheng P, Xiao J, Lu Z, Lu Y, Ni J, Chen C, Wang X, Yang L, Wan R (2016) The circadian clock gene Bmal1 acts as a potential anti-oncogene in pancreatic cancer by activating the p53 tumor suppressor pathway. *Cancer Lett* 371:314-325.

Kalaszczynska I, Geng Y, Iino T, Mizuno S, Choi Y, Kondratiuk I, Silver DP, Wolgemuth DJ, Akashi K, Sicinski P (2009) Cyclin A is redundant in fibroblasts but essential in hematopoietic and embryonic stem cells. *Cell* 138:352-365.

Koff A, Giordano A, Desai D, Yamashita K, Harper JW, Elledge S, Nishimoto T, Morgan DO, Franza SR, Roberts JM (1992) Formation and activation of a cyclin E-CDK2 complex during the G1 phase of the human cell cycle. *Science* 257:1689-1694.

Kowalska E, Ripperger JA, Hoegger DC, Bruegger P, Buch T, Birchler T, Mueller A, Albrecht U, Contaldo C, Brown SA (2013) NONO couples the circadian clock to the cell cycle. *Proc Natl Acad Sci USA* 110:1592-1599.

Leloup JC, Goldbeter A (2003) Toward a detailed computational model for the mammalian circadian clock. *Proc Natl Acad Sci USA* 110:7051-7056.

Leloup JC, Goldbeter A (2004) Modeling the mammalian circadian clock: Sensitivity analysis and multiplicity of oscillatory mechanisms. *J Theor Biol* 230:541-562.

Lindqvist A, Rodriguez-Bravo R, Medema RH (2009) The decision to enter mitosis: feedback and redundancy in the mitotic entry network. *Cell Biol* 185:193-202.

Mohawk JA, Green CB, Takahashi JS (2012) Central and peripheral circadian clocks in mammals. *Annu Rev Neurosci* 35: 445-462.

Masri S, Cervantes M, Sassone-Corsi P (2013) The circadian clock and cell cycle: interconnected biological circuits. *Curr Opin Cell Biol* 25:730-734.

Matsuo T, Yamaguchi S, Mitsui S, Emi A, Shimoda F, Okamura H (2003) Control mechanism of the circadian clock for timing of cell division in vivo. *Science* 302:255-259.

Mueller PR, Coleman TR, Kumagai A, Dunphy WG (1995) Myt1: a membrane-associated inhibitory kinase that phosphorylates Cdc2 on both threonine-14 and tyrosine-15. *Science* 270:86-90.

Mullenders J, Fabius AW, Madiredjo M, Bernards R, Beijersbergen RL (2009) A large scale shRNA barcode screen identifies the circadian clock component ARNTL as putative regulator of the p53 tumor suppressor pathway. PLoS One 4: e4798.

Nagoshi E, Saini C, Bauer C, Laroche T, Naef F, Schibler U (2004) Circadian gene expression in individual fibroblasts: cell-autonomous and self-sustained oscillators pass time to daughter cells. Cell 119:693-705.

Pagano M, Pepperkok R, Verde F, Ansorge W, Draetta G (1992) Cyclin A is required at two points in the human cell cycle. *EMBO J* 11: 961-971.

Paijmans J, Bosman M, Ten Wolde PR, Lubensky DK (2016) Discrete gene replication events drive coupling between the cell cycle and circadian clocks. *Proc Natl Acad Sci* USA 113:4063-4068.

Parker LL, Piwnica-Worms H (1992) Inactivation of the p34cdc2-cyclin B complex by the human WEE1 tyrosine kinase. *Science* 257:1955-1957.

Stojkovic K, Wing SS, Cermakian N (2014) A central role for ubiquitination within a circadian clock protein modification code. *Front Mol Neurosci* 10.3389.

Takahashi JS, Hong HK, Ko CH, McDearmon EL (2008) The genetics of mammalian circadian order and disorder: implications for physiology and disease. *Nat Rev Genet* 9:764-775.

Traynard P, Feillet C, Soliman S, Delaunay F, Fages F (2016) Model-based investigation of the circadian clock and cell cycle coupling in mouse embryonic fibroblasts: Prediction of RevErb-α up-regulation during mitosis. *Biosystems* 149:59-69.

Tyson J, Novak B (2008) Temporal organization of the cell cycle. *Curr Biol* 18, R759-R768.

Zhao X, Hirota T, Han X, Cho H, Chong LW, Lamia K, Liu S, Atkins AR, Banayo E, Liddle C, Yu RT, Yates JR 3rd, Kay SA, Downes M, Evans RM (2016) Circadian amplitude regulation via FBXW7-targeted REV-ERBα degradation. *Cell* 165:1644-1657.

Supplementary Methods and Information

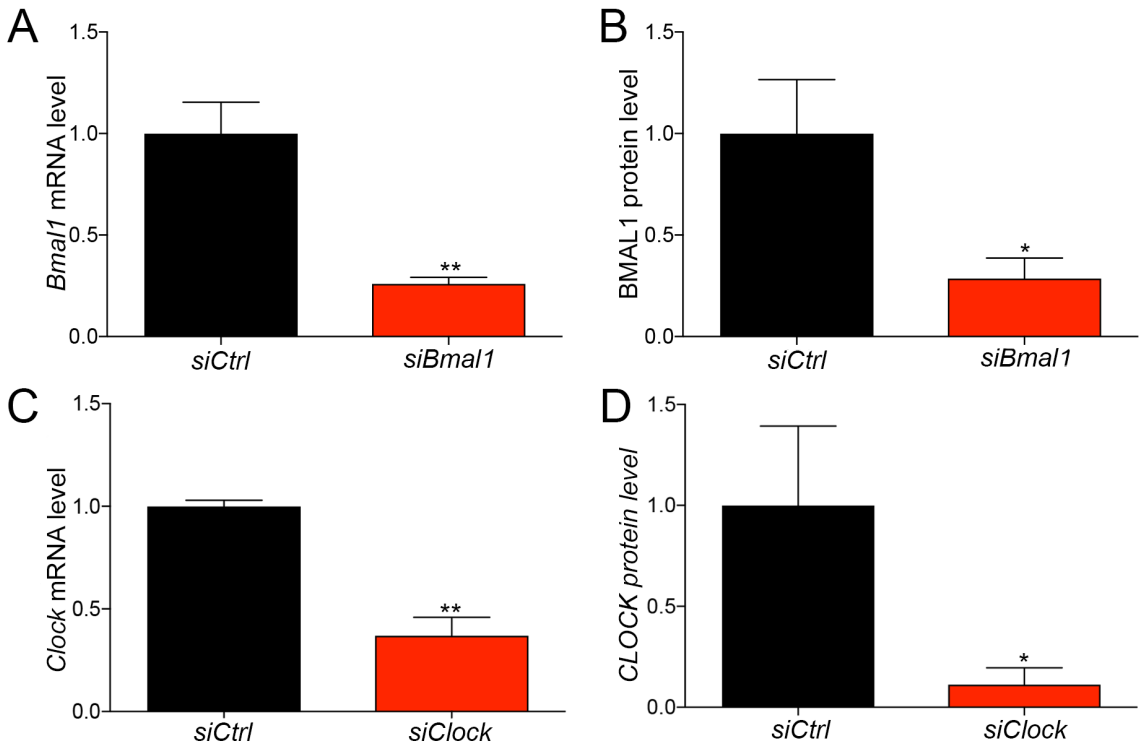

Figure S1. *Bmal1* and *Clock* mRNA and BMAL1 and CLOCK protein levels in *siBmal1* and *siClock* cells. NIH3T3[3C] cells were transiently transfected with Silencer® Select Pre-designed control, *Bmal1* or *Clock* siRNA to generate *siCtrl, siBmal1* cells and *siClock* cells, respectively. (A) Quantitative RT-PCR analysis of *Bmal1* mRNA level in proliferating *siCtrl* and *siBmal1* cells 72 hours after transient siRNA transfection (n=3). mRNA levels were normalized to that of the *B2M* housekeeping gene and expressed relative to the mRNA level in *siCtrl* cells, which was set as 1. Error bars indicate SE. ** $p<0.01$. (B) Western blot analysis of BMAL1 protein levels in *siCtrl* and *siBmal1* cell lysates 72 hours after transient siRNA transfection (n=3). Protein levels were normalized to β-actin protein levels. Error bars indicate SE.* $p=0.02$. (C) Quantitative RT-PCR analysis of *Clock* mRNA level in proliferating *siCtrl* and *siClock* cells 72 hours after transient siRNA transfection (n=3). mRNA levels were normalized to that of the *B2M* housekeeping gene and expressed relative to the mRNA level in *siCtrl* cells, which was set as 1. Error bars indicate SE. ** $p<0.01$. (D) Western blot analysis of CLOCK protein levels in *siCtrl* and *siClock* cell lysates 72 hours after transient siRNA transfection (n=3). Protein levels were normalized to β-actin protein levels. Error bars indicate SE. * $p=0.03$.

Detailed description of the mathematical modeling of the cicadian clock-cell cycle connection

To study the interaction between the circadian clock and the cell cycle we used two computational models previously proposed for the mammalian circadian clock and for the mammalian cell cycle, respectively. The model for the mammalian circadian clock incorporates the positive and negative regulations involving the PER, CRY, CLOCK, BMAL1 and REV-ERBα proteins (Leloup & Goldbeter, 2003, 2004). For simplicity, the PER1 and PER2 proteins, on one hand, and the CRY1 and CRY2 proteins on the other hand, are considered as a single entity referred to as PER and CRY, respectively; moreover, the CLOCK protein is assumed to be expressed constitutively and to instantaneously form a complex with BMAL1. This model accounts for the occurrence of circadian oscillations of the above-mentioned proteins and their mRNAs in a variety of experimental conditions (Leloup & Goldbeter, 2003, 2004).

The model for the mammalian cell cycle is based on the regulatory properties of the CDK network that drives the transitions between the successive phases of the cell cycle (Gérard & Goldbeter, 2009, 2014). The model contains four CDK modules, each of which controls transition to a particular cell cycle phase. Thus, Cyclin D/CDK4-6 and Cyclin E/CDK2 promote progression in G1 and elicit the G1/S transition; the activation of Cyclin A/CDK2 ensures progression in S and G2, while the peak of Cyclin B/CDK1 activity brings about progression into mitosis. Exit from the quiescent state is triggered above a critical level of growth factor by the synthesis of Cyclin D, which allows cells to enter the G1 phase. Synthesis of the various cyclins is regulated through the balance between the antagonistic effects exerted by the transcription factor E2F and the tumor suppressor pRB, which respectively promote and inhibit cell cycle progression. Additional regulations in this model for the CDK network bear on the control exerted by the proteins SKP2, CDH1, or CDC20 on the degradation of cyclins E, A, and B at the G1/S or G2/M transitions, respectively. Moreover, the activity of each cyclin/CDK complex can itself be regulated through CDK phosphorylation-dephosphorylation. At suprathreshold levels of growth factor sustained oscillations spontaneously occur in the CDK network, which may be associated with cellular proliferation since they correspond to the repetitive, sequential activation of the various cyclin-CDK complexes responsible for the ordered progression along the successive phases of the cell cycle (Gérard & Goldbeter, 2009, 2014).

The circadian clock model is governed by 19 kinetic equations (Leloup & Goldbeter, 2003) while the model for the mammalian cell cycle is described by 39 differential equations (Gérard & Goldbeter, 2012). In a previous study the cell cycle was coupled to the circadian clock via the circadian control of WEE1, p21 or Cyclin E; any one of these three modes of coupling can lead to entrainment of the cell cycle by the circadian clock over a range of cell cycle durations prior to coupling (see Gérard & Goldbeter, 2012 for a computational study of circadian entrainment of the cell cycle resulting from these various modes of coupling, and for a list of kinetic equations for the coupled cell cycle-circadian clock system). Here we focus on the case where the cell cycle is coupled to the circadian control via the induction of

Wee1 gene expression by BMAL1, and also introduce coupling via the induction of *Cyclin B1* gene expression by BMAL1, as suggested by the experiments reported in the present study.

To describe the coupling of the cell cycle to the circadian clock via the kinase WEE1 we incorporate in the CDK network model an additional kinetic equation for the mRNA of the *Wee1* gene, which includes the induction of *Wee1* expression by CLOCK/BMAL1. The equations (1) and (2) describing the coupling of the cell cycle to the circadian clock through activation of the transcription of the *Wee1* gene by CLOCK/BMAL1 are:

$$\frac{dMw}{dt} = \left(v_{swee1} + v_{sw} \cdot \frac{Bn^{nmw}}{K_{aw}{}^{nmw} + Bn^{nmw}} - V_{dmw} \cdot \frac{Mw}{K_{dmw} + Mw}\right) \cdot eps \tag{1}$$

$$\frac{dWee1}{dt} = (k_{sw} \cdot Mw - V_{m7b} \cdot (Mb + i_b) \cdot \frac{Wee1}{K_{7b} + Wee1} + V_{m8b} \cdot \frac{Wee1p}{K_{8b} + Wee1p} - k_{dwee1} \cdot Wee1) \cdot eps \tag{2}$$

These equations replace equation [38] in our previous model (Gérard & Goldbeter; 2012). Here, equation (1) describes the time evolution of the *Wee1* mRNA positively regulated by the circadian clock complex, CLOCK/BMAL1 (*Bn*), with an activation constant K_{aw}, while equation (2) shows the time evolution of the kinase WEE1. The synthesis of this protein kinase combines two terms: the basal rate of WEE1 synthesis (ν_{swee1}) is independent from the circadian clock, while the second term, (K_{sw}. *Mw*), reflects WEE1 synthesis at a rate proportional to the *Wee1* mRNA controlled by CLOCK/BMAL1 in a circadian manner. The total amount of *Wee1* mRNA can therefore be viewed as the sum of two terms, (ν_{swee1}/K_{sw}) + *Mw* which are respectively independent from, and dependent on the circadian clock. The coupling strength is expressed by parameter ν_{sw}, which measures the magnitude of the *Wee1* mRNA synthesized under control by the circadian clock. An alternative measure of coupling strength is provided by the parameter K_{aw}, which characterizes the activation of Wee1 expression by CLOCK/BMAL1; the strength of the coupling to the circadian clock increases K_{aw} as progressively decreases.

A similar approach was used to describe the coupling of the cell cycle to the circadian clock via Cyclin B1. Thus, we incorporated in the model for the CDK network an additional kinetic equation for the *Cyclin B1* (*CcnB1*) mRNA, which includes the induction of *Cyclin B1* expression by CLOCK/BMAL1. The equations (3)and (4) describing the coupling of the cell cycle to the circadian clock through the activation of the transcription of the *Cyclin B1* gene by CLOCK/BMAL1 are:

$$\frac{dMcb}{dt} = \left(v_{cb} + v_{scb} \cdot \frac{Bn^{ncb}}{K_{acb}{}^{ncb} + Bn^{ncb}} - V_{dmcb} \cdot \frac{Mcb}{K_{dmcb} + Mcb}\right).eps \tag{3}$$

$$\frac{dCb}{dt} = \left(k_{cb} \cdot Mcb - k_{com4} \cdot Cb \cdot (Cdk1_{tot} - (Mbi + Mb + Mbp27)) + k_{decom4} \cdot Mbi - V_{db} \cdot \frac{Cb}{K_{db} + Cb} \cdot \left(\frac{Cdc20a}{K_{dbcdc20} + Cdc20a} + \frac{Cdh1a}{K_{dbcdh1} + Cdh1a}\right) - k_{ddb} \cdot Cb\right) \cdot eps \tag{4}$$

Equations (3) and (4) replace equation [30] in (Gérard & Goldbeter, 2009).

The synthesis of the *Cyclin B* mRNA, *Mcb*, is described by two terms: the first term is the basal synthesis rate (v_{cb}), which is independent of CLOCK/BMAL1, and the second term ($v_{scb} \cdot \frac{Bn^{ncb}}{K_{acb}{}^{ncb} + Bn^{ncb}}$) reflects the induction by CLOCK/BMAL1. The parameter (v_{scb}) represents the coupling strength, which measures the magnitude of the *Cyclin B* mRNA synthesized under the control by the circadian clock.

To model the impact of knockdown of *Bmal1* gene expression, we reduce the rate of *Bmal1* mRNA synthesis, v_{sB} in the model for the circadian clock. In this model, we consider that the level of *Clock* gene expression is constant and that BMAL1 instantaneously forms a complex with CLOCK. Parameter values used for numerical simulations in Figs 4 and 5 are listed in SI Appendix Table S1. The autonomous period of the cell cycle is 21.1 h, which value is obtained by setting the scaling parameter *eps* = 20.45. The period of the circadian clock is 18 h which is obtained by setting the scaling parameter *delta* = 1.336. Knocking down BMAL1 is achieved in the model by reducing by 70% the rate of *Bmal1* mRNA synthesis, v_{sB}, from 1.55 nM/h in (A) and (C) to 0.465 nM/h in (B) and (D).

The initial values for the 19 concentration variables in the circadian clock model are all equal to 0.1 nM. The initial values for the 41 concentration variables in the cell cycle part of the model are (in μM): AP1=0.01; pRB=1; pRBc1=0.25; pRBp=0.1; pRBc2=0.01; pRBpp=0.01; E2F=0.1; E2Fp=0.05; Cd=0.01; Mdi=0.01; Md=0.01; Mdp27=0.01; Ce=0.01; Mei=0.01; Me=0.01; Skp2=0.01; Mep27=0.01; Pei=0.01; Pe=0.01; Ca=0.01; Mai=0.01; Ma=0.01; Map27=0.01; p27=0.25; p27p=0.01; Cdh1i=0.01; Cdh1a=0.01; Pai=0.01; Pa=0.01; Mcb=0.01; Cb=0.01; Mbi=0.01; Mb=0.01; Mbp27=0.01; Cdc20i=0.01; Cdc20a=0.01; Pbi=0.01; Pb=0.01; Mw=0.01; WEE1=0.1; WEE1p=0.01.

References

Gérard C, Goldbeter A (2009) Temporal self-organization of the cyclin/Cdk network driving the mammalian cell cycle. *Proc Natl Acad Sci USA* 106:21643-21648.

Gérard C, Goldbeter A (2012) Entrainment of the mammalian cell cycle by the circadian clock: Modeling two coupled cellular rhythms. *PLoS Comput Biol* 8:e1002516.

Gérard C, Goldbeter A (2014) The balance between cell cycle arrest and cell proliferation: control by the extracellular matrix and by contact inhibition. *Interface Focus* 4:20130075.

Leloup JC, Goldbeter A (2003) Toward a detailed computational model for the mammalian circadian clock. *Proc Natl Acad Sci USA* 110:7051-7056.

Leloup JC, Goldbeter A (2004) Modeling the mammalian circadian clock: Sensitivity analysis and multiplicity of oscillatory mechanisms. *J Theor Biol* 230:541-562.

Supplementary tables

Table S1: Parameters of the model

Parameter values used for the numerical simulations as presented in Figures 4 and 5. Indicated are the parameter values for the circadian clock, the cell cycle, and the coupling of the circadian clock and cell cycle through Wee1 (Gérard and Goldbeter, 2009, 2012). The last section of the table lists the parameter values used to extend the aforementioned coupling model to circadian control of Cyclin B1 (see equations 3 and 4 in the detailed description of the mathematical modeling of the circadian clock - cell cycle connection).

Symbol	Definition	Value in model
Circadian clock Parameters are (with some modifications) based on those provided in Supporting Figure 8 in Leloup and Goldbeter (2003; see http://www.pnas.org/content/100/12/7051/suppl/DC1) and on Table 1 in Leloup and Goldbeter (2004).		
delta	Scaling factor used to modify the time scale of circadian clock	1.336
k_1	Rate constant for entry of the PER/CRY complex into the nucleus	0.8 h^{-1}
k_2	Rate constant for exit of the PER/CRY complex from the nucleus	0.4 h^{-1}
k_3	Rate constant for the formation of the PER/CRY complex	0.8 nM^{-1} h^{-1}
k_4	Rate constant for dissociation of the PER/CRY complex	0.4 h^{-1}
k_5	Rate constant for entry of the BMAL1 protein into the nucleus	0.8 h^{-1}
k_6	Rate constant for exit of the BMAL1 protein from the nucleus	0.4 h^{-1}
k_7	Rate constant for the formation of the inactive PER/CRY/CLOCK/BMAL1 complex	1 nM^{-1} h^{-1}
k_8	Rate constant for the dissociation of the PER/CRY/CLOCK/BMAL1 complex	0.2 h^{-1}
k_9	Rate constant for entry of the REV-ERBα protein into the nucleus	0.8 h^{-1}
k_{10}	Rate constant for exit of the REV-ERBα protein from the nucleus	0.4 h^{-1}
K_{AP}	Constant for activation by CLOCK-BMAL1 (Bn) of Per mRNA synthesis	0.6 nM
K_{AC}	Constant for activation by CLOCK-BMAL1 (Bn) of Cry mRNA synthesis	0.6 nM
K_{AR}	Constant for activation by CLOCK-BMAL1 (Bn) of Rev-erbα mRNA synthesis	0.6 nM
K_{IB}	Constant of inhibition by Rev-ERBα protein of Bmal1 mRNA synthesis	1 nM
k_{dmb}	Nonspecific degradation rate constant for Bmal1 mRNA	0.02 h^{-1}
k_{dmc}	Nonspecific degradation rate constant for Cry mRNA	0.02 h^{-1}
k_{dmp}	Nonspecific degradation rate constant for Per mRNA	0.02 h^{-1}
k_{dmr}	Nonspecific degradation rate constant for Rev-erbα mRNA	0.02 h^{-1}
k_{dn}	Nonspecific degradation rate constant for other proteins	0.02 h^{-1}
k_{dnc}	Nonspecific degradation rate constant for cytosolic non-phosphorylated CRY	0.02 h^{-1}
K_d	Michaelis constant for protein degradation	0.3 nM
K_{dp}	Michaelis constant for protein dephosphorylation	0.1 nM

K_p	Michaelis constant for protein phosphorylation	1.006 nM
K_{mB}	Michaelis constant for degradation of *Bmal1* mRNA	0.4 nM
K_{mC}	Michaelis constant for degradation of *Cry* mRNA	0.4 nM
K_{mP}	Michaelis constant for degradation of *Per* mRNA	0.3 nM
K_{mR}	Michaelis constant for degradation of *Rev-erbα* mRNA	0.4 nM
k_{sB}	Rate constant for synthesis of BMAL1 protein	0.32 h^{-1}
k_{sC}	Rate constant for synthesis of CRY protein	3.2 h^{-1}
k_{sP}	Rate constant for synthesis of PER protein	1.2 h^{-1}
k_{sR}	Rate constant for synthesis of REV-ERBα protein	1.7 h^{-1}
n	Degree of cooperativity of activation of *Per* and *Cry* expression by BMAL1	2
m	Degree of cooperativity of repression of *Bmal1* expression by REV-ERBα	2
h	Degree of cooperativity of activation of *Rev-erbα* expression by BMAL1	2
V_{1B}	Maximum rate of cytosolic BMAL1 phosphorylation	0.07 nM h^{-1}
V_{1C}	Maximum rate of cytosolic CRY phosphorylation	1.2 nM h^{-1}
V_{1P}	Maximum rate of cytosolic PER phosphorylation	9.6 nM h^{-1}
V_{1PC}	Maximum rate of phosphorylation of cytosolic PER-CRY complex	2.4 nM h^{-1}
V_{2B}	Maximum rate of cytosolic BMAL1 dephosphorylation	2 nM h^{-1}
V_{2C}	Maximum rate of cytosolic CRY dephosphorylation	0.2 nM h^{-1}
V_{2P}	Maximum rate of cytosolic PER dephosphorylation	0.6 nM h^{-1}
V_{2PC}	Maximum rate of cytosolic PER–CRY complex dephosphorylation	0.2 nM h^{-1}
V_{3B}	Maximum rate of nuclear BMAL1 phosphorylation	0.07 nM h^{-1}
V_{3PC}	Maximum rate of phosphorylation of nuclear PER/CRY complex	2.4 nM h^{-1}
V_{4B}	Maximum rate of nuclear BMAL1 dephosphorylation	4 nM h^{-1}
V_{4PC}	Maximum rate of dephosphorylation of nuclear PER/CRY complex	0.2 nM h^{-1}
V_{phos}	Phosphorylation rate	0.4 nM h^{-1}
v_{dBC}	Maximum rate of degradation of cytosolic phosphorylated BMAL1	3 nM h^{-1}
v_{dBN}	Maximum rate of degradation of nuclear phosphorylated BMAL1	3 nM h^{-1}
v_{dCC}	Maximum rate of degradation of cytosolic phosphorylated CRY	1.4 nM h^{-1}
v_{dIN}	Maximum rate of degradation of nuclear PER/CRY/CLOCK/BMAL1 complex	1.6 nM h^{-1}
v_{dPC}	Maximum rate of degradation of cytosolic phosphorylated PER	3.4 nM h^{-1}
v_{dPCC}	Maximum rate of degradation of cytosolic phosphorylated PER/CRY complex	1.4 nM h^{-1}
v_{dPCN}	Maximum rate of degradation of nuclear phosphorylated PER/CRY complex	1.4 nM h^{-1}
v_{dRC}	Maximum rate of degradation of cytosolic REV-ERBα	4.4 nM h^{-1}
v_{dRN}	Maximum rate of degradation of nuclear REV-ERBα	0.8 nM h^{-1}
v_{mB}	Maximum rate of *Bmal1* mRNA degradation	1.3 nM h^{-1}
v_{mC}	Maximum rate of *Cry* mRNA degradation	2.0 nM h^{-1}
v_{mR}	Maximum rate of *Rev-erbα* mRNA degradation	1.6 nM h^{-1}
v_{mP}	Maximum rate of *Per* mRNA degradation	2.2 nM h^{-1}

v_{sB}	Maximum rate of *Bmal1* mRNA synthesis	1.55 nM h^{-1}
v_{sC}	Maximum rate of *Cry* mRNA synthesis	2.2 nM h^{-1}
v_{sP}	Maximum rate of *Per* mRNA synthesis	2.4 nM h^{-1}
v_{sR}	Maximum rate of *Rev-erbα* mRNA synthesis	1.6 nM h^{-1}
Cell cycle Parameters are (with some modifications) based on those provided in Supporting Table S2 in Gérard and Goldbeter (2009; see http://www.pnas.org/content/106/51/21643/suppl/DCSupplemental).		
GF	Growth factor	1
K_{agf}	Michaelis constant for synthesis of AP1 induced by growth factor	0.1 μM
k_{dap1}	Apparent first-order rate constant for AP1 transcription factor degradation	0.15 h^{-1}
eps	Scaling factor used to modify the time scale of cell cycle	20.45
v_{sap1}	Rate of synthesis of the transcription factor AP1 depending on growth factor GF	1 μM h^{-1}
k_{de2f}	Apparent first-order rate constant for non-specific E2F degradation	0.002 h^{-1}
k_{de2fp}	Apparent first-order rate constant for E2Fp degradation	1.1 h^{-1}
k_{dprb}	Apparent first-order rate constant for pRB degradation	0.01 h^{-1}
k_{dprbp}	Apparent first-order rate constant for pRBp degradation	0.06 h^{-1}
k_{dprbpp}	Apparent first-order rate constant for pRBpp degradation	0.04 h^{-1}
k_{pc1}	Bimolecular rate constant for binding of pRB to E2F	0.05 μM^{-1} h^{-1}
k_{pc2}	Rate constant for dissociation of complex between pRB and E2F	0.5 h^{-1}
k_{pc3}	Bimolecular rate constant for binding of pRBp to E2F	0.025 μM^{-1} h^{-1}
k_{pc4}	Rate constant for dissociation of complex between pRBp and E2F	0.5 h^{-1}
K_1	Michaelis constant for pRB phosphorylation	0.1 μM
K_2	Michaelis constant for pRBp dephosphorylation	0.1 μM
K_3	Michaelis constant for pRBp phosphorylation	0.1 μM
K_4	Michaelis constant for pRBpp dephosphorylation	0.1 μM
V_1	Rate constant for phosphorylation of pRB	2.2 h^{-1}
V_2	Maximum rate of dephosphorylation of pRBp	2 μM h^{-1}
V_3	Rate constant for phosphorylation of pRBp	1 h^{-1}
V_4	Maximum rate of dephosphorylation of pRBpp	2 μM h^{-1}
K_{1e2f}	Michaelis constant for E2F phosphorylation by Cyclin A/Cdk2	5 μM
K_{2e2f}	Michaelis constant for E2F dephosphorylation	5 μM
V_{1e2f}	Rate constant for phosphorylation of E2F by Cyclin A/Cdk2	4 h^{-1}
V_{2e2f}	Maximum rate of dephosphorylation of E2F	0.75 μM h^{-1}
v_{se2f}	Basal rate of synthesis of E2F	0.15 μM h^{-1}
v_{sprb}	Basal rate of synthesis of pRB	0.8 μM h^{-1}
$Cdk4_{tot}$	Total concentration of Cdk4-6 kinase	1.5 μM
K_{i7}	Constant of inhibition by pRB of Cyclin D synthesis	0.1 μM
K_{i8}	Constant of inhibition by pRBp of Cyclin D synthesis	2 μM

k_{cd1}	Rate constant for Cyclin D synthesis induced by AP1	0.4 h^{-1}
k_{cd2}	Rate constant for Cyclin D synthesis induced by E2F	0.005 h^{-1}
k_{decom1}	Rate constant for dissociation of complex between Cyclin D and Cdk4-6	0.1 h^{-1}
k_{com1}	Bimolecular rate constant for binding of Cyclin D to Cdk4-6	0.175 μM^{-1} h^{-1}
k_{c1}	Bimolecular rate constant for binding of Cyclin D/Cdk4-6 to p27	0.15 μM^{-1} h^{-1}
k_{c2}	Rate constant for dissociation of complex between Cyclin D/Cdk4-6 and p27	0.05 h^{-1}
k_{ddd}	Apparent first-order rate constant for non-specific Cyclin D protein degradation	0.005 h^{-1}
K_{dd}	Michaelis constant for Cyclin D degradation	0.1 μM
K_{1d}	Michaelis constant for Cyclin D/Cdk4-6 (inactive) activation	0.1 μM
K_{2d}	Michaelis constant for Cyclin D/Cdk4-6 (active) inactivation	0.1 μM
V_{dd}	Maximum rate of degradation of Cyclin D	5 $\mu M \cdot h^{-1}$
V_{m1d}	Maximum rate of activation of Cyclin D/Cdk4-6 (inactive)	1 $\mu M \cdot h^{-1}$
V_{m2d}	Maximum rate of inactivation of Cyclin D/Cdk4-6 (active)	0.2 $\mu M \cdot h^{-1}$
a_e	Factor measuring the contribution of Polo-like kinase 3 (Plk3) to phosphorylation and activation of Cdc25 phosphatase (Pei)	0.25 μM
$Cdk2_{tot}$	Total concentration of Cdk2 kinase	2 μM
i_{b1}	Factor measuring the contribution of kinase Myt1 to phosphorylation and inhibition of Cyclin E/Cdk2	0.5 μM
K_{i9}	Constant of inhibition by pRB of Cyclin E synthesis	0.1 μM
K_{i10}	Constant of inhibition by pRBp of Cyclin E synthesis	2 μM
k_{ce}	Rate constant for Cyclin E synthesis induced by E2F	0.29 h^{-1}
k_{c3}	Bimolecular rate constant for binding of Cyclin E/Cdk2 to p27	0.2 μM^{-1} h^{-1}
k_{c4}	Rate constant for dissociation of complex between Cyclin E/Cdk2 and p27	0.1 h^{-1}
k_{decom2}	Rate constant for dissociation of complex between Cyclin E and Cdk2	0.1 h^{-1}
k_{com2}	Bimolecular rate constant for binding of Cyclin E to Cdk2	0.2 μM^{-1} h^{-1}
k_{dde}	Apparent first-order rate constant for non-specific Cyclin E degradation	0.005 h^{-1}
k_{ddskp2}	Apparent first-order rate constant for non-specific Skp2 degradation	0.005 h^{-1}
k_{dpe}	Apparent first-order rate constant for degradation of active Cdc25 phosphatase (Pe)	0.075 h^{-1}
k_{dpei}	Apparent first-order rate constant for degradation of inactive Cdc25 phosphatase (Pei)	0.15 h^{-1}
K_{de}	Michaelis constant for Cyclin E degradation	0.1 μM
$K_{dceskp2}$	Michaelis constant for activation by Skp2 of Cyclin E degradation	2 μM
K_{dskp2}	Michaelis constant for Skp2 degradation	0.5 μM
K_{cdh1}	Michaelis constant for activation by Cdh1 of Skp2 degradation	0.4 μM
K_{1e}	Michaelis constant for Cyclin E/Cdk2 (inactive) activation through dephosphorylation by phosphatase Cdc25 (Pe)	0.1 μM
K_{2e}	Michaelis constant for Cyclin E/Cdk2 (active) inactivation through phosphorylation by kinases WEE1 and Myt1	0.1 μM
K_{5e}	Michaelis constant for Cdc25 (Pei) activation through phosphorylation by Cyclin E/Cdk2 and Plk3	0.1 μM
K_{6e}	Michaelis constant for Cdc25 (Pe) inactivation	0.1 μM
V_{de}	Maximum rate of Cyclin E degradation	3 μM h^{-1}

V_{dskp2}	Maximum rate of Skp2 degradation	1.1 μM h^{-1}
V_{m1e}	Rate constant for activation of Cyclin E/Cdk2 (inactive) through dephosphorylation by phosphatase Cdc25 (Pe)	2 h^{-1}
V_{m2e}	Rate constant for inactivation of Cyclin E/Cdk2 (active) through phosphorylation by kinases WEE1 and Myt1	1.4 h^{-1}
V_{m5e}	Rate constant for activation of phosphatase Cdc25 through phosphorylation by Cyclin E/Cdk2 and Polo-like kinase 3	5 h^{-1}
V_{6e}	Maximum rate of inactivation of phosphatase Cdc25 through phosphorylation	0.8 μM h^{-1}
v_{spei}	Rate of synthesis of phosphatase Cdc25 acting on Cyclin E/Cdk2	0.13 μM h^{-1}
v_{sskp2}	Maximum rate of synthesis of Skp2	0.15 μM h^{-1}
x_{e1}	Factor measuring basal, Chk1-independent contribution to the rate of inactivation through phosphorylation of phosphatase Cdc25 (Pe)	1
a_a	Factor measuring the contribution of Polo-like kinase 3 (Plk3) to phosphorylation and activation of phosphatase Cdc25 (Pa)	0.2 μM
i_{b2}	Factor measuring the contribution of kinase Myt1 to phosphorylation and inhibition of Cyclin A/Cdk2	0.5 μM
K_{i11}	Constant of inhibition by pRB of Cyclin A synthesis	0.1 μM
K_{i12}	Constant of inhibition by pRBp of Cyclin A synthesis	2 μM
K_{i13}	Constant of inhibition by pRB of p27 synthesis	0.1 μM
K_{i14}	Constant of inhibition by pRBp of p27 synthesis	2 μM
k_{ca}	Rate constant for Cyclin A synthesis induced by E2F	0.0375 h^{-1}
k_{decom3}	Rate constant for dissociation of complex between Cyclin A and Cdk2	0.1 h^{-1}
k_{com3}	Bimolecular rate constant for binding of Cyclin A to Cdk2	0.2 μM^{-1} h^{-1}
k_{c5}	Bimolecular rate constant for binding of active Cyclin A/Cdk2 to p27	0.15 μM^{-1} h^{-1}
k_{c6}	Rate constant for dissociation of complex between Cyclin A/Cdk2 and p27	0.125 h^{-1}
k_{dda}	Apparent first-order rate constant for non-specific Cyclin A degradation	0.005 h^{-1}
k_{ddp27}	Apparent first-order rate constant for non-specific p27 degradation	0.06 h^{-1}
k_{ddp27p}	Apparent first-order rate constant for non-specific p27p degradation	0.01 h^{-1}
k_{dcdh1a}	Apparent first-order rate constant for degradation of active Cdh1	0.1 h^{-1}
k_{dcdh1i}	Apparent first-order rate constant for degradation of inactive Cdh1	0.2 h^{-1}
k_{dpa}	Apparent first-order rate constant for degradation of active phosphatase Cdc25 (Pa)	0.075 h^{-1}
k_{dpai}	Apparent first-order rate constant for degradation of inactive phosphatase Cdc25 (Pai)	0.15 h^{-1}
K_{da}	Michaelis constant for Cyclin A degradation	1.1 μM
K_{dp27p}	Michaelis constant for p27p degradation	0.1 μM
$K_{dp27skp2}$	Michaelis constant for activation by Skp2 of p27p degradation	0.1 μM
K_{acdc20}	Michaelis constant for activation by Cdc20 of Cyclin A degradation	2 μM
K_{1a}	Michaelis constant for Cyclin A/Cdk2 (inactive) activation through dephosphorylation by Cdc25 (Pa)	0.1 μM
K_{2a}	Michaelis constant for Cyclin A/Cdk2 (active) inactivation through phosphorylation by kinases WEE1 and Myt1	0.1 μM
K_{1cdh1}	Michaelis constant for Cdh1 (inactive) activation through dephosphorylation	0.01 μM
K_{2cdh1}	Michaelis constant for Cdh1 (active) inactivation through phosphorylation by Cyclin A/Cdk2 and Cyclin B/Cdk1	0.01 μM
K_{5a}	Michaelis constant for Cdc25 (Pai) activation through phosphorylation by Cyclin A/Cdk2 and kinase Plk3	0.1 μM

K_{6a}	Michaelis constant for Cdc25 (Pa) inactivation	0.1 μM
K_{1p27}	Michaelis constant for p27 phosphorylation by Cyclin E/Cdk2	0.5 μM
K_{2p27}	Michaelis constant of p27p dephosphorylation	0.5 μM
V_{dp27p}	Maximum rate of p27p degradation	5 μM h^{-1}
V_{da}	Maximum rate of Cyclin A degradation	2.5 μM h^{-1}
V_{m1a}	Rate constant for activation of Cyclin A/Cdk2 (inactive) through dephosphorylation by phosphatase Cdc25 (Pa)	2 h^{-1}
V_{m2a}	Rate constant for inactivation of Cyclin A/Cdk2 (active) through phosphorylation by kinases WEE1 and Myt1	1.85 h^{-1}
V_{m5a}	Rate constant for activation of phosphatase Cdc25 (Pai) through phosphorylation by Cyclin A/Cdk2 and kinase Plk3	4 h^{-1}
V_{6a}	Maximum rate of phosphatase Cdc25 (Pa) inactivation	1 μM h^{-1}
v_{scdh1a}	Rate of synthesis of active Cdh1	0.11 μM h^{-1}
v_{spai}	Rate of synthesis of phosphatase Cdc25 (Pai) acting on Cyclin A/Cdk2	0.105 μM h^{-1}
v_{s1p27}	Basal rate of synthesis of p27	0.8 μM h^{-1}
v_{s2p27}	Rate constant for synthesis of p27 induced by E2F	0.1 h^{-1}
V_{1cdh1}	Maximum activation rate of Cdh1 (inactive) through dephosphorylation	1.25 μM h^{-1}
V_{2cdh1}	Rate constant for inactivation of Cdh1 (active) through phosphorylation by Cyclin A/Cdk2 and Cyclin B/Cdk1	8 h^{-1}
V_{1p27}	Rate constant for inactivation of p27 through phosphorylation by Cyclin E/Cdk2	100 h^{-1}
V_{2p27}	Maximum rate of activation of p27p through dephosphorylation	0.1 μM h^{-1}
x_{a1}	Factor measuring basal, Chk1-independent contribution to the inactivation rate of phosphatase Cdc25 (Pa)	1
a_b	Factor measuring the contribution of Polo-like kinase 1 (Plk1) to phosphorylation and activation of Cdc25 phosphatase (Pbi)	0.11 μM
$Cdk1_{tot}$	Total concentration of the Cdk1 kinase	0.5 μM
i_b	Factor measuring the contribution of kinase(s) other than Cdk1 to phosphorylation and inactivation of kinase WEE1	0.75 μM
i_{b3}	Factor measuring the contribution of kinase Myt1 to phosphorylation and inhibition of Cyclin B/Cdk1	0.5 μM
k_{c7}	Bimolecular rate constant for binding of Cyclin B/Cdk1 (active) to p27	0.12 μM^{-1} h^{-1}
k_{c8}	Rate constant for dissociation of complex between Cyclin B/Cdk1 and p27	0.2 h^{-1}
k_{decom4}	Rate constant for dissociation of complex between Cyclin B and Cdk1	0.1 h^{-1}
k_{com4}	Bimolecular rate constant for binding of Cyclin B to Cdk1	0.25 μM^{-1} h^{-1}
$k_{dcdc20a}$	Apparent first-order rate constant for degradation of active Cdc20	0.05 h^{-1}
$k_{dcdc20i}$	Apparent first-order rate constant for degradation of inactive Cdc20	0.14 h^{-1}
k_{ddb}	Apparent first-order rate constant for non-specific Cyclin B degradation	0.005 h^{-1}
k_{dpb}	Apparent first-order rate constant for degradation of active phosphatase Cdc25 (Pb)	0.1 h^{-1}
k_{dpbi}	Apparent first-order rate constant for degradation of inactive phosphatase Cdc25 (Pbi)	0.2 h^{-1}
k_{dwee1}	Apparent first-order rate constant for degradation of active kinase WEE1	0.1 h^{-1}
k_{dwee1p}	Apparent first-order rate constant for degradation of inactive kinase WEE1	0.2 h^{-1}
K_{db}	Michaelis constant for Cyclin B degradation	0.005 μM
$K_{dbcdc20}$	Michaelis constant for activation by Cdc20 (active) of Cyclin B degradation	0.2 μM

K_{dbcdh1}	Michaelis constant for activation by Cdh1 (active) of Cyclin B degradation	0.1 μM
K_{1b}	Michaelis constant for Cyclin B/Cdk1 (inactive) activation through dephosphorylation by phosphatase Cdc25 (Pb)	0.1 μM
K_{2b}	Michaelis constant for Cyclin B/Cdk1 (active) inactivation through phosphorylation by kinases WEE1 and Myt1	0.1 μM
K_{3b}	Michaelis constant for Cdc20 (inactive) activation through phosphorylation by Cyclin B/Cdk1	0.1 μM
K_{4b}	Michaelis constant for Cdc20 (active) inactivation through dephosphorylation	0.1 μM
K_{5b}	Michaelis constant for Cdc25 (Pbi) activation through phosphorylation by Cyclin B/Cdk1 and kinase Plk1	0.1 μM
K_{6b}	Michaelis constant for Cdc25 (Pb) inactivation	0.1 μM
K_{7b}	Michaelis constant for Wee1 inactivation through phosphorylation by Cyclin B/Cdk1 and kinase Plk1	0.1 μM
K_{8b}	Michaelis constant for Wee1 activation through dephosphorylation	0.1 μM
V_{db}	Maximum rate of Cyclin B degradation	0.06 μM h^{-1}
V_{m1b}	Rate constant for activation of Cyclin B/Cdk1 (inactive) through dephosphorylation by phosphatase Cdc25 (Pb)	3.9 h^{-1}
V_{m2b}	Rate constant for inactivation of Cyclin B/Cdk1 (active) through phosphorylation by kinases WEE1 and Myt1	2.1 h^{-1}
$v_{scdc20i}$	Rate of synthesis of Cdc20 (inactive)	0.1μM h^{-1}
V_{m3b}	Rate constant for activation of Cdc20 (inactive) through phosphorylation by Cyclin B/Cdk1	8 h^{-1}
V_{m4b}	Maximum rate of Cdc20 (active) inactivation through dephosphorylation	0.7μM h^{-1}
V_{m5b}	Rate constant for activation of phosphatase Cdc25 (Pbi) through phosphorylation by Cyclin B/Cdk1 and kinase Plk1	5 h^{-1}
V_{6b}	Maximum inactivation rate of phosphatase Cdc25 (Pb)	1 μM h^{-1}
V_{m7b}	Rate constant for inactivation of kinase WEE1 through phosphorylation by Cyclin B/Cdk1 and kinase Plk1	1.2 h^{-1}
V_{m8b}	Maximum rate of kinase Wee1 activation through dephosphorylation	1 μM h^{-1}
v_{spbi}	Rate of synthesis of phosphatase Cdc25 (Pbi) acting on Cyclin B/Cdk1	0.12 μM h^{-1}
x_{b1}	Factor measuring basal, Chk1-independent contribution to the rate of phosphatase Cdc25 (Pb) inactivation	1

Coupling the mammalian cell cycle to the circadian clock through Wee1

Parameters are (with some modifications) based on those given in Supporting Information to Gérard and Goldbeter (2009; see http://www.pnas.org/content/106/51/21643/suppl/DCSupplemental) and in Figure 2 in Gérard and Goldbeter (2012).

K_{dmw}	Michaelis constant for the degradation of *Wee1* mRNA (Mw)	0.5 μM
K_{aw}	Threshold constant for activation by CLOCK/BMAL1 (Bn) of *Wee1* mRNA (Mw) synthesis	4 nM
nmw	Degree of cooperativity for the activation by CLOCK/BMAL1 (Bn) of *Wee1* mRNA (Mw) synthesis	4
V_{dmw}	Maximum rate of degradation of *Wee1* mRNA (Mw)	2.445×10^{-2} μM h^{-1}
v_{swee1}	Rate of synthesis of *Wee1* mRNA (Mw) independent from coupling to the circadian clock	5.721×10^{-4} μM h^{-1}
v_{sw}	Rate of synthesis of Mw depending on CLOCK/BMAL1 (Bn)	6.846×10^{-3} μM h^{-1}
k_{sw}	Rate constant for synthesis of WEE1 protein	5 h^{-1}

Coupling the mammalian cell cycle to the circadian clock through Cyclin B This study		
K_{dmcb}	Michaelis constant for the degradation of *Cyclin B* mRNA (Mcb)	0.5 μM
K_{acb}	Threshold constant for activation by CLOCK/BMAL1 (Bn) of *Cyclin B* mRNA (Mcb) synthesis	4 nM
ncb	Degree of cooperativity for the activation by CLOCK/BMAL1 (Bn) of *Cyclin B* mRNA (Mcb) synthesis	4
V_{dmcb}	Maximum rate of degradation of *cyclin B* mRNA (Mcb)	2.445×10^{2}μMh^{-1}
v_{cb}	Rate of synthesis of *cyclin B* mRNA independent from coupling to the circadian clock	5.263×10^{4}μMh^{1}
v_{scb}	Rate of synthesis of *cyclin B* mRNA depending on CLOCK/BMAL1 (Bn)	9.78×10^{5}μMh^{1}
k_{cb}	Rate of synthesis of Cyclin B protein	5 h^{-1}

References

Gérard C, Goldbeter A (2009) Temporal self-organization of the cyclin/Cdk network driving the mammalian cell cycle. Proc Natl Acad Sci USA 106:21643-21648.

Gérard C, Goldbeter A (2012) Entrainment of the mammalian cell cycle by the circadian clock: Modeling two coupled cellular rhythms. PLoS Comput Biol 8:e1002516.

Leloup JC, Goldbeter A (2003) Toward a detailed computational model for the mammalian circadian clock. Proc Natl Acad Sci USA 110:7051-7056.

Leloup JC, Goldbeter A (2004) Modeling the mammalian circadian clock: Sensitivity analysis and multiplicity of oscillatory mechanisms. J Theor Biol 230:541-562.

CHAPTER 3

The circadian clock proteins CRY1 and CRY2 control the cell cycle G1/S transition and mitotic progression

Names: Elham Farshadi, Karlijn Houkes, Roel Janssens, Gijsbertus T.J. van der Horst, Inês Chaves*

Key words: Circadian clock, Cell cycle, Cryptochromes, Cyclin E, Mitosis

Abstract

The circadian clock and the cell cycle are two intracellular oscillators that employ cyclic gene expression and protein degradation to impose diurnal rhythmicity on behavior, physiology and metabolism, and to drive cell division, respectively. Recently, we have used the NIH3T3^{3C} mouse cell line, carrying fluorescent reporter genes for clock and cell cycle phase, to show that the circadian clock and the cell cycle are 1:1 phase coupled in proliferating cells. Previously we have shown the impact of positive circadian elements (CLOCK/BMAL1) on cell cycle progression. In the present study, we have investigated the impact of negative circadian elements on cell cycle progression and on the coupling between these two systems. To this end, we knocked out cryptochrome genes in NIH3T3^{3C} cells and analyzed timing of cell cycle progression at the single cell and population levels. Cryptochrome deficiency shortened the total cell cycle length. Notably, Cry deficient cells spend less time in G1 before entering S phase, which is supported by the elevated levels of Cyclin E in G1/S and early S phase cells. In addition, subsequent molecular analysis revealed involvement of cryptochromes on mitotic progression by modulating the phosphorylation of mitotic substrates. In conclusion, we show that cryptochromes modulate cell cycle progression at two different levels, by regulating G1/S transition and mitotic progression.

Introduction

The circadian clock and the cell cycle are two biological oscillators that interact closely with each other via intracellular molecular connections. They follow sequential events of transcription, translation, protein modification and degradation that drive their timed and cyclic events.

All living organisms possess an internal timing system called the "circadian clock", to adjust behavior, physiology and metabolism to the environmental changes that are instigated by the rotation of the earth around its own axis, i.e. the day and night (Pittendrigh et al., 1996). Mammals possess a master circadian clock which is centrally located in the suprachiasmatic nucleus of the brain (SCN) (Ralph et al., 1990). SCN neurons receive light input signals from photoreceptors located in the inner nuclear layer of the retina, to remain synchronized to the day/night cycle (Gooley et al., 2001). Subsequently, the SCN neurons transmit clock synchronizing signals via hormonal and neural cues to the peripheral clocks that are located in almost every single cell of an organism (Welsh et al., 2004). At the molecular level, both central and peripheral cells generate circadian rhythms through the same set of clock genes that act in autoregulatory transcriptional-translational feedback loops (TTFL) (Reppert et al., 2001; Yagita et al., 2002). The positive limb of the molecular oscillator consists of the Brain and Muscle Arnt-Like 1 (*Bmal1*) and Circadian Locomotor Output Cycles Kaput (*Clock*) genes (Bunger et al., 2000). The CLOCK/BMAL1 heterodimer acts as transcriptional activator of E-box promoter element containing genes, including the period (*Per1* and *Per2*), cryptochrome *(Cry1 and Cry2),* and nuclear hormone receptor *Rev-Erbα* clock genes (Takahashi et al., 2008). PER and CRY proteins, which make up the negative limb, accumulate in the cytoplasm and translocate to the nucleus, where they repress the activity of the CLOCK/BMAL1 heterodimer, thereby also inhibiting transcription of their own genes (Takahashi et al., 2008; Mohawk et al., 2012). Moreover, the CLOCK/BMAL1 heterodimer induces transcription of E-box containing Clock Controlled Genes (CCG), comprising over 10% of the cellular transcriptome (Miller et al., 2007). Thus, circadian transcription couples the circadian oscillator to a wide variety of physiological processes such as hormone secretion, drug and xenobiotic metabolism, and cell cycle progression (Takahashi et al., 2008).

Like the circadian clock, the cell cycle is a highly regulated oscillatory system, driven by cyclic gene expression and protein degradation. During the cell cycle, cells duplicate their genome in S-phase (S), followed by the separation of the genome in two daughter cells in mitosis (M). These two important phases of the cell cycle are separated by two gap phases, G1 and G2, that allow the cells to prepare for DNA replication and cell division, respectively (Norbury & Nurse 1992). Progression through the cell cycle relies on the rhythmic activity of cyclin-CDK kinase complexes. Cyclins are regulatory subunits that are produced at a specific phase of the cell cycle and subsequently associate with their catalytic subunits, the Cyclin-Dependent Kinases (CDKs) (Tyson & Novak, 2008). Specific combination of cyclin-CDK complexes triggers various cell cycle events such as DNA replication and mitosis. In addition, degradation of the cyclins at the end of each cell cycle phase is equally important

for cell cycle progression as it attenuates the kinase activity of the CDK partner, thereby allowing the cell to move forward and blocking the way back. Thus, cyclic activity of the cyclins and their associated CDK partners regulates cell cycle progression in a sequential and uni-directional manner.

Evidence is increasing that the circadian and cell cycle systems are not independent, but rather are coupled. Single cell studies, making use of a mouse fibroblast cell line (NIH3T3) expressing a clock reporter (Bieler et al., 2014) or a clock reporter together with two cell cycle markers (NIH3T3^{3C}) (Feillet et al., 2014,2015), have shown that these two oscillators are phase coupled at a 1:1 ratio. Several other studies have shown the existence of molecular connections between these two cyclic processes. For instance, transcription of *Wee1,* an important kinase for G2/M transition *(*Matsuo et al., 2003), of tumor suppressor gene *P21* (Gréchez-Cassiau et al., 2008), and of *P16-INK4* (Kowalska et al., 2013) is driven by the circadian clock. Conversely, the cell cycle gene *p53* negatively regulates *Per2* expression (Miki et al.,2013).

Although it is clear that the circadian clock and cell cycle are interconnected, little is known about how disruption of one of the systems can impact the other. This question can be addressed by genetically disrupting the circadian clock and investigating how this impacts cell cycle progression, and vice versa. It is also important to assess how a dysregulated communication between the two systems impacts disease and cancer predisposition. Previously we have shown that siRNA mediated knock down of *Bmal1* or *Clock* gene expression prolonged the total cell cycle length by delaying G2/M transition. At the molecular level, the CLOCK/BMAL1 heterodimer was shown to induce expression of Cyclin B1, thereby promoting G2/M transition and overruling the CLOCK/BMAL1-mediated induction of the G2/M transition inhibitor gene Wee1 (Farshadi et al., unpublished). Since positive and negative elements of the circadian transcription-translation feedback loop act oppositely on the expression of clock controlled genes, the question arises if, and how the negative circadian elements (CRY and PER) may regulate cell cycle progression.

In the current study, we have knocked out the endogenous cryptochrome genes (*Cry1* and *Cry2*) in the NIH3T3^{3C} mouse fibroblast cell line by CRISPR/Cas9 mediated technology and investigated cell cycle progression We show that the absence of cryptochrome proteins affects the cell cycle. Importantly, we shed light on the possible molecular mechanisms of this cryptochrome-mediated regulation of cell cycle progression.

Material and methods

Cell culture

NIH3T3^{3C} cells containing *Rev-Erbα-VNP* clock reporter and FUCCI *hCdt1-mKOrange* and *hGeminin-CFP* FUCCI cell cycle reporter genes (Feillet et al., 2014) were cultured in

Dulbecco's Modified Eagle's Medium (DMEM)/F10 (Lonza) containing 10% Fetal Bovine Serum (FBS) (Gibco), 100 U/ml Penicillin and 100 µg/ml Streptomycin in a standard humidified incubator at 37°C and 5% CO_2 (pH7.7).

In a subset of experiments, the cell cycle of proliferating cells (seeded on 6-well plates at a density of 80.000 cells per well) was synchronized by treatment of cell cultures with 2.5 mM thymidine (Sigma) treatment for 24 hours, which arrests most of the cells at the G1/S transition or early S phase. Cells were released from thymidine block by washing 3 times with PBS and harvested at the indicated time points.

To collect cells in mitosis, cell cultures (seeded on 10cm dishes at a density of 280.000 cells per dish) were treated with nocodazole (0.25 µg/ml, Sigma) for 12 hour. After incubation with nocodazole, cells were harvested with a gentle mitotic shake off. After washing with PBS, mitotic cells were reseeded in fresh medium and harvested at the indicated time points.

Generation of Cry1/Cry2 double knock out NIH3T3^{3C} cell line

The CRISPR/Cas9 genome editing approach was applied to knock out the *Cry1* and *Cry2* genes and obtain cryptochrome deficient NIH3T3^{3C} cells. Specific sgRNA sequences, targeting exon one of the *Cry* genes, were cloned into a blasticidine resistance selection marker containing back bone plasmid, containing a doxycycline inducible H1 promoter. The guide sequences are as follows: *Cry1:* Oligo 1= 5' GGT CGA GGA TAT AGA CGC AG 3'; Oligo 2= 5' CT GCG TCT ATA TCC TCG ACC; *Cry2:* Oligo 1= 5' TTT GCG GAA CCA GTG CAC CG 3'; Oligo 2= 5' CG GTG CAC TGG TTC CGC AAA 3'.

NIH3T3^{3C} cells were seeded on 6 well plates and were transfected the day after, at 70% confluency, simultaneously with the vectors containing the desired gRNAs for *Cry1*, *Cry2*, and Cas9 plasmid using Polyplus jetPei transfection reagent (Westburg). Transfection was carried out according to the manufacturer's protocol. Transfected cells were selected using 5ug/ml Blasticidine for several days. Subsequently, single cells were seeded on a 96 wells plate to obtain pure clones.

Isolated clones were screened for *Cry* gene inactivation by sequencing. To this end, genomic DNA around the exon 1 of *Cry1* and *Cry2* genes was PCR amplified using a Phusion High-Fidelity DNA Polymerase PCR Master kit (Thermo Fisher) according to manufacturer's protocol, using the following primers: *Cry1*: forward: 5' CGA TCG ATT GAT TTC CCA AG 3'; Reverse: 5' CTG GAA GGT ATG CGT GTC CT 3'; *Cry2*: forward: 5' GTT AGA AAG GGC CCG GTA AC 3'; Reverse: 5' CAG ATC CTC CCT CAG GTT GA 3'. Gel extracted PCR products were sent for Sanger sequencing. The sequencing results were analyzed by the TIDE (Tracking of Indels by DEcomposition) algorithm (https://tide.nki.nl) (Brinkman et al., 2014).

Real time bioluminescence monitoring of circadian performance

To monitor circadian oscillations in real time, cells were seeded in 35mm petri dishes. After 24 hours, at 60-70% confluency, the cells were transfected with a Bmal1::Luciferase reporter construct (1 µg/dish) using X-tremeGENE HP DNA Transfection Reagent (Roche) according to the manufacturer's protocol. After reaching confluency cell cultures were treated with forskolin (dissolved in 100% ethanol, added to a final concentration of 10µM) to synchronize the circadian clocks and subsequently cultured in medium buffered with 25 mM HEPES and containing 0.1 mM luciferin (Caliper Life Science, Hopkinton, MA, USA). The bioluminescence signal was monitored for 7 days (60 sec measurements at 10 min intervals) in a standard dry incubator using a LumiCycle 32-channel automated luminometer (Actimetrics), placed in a dry incubator at 37 °C. Prior to placing dishes in the LumiCycle, the lid was replaced by a glass coverslip and sealed with parafilm. The data were extracted and analyzed using Microsoft Excel.

Time-lapse fluorescence microscopy

For time-lapse recording of circadian clock and cell cycle progression, cells were seeded on 4 well poly-L-lysine coated glass bottom dishes (D141410, Matsunami Glass Ind.) at a density of 6000 cells per well. After 24 hours, dishes were placed in the temperature (37°C), CO_2 (5%) and humidity controlled chamber of a live cell imaging Zeiss LSM510/Axiovert 200M confocal microscope, equipped with a 10x Ph objective. Images were taken every 30 min for 48 hours or more using a Coolsnap HQ/Andor Neo sCMOS camera. Live cell imaging was conducted using the following parameters (as set up in Zeiss 200 software): Venus (green): 1000 ms (filter cube: Ex= 475/40 nm, DM= 500 nm, Em= 530/50 nm); mKO2 (red): 300 ms (filter cube: Ex= 534/20 nm, DM=552 nm, Em: 572/38 nm); CFP (blue): 300 ms (filter cube: Ex= 458/17 nm, DM=450 nm, Em: 479/40 nm). A bright field image for each frame was also acquired to ease cell tracking and analysis. The ConvertZeissTLV3 program was used to merge the acquired images into a single file to generate a movie, which was used for further analysis. Single cell numerical time series for each of the fluorescent markers were generated using the LineageTracker plugin for ImageJ. (https://github.com/pkrusche/lineagetracker.jsonexport). Time series were analyzed for circadian cycle length, cell cycle length and G1 and S/G2/M cell cycle phase length. The G1 phase is defined as the interval between the peaks of hGeminin-CFP and hCDT1-mKOrange expression. Oppositely, the S/G2/M phase is defined as the interval between the peaks of hCDT1-mKOrange and hGeminin-CFP expression

Flow cytometry

To analyze the cell cycle distribution by quantification of DNA content, cells were seeded and harvested at 50% confluency. Next, cells were washed with PBS, and fixed overnight at 4°C with cold 70% ethanol. Then, the fixed cells were washed with PBS, treated for 15 min

at 37°C with PBS containing 100 μg/ml bovine pancreas RNase (Calbiochem), and left overnight at 4°C in PBS with 40 μg/ml propidium iodide (PI; Life Technologies). To detect mitotic cells, fixed cells were stained for the presence of the MPM-2 phospho-epitope on DNA topoisomerase IIα, using mouse anti-MPM2 primary antibodies (Merck-Millipore; dilution 1:200; 1 h, 0°C) and goat-anti mouse FITC secondary antibodies (Abcam; dilution 1:50, 30 min, 0°C). Cells were analyzed using a Becton Dickinson LSRFortessa™ Cell Analyzer (BD Biosiences). PI and FITC fluorescence intensities were measured at 610 nm and 530 nm, respectively. For each condition, at least 10,000 cells were counted. Frequency histograms were made using BD FACSDiva™ software (BD Biosciences).

Western blot analysis

Protein levels were determined by Western blot analysis. After harvesting cells were lysed for 30 min on ice in RIPA lysis buffer, containing 5.15 mM NaCl, 2 mM Tris-HCl pH8.0, 0.5% NaDOC, 0.1% SDS, 0.1% TX-100, 10 mM EDTA, a PhosSTOP phosphatase inhibitor tablet (Roche) and a Pierce Protease inhibitor tablet (Thermofisher). Lysed cells were cleared by centrifugation at 13000 rpm for 10 min at 4°C and supernatant was collected. 2x sample buffer (130 mM TrisCl pH 8.0, 20% glycerol, 4.6% SDS, 0.02% bromophenol blue, 100 mM DTT or 10% 2-mercaptoethanol) was added (1:1). Samples were heated at 95°C for 5 min. Proteins were kept on ice for at least 5 min before loading on a Bis-Tris Plus 4-12% polyacrylamide gel (Novex®, Life technologies). The proteins were size separated in 10% running buffer composed of 0.25 M Trizma base, 1.92 M Glycine and 1% SDS. Proteins where transferred to a Polyvinylidene fluoride (PVDF) membrane in 20% methanol and 10% transfer buffer (1.2 M Trizma base, 0.4 M Glycine). The membrane was cut into different pieces for each protein according to their size, using the Precision Plus Protein Standard (Bio-Rad) as a guide for protein size. The membranes were blocked with 4% skim milk and incubated with the primary antibody of interest (listed below) overnight at 4°C. After 3x washing with PBS/0.05%Tween, membranes were incubated with the secondary antibodies (1:2000 dilution) for 1 hour at 4°C. Protein bands were visualized using a SuperSignal® West Femto Maximum Sensitivity Substrate Kit (#34094) and autoradiography. Band intensities were quantified by Fiji® software and normalized against β-actin protein levels. Next, intensities were normalized to the average intensity of the blot to quantitatively compare different blots.

Antibodies used: Santa Cruz Actin C-2 (sc8432, dilution 1:750), Cyclin B1 (sc245, dilution 1:2000), Cyclin A1 (sc751, dilution 1:1000), WEE1 (sc325, dilution 1:500), and BMAL1 (sc48790, dilution 1:2000). Abcam Cry1 (ab104736, dilution 1:500), Cry2 (ab38872, dilution 1:400), Cyclin E (ab7959, dilution 1:300), Cyclin D (ab134175, dilution 1:1000). Secondary antibodies: goat anti-rabbit IgG (H+L)-HRP conjugate (P0260, Dako) or rabbit anti-mouse IgG (H+L)-HRP conjugate (P0448, Dako).

Statistical analysis

All statistical analyses were carried out with GraphPad software. For single cell studies, after performing the normality test, the two-tailed Mann-Whitney test was used to analyze the duration of the circadian and cell cycle (including G1, S/G2/M phase). For Western blot, flow cytometry, and immunofluorescence experiments, the two-tailed Student's t-test was applied.

Results

Generation and validation of *Cry dko* NIH3T3^{3C} cell lines

To inactivate the endogenous *Cry1* and *Cry2* genes in the NIH3T3^{3C} cell line, containing Rev-Erbα-VNP clock reporter, and hCdt1-mKOrange and hGeminin-CFP FUCCI cell cycle reporter genes, we applied the CRISPR/Cas9 gene editing method. NIH3T3^{3C} cells were simultaneously transfected with the gRNAs targeting *Cry1* and *Cry2* genes together with a Cas9 plasmid. Transfected cells were selected and sequenced to validate the targeting efficiency for both *Cry*1 and *Cry2* loci. Next, we selected single clones, followed by sequencing to further validate the clones. Two of the targeted clones, hereafter referred to as *Cry* dko1 and *Cry* dko2, were further analysed. In addition, one of the non-target clones was selected as the negative control *(ntCtrl*).

To quantify the editing efficacy and identify the type and frequency of Indels (Insertions and deletions) in the selected clones, a TIDE (Tracking of Indels by DEcomposition) analysis (Brinkman et al., 2014) was performed. As shown in Fig. S1A, the expected Cas9 break site for the *Cry1* and *Cry2* loci is located at the right position in the *Cry dko1* and *Cry dko2* clones. In addition, we checked type (inseration or deletion), and size of the mutations in *Cry dko1* and *dko2* clones (Fig. S1B). Fig. 1, represent the position of the aberrant sequences in the *Cry1* and *Cry2* loci for *Cry dko1* and *Cry dko2* cells. As it is shown for the *Cry1* locus *(*Fig. 1A), aberrant sequences and large deletions start in the coding region 87 base pairs downstream of the ATG start codon in both targeted clones. Based on these large deletions, no functional CRY1 protein is expected. For the *Cry2* Locus*, Cry* dko1 and *Cry* dko2 cells carry a +1 insertion of a thymidine at nucleotide 68 downstream of the ATG start codon (Fig. 1B; supplementary Fig.1B). This mutation caused a frame shift that generates non-functional CRY2 protein (Fig. 1B). In conclusion, according to the sequencing results, no functional CRY1 and CRY2 proteins are expected in the selected clones.

We next compared the circadian performance of *Cry dko* clones and the Non-target control (*ntCtrl*) to that of the parental cell line (*Ctrl*) by transiently transfecting the cells with a Bmal1::luciferase reporter construct and subsequent time lapse recording of the bioluminescence signal for 6 days. As shown in Fig. 1C, a robust oscillation in bioluminescence is observed in the non-target control, with an amplitude and period that compares well to that of the parental *Ctrl* line, indicating that the CRISP/Cas9 procedure did not affect clock peformance. As expected on the basis of the loss of circadian rhythmicity in *Cry1*$^{-/-}$*Cry2*$^{-/-}$ double

knockout mice and fibroblasts (van der Horst et al., 1999; Yagita et al., 2001), no oscillations could be detected in the *Cry dko1* and *Cry dko2* cells. From these data we conclude that we have successfully inactivated the *Cry1* and *Cry2* alleles in *Cry dko1* and *Cry dko2* cells.

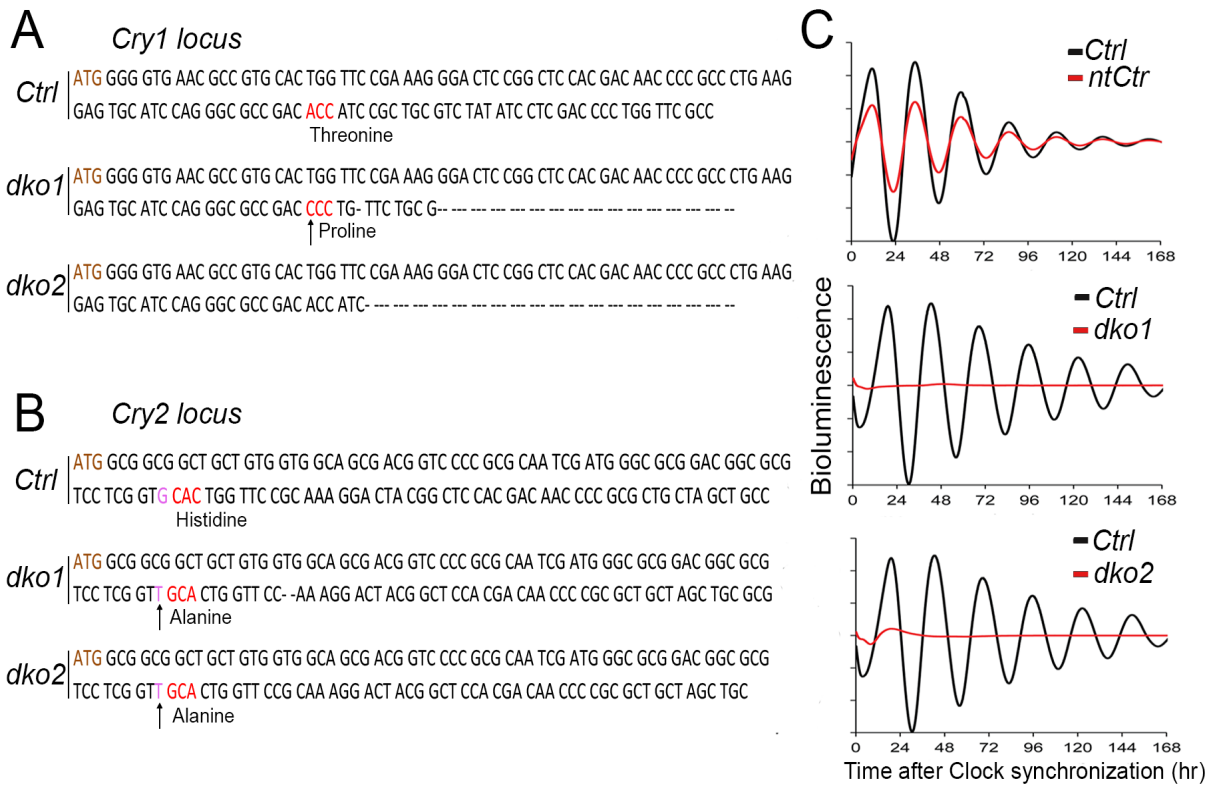

Figure 1. Characterization of the CRY deficient clones. Sequence alignment of the control and test samples for *Cry1* (panel A) and *Cry2* loci (panel B) in *Ctrl* (top row) *Cry1 dko1* (middle row) and *dko2* (bottom row) cells. In *Cry1* locus, Substitution of a single nucleotide is shown by arrow in *Cry dko1* clone. Mismatches and deletions between the control sequence and the targeted sequences are shown by dashes. In *Cry2* locus, the position of the inserted nucleotide is shown by an arrow. Change in the reading frame is shown in red. (C) Representative example of bioluminescence rhythms in confluent cultures of *Ctrl* and *ntCtrl* (top panel), *Ctrl* and *Cry dko1* (middle panel), *Ctrl* and *Cry dko2* (bottom panel). Cells are transfected with a Bmal1::Luciferase reporter construct and synchronized with Forskolin (clock synchronizer). Y- axis represents the base line subtracted bioluminescence value.

Absence of Cryptochromes shortens the cell cycle

We next analyzed clock performance and cell cycle progression in proliferating *Cry dko1* cells at the single cell level by time lapse confocal microscopy. Fig. 2A shows a representative example of an individual proliferating *Ctrl* cell (upper panel), and a *Cry dko1* cell (lower panel) spanning the circadian cycles and G1/S/G2/M cycles over the period of 68 hours. In line with earlier observations (Feillet et al., 2014; Farshadi et al, un published) proliferating

Ctrl cells show clock phase-coupled cell proliferation patterns with a clock and cell cycle period (as calculated from the time interval between two peaks of REV-ERBα-VNP and hCdt1-mKOrange fluorescence respectively) of 17.5 ± 0.4 h and 17.6 ± 0.4 h respectively (n=40 cells). Surprisingly, as confluent *Cry* dko1 cells are completely arrhythmic, a markedly attenuated oscillation of the REV-ERB-VNP clock marker could still be observed with a periodicity of 15.5 ± 0.3 h (n=40 cells). Moreover, the circadian clock of *Cry1* dko1 cells appears still 1:1 phase coupled to the cell cycle, having a comparable period of 15.5 ± 0.3 h. These data suggest that proliferating *Cry dko1* cells may still have a partially functional clock. Further comparison of the total cell cycle length of *Ctrl* and *Cry dko1* cells revealed that inactivation of the Cryptochrome genes significantly ($p<0.001$) shortened the total cell cycle length from 17.6 ± 0.4 h to 15.7± 0.2 h (mean ± SEM Fig. 2B).

Next, we quantified the length of the G1 and combined S, G2 and M (hereafter referred to as S/G2/M) phases in *Ctrl* and *Cry dko* cells. The G1 phase is defined as the interval between the peaks of hGeminin-CFP and hCDT1-mKOrange expression, and the S/G2/M phase as the interval between the peaks of hCDT1-mKOrange and hGeminin-CFP expression. As shown in Fig. 2B, the mean length of the G1 phase decreased significantly from 7.9 ± 0.2 h in *Ctrl* cells to 5.9 ± 0.1 h in *Cry dko* cells (mean ± SEM $p <0.0001$). The average length of S/G2/M was comparable in both conditions (9.6 ± 0.2 h in *Ctrl* cells and 9.8 ± 0.1 h in *Cry dko1* cells, $p= 0.4$) (Fig. 2*B*). Similar results were obtained with *Cry dko2* cells (supplementary Fig. 2A). Taken together, the single cell data show a modulating role of cryptochrome proteins on the G1 phase of the cell cycle.

Altered cell cycle distribution in the absence of *cryptochromes*

The single cell experiments showed that knocking out *Cry genes* shortens the G1 phase of the cell cycle, without affecting the overall S/G2/M phase length. To uncover potential alterations in S, G2 and M phase, we analyzed the cell cycle phase distribution of proliferating *Cry dko*1 cell cultures by flow cytometry. Fig. 2C shows a representative example of the cell cycle distribution of Propidium Iodide (PI) stained *Ctrl* and *Cry dko1* cells. In line with the single cell experiments, quantification of the cell cycle phase distribution (Fig. 2*D)* revealed a significant decrease in the percentage of G1 *dko1* cells, as compared to *Ctrl* cells (48.4 ± 0.9 % and 44.3 ± 0.4 % for *Ctrl* and *Cry dko1* cells; n=3, $p=0.02$). Interestingly, whereas the overall length of the combined S, G2 and M phase of *dko* cells was not altered, the distribution of S and G2/M phase cells was dramatically shifted in *Cry1/Cry2* knockout cells. The percentage of S phase cells significantly decreased from 20.7 ± 0.9 % in *Ctrl* cells to 13.5 ± 0.2 % in *Cry dko* cells ($p=0.01$) (Fig. 2*D*). In contrast, the percentage of cells in G2 and M phase increased significantly ($p<0.0001$) from 28.0 ± 0.4 % in controls to 38.3 ± 0.3 % (mean ± SEM; n=3) in *Cry dko* cells. To discriminate between G2 and M phase cells, we also stained the cells with an antibody against the mitosis-specific MPM-2 phospho-epitope on DNA topoisomerase IIα.

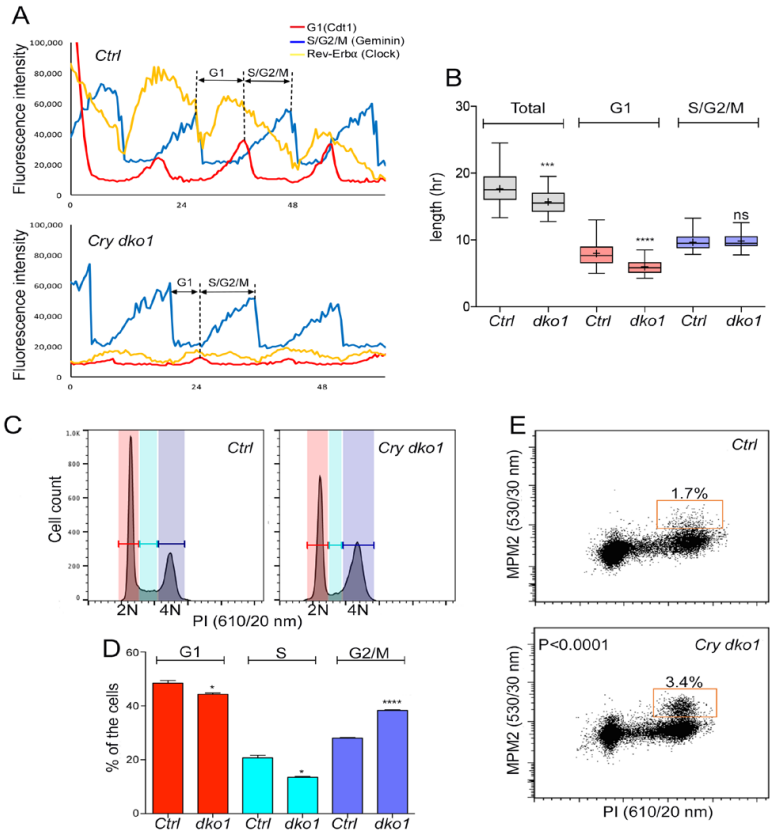

Figure 2. Cell cycle dynamics in the absence of cryptochromes. (A) Representative examples of time-lapse confocal imaging of a *Ctrl* (NIH3T3^{3C}) (upper panel) and a *Cry dko* cell (lower panel). Plotted are fluorescence intensities of circadian clock (Rev-Erbα-VNP; yellow), and of G1 (hCdt1-mKOrange; red) and S/G2/M (hGeminin-CFP; blue) cell cycle markers over a 68-hour period. The G1 phase is defined as the interval between the peaks of hGeminin-CFP and hCDT1-mKOrange expression. S/G2/M is defined as the interval between the peaks of hCDT1-mKOrange and hGeminin-CFP expression. (*B*) Box-whisker plot showing the length of the total cell cycle (grey), G1 (red) and S/G2/M (blue) in *Ctrl* and *Cry* dko cells (n= 40 cells per condition). The range between the highest and lowest values is shown. The solid line and cross within the box represent the median and mean value, respectively. The lowest and highest boundaries of the box indicate the 25 and 75 percentiles, respectively. *** p<0.001 and **** p<0.0001 (Mann Whitney test). C) Flow cytometric analysis of cell cycle phase distribution in Ctrl and *Cry* dko cells. Shown are representative examples of propidium iodide (PI) stained Ctrl and *Cry* dko cells, analyzed for DNA content (n=3 experiments). The vertical axis indicates the relative number of cells and the horizontal axis indicates the relative PI fluorescence intensity. The 2N and 4N peaks and intermediate region correspond to G1, G2/M and S phase, respectively. (*D*) Quantification of cell cycle phase distribution of proliferating *Ctrl* and *Cry dko* cells. Shown is the average of 3 biological replicates (20000 cell counts/per sample). The data were analyzed using the two-tailed paired Student's t-test. Error bars indicate the SEM. (*C*) Representative example of flow cytometry analysis to determine of the number of mitotic cells. The bivariate dot plots show DNA content (PI) and mitotic phosphoproteins content (MPM2 stain) on the X and Y axis, respectively. The box marks cells stained positive for MPM2.

As shown in Fig. 2E, we observed a highly significant increase ($p<0.001$) in the percentage of MPM2-positive cells from 1.7 ± 0.2 % in controls to 3.4 ± 0.2 % (mean ± SEM; n=3) in *Cry dko* cells. Similar data were obtained for the *Cry dko2* clone (supplementary Fig. 2B). In conclusion, cell cycle profile analysis shows relatively less cells in G1 and S, but more cells in G2 and mitosis in the CRY deficient clones.

Cryptochromes regulate two cell cycle check points

Phase specific and timed expression and degradation of different Cyclins is important for regulated cell cycle progression. We therefore next studied the kinetics of different cell cycle regulators in proliferating CRY deficient cells. To this end, we used a thymidine block (which arrests the cells at G1/S), followed by a release protocol. Cells were harvested 0, 2, 4, 6, 8, and 10 hours after release from the thymidine block and expression levels of the various cyclins in exponentially proliferating *Ctrl* and *Cry dko* cells were examined by western blot analysis. Cyclin E peaks at late G1 and is an important molecule for the G1/S transition (Koff et al., 1992; Jackson et al., 1995). As shown in Figs. 3A and B, at the G1/S transition and the beginning of S phase (time points 0 and 2 hours after thymidine release), an elevated level of Cyclin E is observed ($p=0.01$ and $p=0.04$ respectively). Therefore, higher Cyclin E protein levels explain the shortening of the G1 phase.

Next, we analyzed Cyclin A2 protein levels in *Ctrl* and *Cry dko1* cells upon release from a thymidine block (Fig. 3A and C). Calculations of the time spent in each of the cell cycle phases based on the flow cytometry data and single cell analysis (Table 1) showed that the approximate total time spent in S and G2 is about 8 hours in both *Ctrl* and *Cry dko1* cells (S and G2-phase cells in total 48% and 51%, at a cell cycle length of 17.6 and 15.7 hours in *Ctrl* and *Cry dko1* cells, respectively). Thereby, mitosis should start approximately 8 hours after thymidine release. Progression through mitosis requires degradation of Cyclin A2 right after break down of the nuclear envelope (Den Elzen et al., 2001). Between the 6 hour and 10 hour time points, Cyclin A2 is degraded by 75% in the *Ctrl* cells, indicating that the cells reached late G2 or early mitosis. In contrast, *Cry dko1* cells only show a 30% reduction in Cyclin A2 protein levels ($p=0.02$ at 10 hours) (Fig. 3C).

Furthermore, Cyclin B1 protein level gradually increased with the same kinetics in *Ctrl* and *Cry dko1* cells during the S and G2 phase, reaching a maximal level 6 hours after thymidine release (Fig. 3A and D). Interestingly, a significant higher level of Cyclin B1 was detected in *Cry dko1* cells 8 and 10 hour after thymidine release ($p<0.01$ at 10 hours; Fig. D). It is well known that exit from mitosis requires degradation of Cyclin B1 (Holloway et al., 1993; Pines et al.,2006). Therefore, failure to degrade Cyclin B1 at the end of mitosis could cause unsuccessful or delayed mitosis. To examine the degradation kinetics of Cyclin B1 at the end of mitosis, we arrested the cells at metaphase with Nocodazol, followed by a release protocol. Cells were harvested 0, 1, 2, 3, 4, 5, and 6 hours after Nocodazol release and analyzed for Cyclin B1 levels. As shown in Fig. 3E and F, although Cyclin B1 appears to be up-regulated in metaphase cells, no clear difference could be observed in the degradation of Cyclin B1 at

the end of mitosis in *Ctrl* and *Cry* dko cells. Therefore, we speculate that the aberrant mitotic profile could be due to a delay in early mitosis.

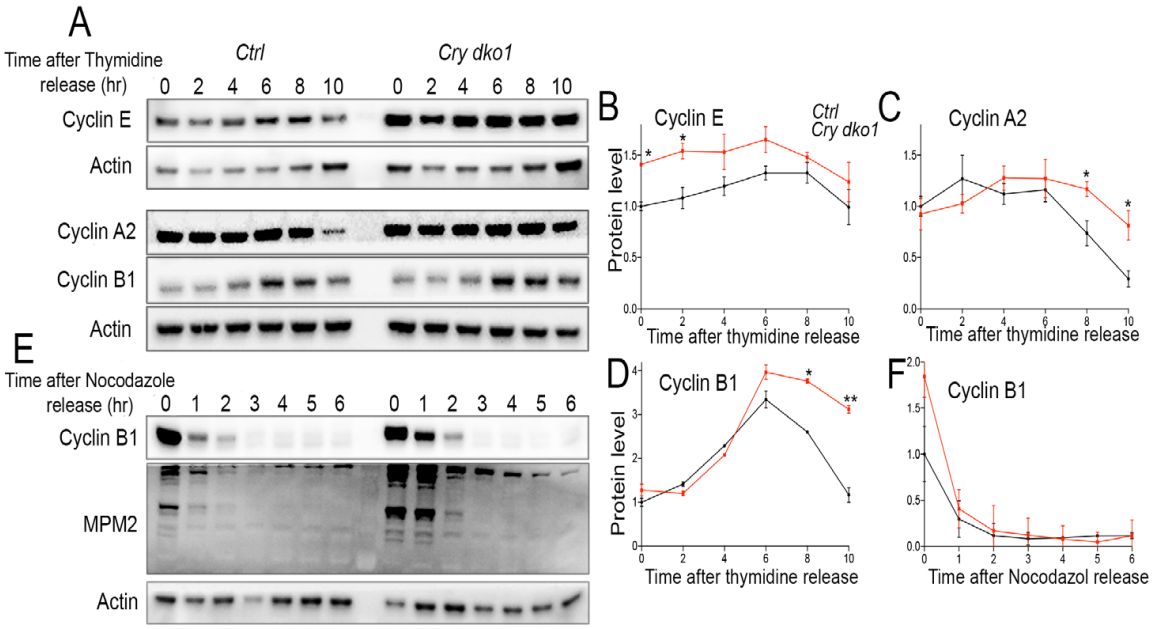

Table 1	G1	S	G2	M	Total cell cycle length
Ctrl	48.4%	20.7%	28.01%	1.7%	17.6 ± 0.4h
	8.5 ± 0.1 h	3.6 ± 0.1 h	4.9 ± 0.05 h	0.3 ± 0.02 h	
Cry dko1	44.3%	13.5%	38.3%	3.4%	15.7 ± 0.2 h
	6.9 ± 0.07 h	2.1 ± 0.04 h	6.2 ± 0.03 h	0.5 ± 0.01 h	
P-Value	P<0.01	P<0.01	P<0.001	P<0.01	

Figure 3. **Cell cycle protein expression in Ctrl and Cry dko cells.** (A) Western blot analysis of Cyclin E, Cyclin A2 and Cyclin B1 protein levels in *Ctrl* and *Cry dko* cells after release from a thymidine block. Shown are representative examples of n=3 independent experiments. Actin was used as a loading control. (*B-D*) Kinetics of Cyclin E (B), Cyclin A2 (C) and Cyclin B1 (D) expression after release from a thymidine block. Expression levels were normalized against actin and are relative to the Ctrl at t=0. Error bars indicate SEM (n=3 experiments). (E) Western blot analysis of Cyclin B1 and MPM2, in *Ctrl* and *Cry dko* cells, after release from a Nocodazol block. Shown are representative examples of n=3 independent experiments. Actin was used as a loading control. (F) Kinetics of Cyclin B1 expression after release from a Nocodazol block. Cyclin B1 expression levels were normalized against actin and are relative to the Ctrl at t=0. Error bars indicate SE (n=3 experiments).

Table 1. Estimated duration of individual cell cycle phases: Percentages were obtained from flow cytometry analysis. The percentage of cells in G2 was calculated as the percentage of cells in G2/M (PI staining) minus the percentage of cells in M (MPM2 staining). The values of total cell cycle length are derived from the single cell analysis.

Phosphorylation of mitotic proteins is highly regulated and is a central mechanism for mitotic progression. These post-translational modifications define stability and activity of mitotic proteins (Olsen et al., 2010). To determine whether this process is affected in the CRY deficient clones, we performed Western blot analysis of the Nocodazol released cells using an antibody against the MPM2 mitotic marker (recognizes a phosphorylated epitope (S/T) found in mitotic phosphoproteins). As shown in Fig. 3E, we observed elevated levels of phosphorylation of mitotic proteins in the *Cry dko1* cells. Taken together, these findings indicated that CRY proteins are required for proper progression through early stages of mitosis.

Discussion

In the present study, we have investigated the impact of the negative elements of the circadian oscillator on cell cycle progression by genetic disruption of the cryptochrome genes. First, we analyzed the clock performance in the *Cry* double knock out cell line compared to control cells. Surprisingly, as based on the population time lapse experiment and according to previous literature (van der Horst et al., 1999; Yagita et al., 2001) we did not expect any circadian oscillation in *Cry* deficient cells, we observed a dampened REV-ERB-VNP in the proliferating *Cry* dko cell lines. This can be explained by assuming that in the absence of the CRY proteins (but with the BMAL1 and CLOCK proteins still functional), the circadian clock may act as an hour glass clock. We hypothesize that during mitosis the clock is reset and CLOCK/BMAL1 heterodimers start to activate E-box genes. However, in the absence of the CRY proteins (representing the negative limb of the TTFL) the oscillation fails to continue and gain amplitude.

Previously, we showed that knocking down the positive circadian elements (*Bmal1* or *Clock*) extended the cell cycle length of proliferating NIH3T3^{3C} cells by about 4 hours. The progression from G2 to M was delayed as a consequence of impaired expression of Cyclin B1. In this study, using NIH3T3^{3C} cells lacking cryptochromes (*Cry dko1* and *dko2*), we show that disruption of the negative circadian elements shortened the total cell cycle by about 2 hours. Our data indicate a shortening of the G1 phase by 2 hours in *Cry* double knock out cells, while no significant changes could be detected in the total S/G2/M length at the single cell level. Interestingly, flow cytometric analysis revealed reduced numbers of cells in both G1 and S, and a significant increase in the percentage of G2/M cells. We have observed a two-fold higher percentage of mitotic cells, which can partially explain the increased 4N population.

Subsequent analysis of important cell cycle regulators in cell cycle synchronized cell cultures revealed involvement of cryptochromes in the regulation of G1/S and M phase. Proliferating *Cry dko* cells are characterized by a shortened G1 phase and express high level of Cyclin E at G1/S. This finding is in good agreement with the observation that overexpression of Cyclin E decreases the time of G1 to S phase transition, which leads to a shortening of G1 (Ohtsubu et al., 1995; Resnitzky et al., 1995). It is known that transcription of Cyclin E is induced by the *Myc* oncogene. On the other hand, *Myc* transcription is directly controlled by circadian clock genes (Fu et al., 2002). Therefore, regulation of Cyclin E by cryptochromes

could occur via *Myc* transcriptional regulation.

Whereas the kinetics of the Cyclin A2 and Cyclin B1 cell cycle regulators during S and G2 was in the normal range, *Cry dko* cells showed an attenuatted degradation of Cyclin A2 and Cyclin B1. It is known that accumulation of Cyclin A2 at late G2 and early M cells will interfere with chromosome alignment and cause a mitotic delay (Den Elzen et al., 2001; Pines et al., 2006). Therefore, in the absence of CRY proteins accumulation of Cyclin A2 at the beginning of mitosis may interfere with mitotic progression, which also could explain the higher mitotic index in Cry dko cells, as determined by flow cytometry.

Active Cyclin A2-CDK2 and Cyclin B1-CDK1 phosphorylate key mitotic substrates (Pines et al., 2006), and these post-translational modifications define activity and stability of the mitotic proteins (Ptacek et al., 2006; Oslen et al., 2010). Timed degradation of Cyclin A2 and Cyclin B1 allows phosphatases to reverse the phosphorylation of mitotic substrates, allowing the cell to progress through mitosis (Domingo-Sananes et al., 2011). Therefore, the observed delayed degradation of these cyclins in the CRY deficient cells may interfere with mitotic progression, by affecting the phosphorylation pattern of mitotic substrates. Interestingly, when we analyzed the level of phosphorylation of mitotic substrates, determined by western blot analysis of nocodazole released cells, we observed elevated levels of phosphorylated MPM2 epitope (mitotic marker). This confirms that phosphorylation of mitotic proteins is de-regulated in the CRY deficient cells.

Circadian oscillation in transcription has been extensively studied, and it is known that at least 10% of the genome is under circadian control (Panda et al., 2002; Zhang et al., 2014). However, recent proteome studies revealed that 40% of the phosphoproteins are significantly oscillating in mouse liver (Robles et al., 2017). This study indicates a prominent role of circadian regulation at the post translational level, such as protein phosphorylation. Taking into account that we have observed a significant increase in the phosphorylation of several mitotic proteins (Figure 3E), and knowing that phosphorylation is a central mechanism of control for both mitosis (Olsen et al., 2010) and circadian rhythms, we speculate that in the absence of CRY proteins the circadian control of the cell cycle is lost in these cells as a consequence of a de-regulated phosphoproteome. To test this hypothesis, a comparative time course phosphoproteomics experiment in the WT and *Cry dko* cell lines using the HighPhos workflow could be performed.

So far, several studies have linked circadian disruption to tumorigenesis. Impaired cryptochrome gene expression has been reported in colorectal (Mazzoccoli et al., 2016) and breast cancer (Hoffman et al., 2010). Our results support the link between cryptochrome deficiency and tumorogenesis by showing a shortened G1/S transition together with elevated levels of Cyclin E in *Cry* double knock out cells. It is known that Cyclin E activity is tightly regulated in normal cells and is frequently de-regulated and overexpressed in cancer cells (Mazumder et al., 2004; Hwang et al., 2005). Therefore, overexpression of Cyclin E is considered as an oncogenic factor. Moreover, impaired mitotic progression may cause chromosomal instability, which is a hallmark of cancer. Therefore, in this study we un-covered the effect of cryptochrome deficiency on cell cycle progression and, to some extent, we shed light on

the underlying mechanism. Improvement of the FUCCi system in NIH3T3^{3C} cell line will allows us to discriminate between each of the S, G2, and M phases and may further help us to un-cover the effect of circadian elements on each specific cell cycle phases.

References:

Bieler J, Cannavo R, Gustafson K, Gobet C, Gatfield D, Naef F (2014) Robust synchronization of coupled circadian and cell cycle oscillators in single mammalian cells. Mol Syst Biol 10:739.

Brinkman EK, Chen T, Amendola M, Van Steensel B (2014) Easy quantitative assessment of genome editing by sequence trace decomposition. Nucleic Scids Res 42:168.

Bunger MK, Wilsbacher LD, Moran SM, Clendenin C, Radcliffe LA, Hogenesch JB, Simon MC, Takahashi JS, Bradfield CA (2000) Mop3 is an essential component of the master circadian pacemaker in mammals. Cell 103, 1009–1017.

Coverley D, Laman H, Laskey RA (2002). Distinct roles for cyclins E and A during DNA replication complex assembly and activation. Nat Cell Biol 4:523-528.

Den Elzen N, Pines j (2001) Cyclin A is desproyed in prometaphase and cann delay chromosome alignment and anaphase. J Cell Biol 153:121-136.

Erlandsson F, Linnman C, Ekholm S, Bengtsson E, Zetterberg A (2000) A detailed analysis of Cyclin A accumulation at the G1/S border in normal and transformed cells. Exp Cell Res 295:86-95.

Feillet C, Krusche P, Tamanini F, Janssens RC, Downey MJ, Martin P, Teboul M, Saito S, Lévi FA, Bretschneider T, van der Horst GTJ, Delaunay F, Rand DA (2014) Phase locking and multiple oscillating attractors for the coupled mammalian clock and cell cycle. Proc Natl Acad Sci USA 111:9828-9833.

Fu L, Pelicano H, Liu J, Huang P, Lee CC (2002) The Circadian Gene Period2 Plays an Important Role in Tumor Suppression and DNA Damage Response In Vivo. Cell 111: 41-50.

Fung TK, Poon RYC (2005) A roller coaster ride with the mitotic cyclins. Sem Cell Dev Biol 16:335-342.

Gavet O, Pines J (2010) Progressive activation of CyclinB1-Cdk1 coordinates entry to mitosis. Dev Cell 18:533-543.

Geley S, Kramer E, Gieffers C, Gannon J, Peters JM, Hunt T (2001) Anaphase-Promoting Complex/Cyclosome–Dependent Proteolysis of Human Cyclin a Starts at the Beginning of Mitosis and Is Not Subject to the Spindle Assembly Checkpoint. J Cell Biol 153:137-148.

Gooley JJ, Lu J, Chou TC, Scammell TE, Saper CB (2001) Melanopsin in cells of origin of the retinohypothalamic tract. Nat Neurosci 4, 1165.

Gréchez-Cassiau A, Rayet B, Guillaumond F, Teboul M, Delaunay F (2008) The circadian clock component BMAL1 is a critical regulator of p21WAF1/CIP1 expression and hepatocyte proliferation. J Biol Chem 283:4535-4542.

Guillemot L, Levy A, Raymondjean M, Rothhut B (2001) Angiotensin II-induced transcriptional activation of the Cyclin D1 gene is mediated by Egr-1 in CHO-AT1A Cells. J Biol Chem 276:39394-39403.

Henley SA, Dick FA (2012) The retinoblastoma family of proteins and their regulatory functions in the mammalian cell division cycle. Cell Div 7:10.

Holloway SL, Glotzer M, King RW, Murray AW (1993) Anaphase is initiated by proteolysis rather than

by the inactivation of maturation-promoting factor. Cell 73:1393–1402.

Hwang HC, Clurman BE (2005) Cyclin E in normal and neoplastic cell cycles. Oncogene 24:2776-2786.

Jackson PK, Chevalier S, Philippe M, Kirschner MW (1995) Early events in DNA replication require cyclin E and are blocked by p21CIP1. J Cell Biol 130:755–769.

Kalaszczynska I, Geng Y, Iino T, Mizuno S, Choi Y, Kondratiuk I, Silver DP, Wolgemuth DJ, Akashi K, Sicinski P (2009) Cyclin A is redundant in fibroblasts but essential in hematopoietic and embryonic stem cells. Cell 138:352-365.

Keck JM, Summers MK, Tedesco D, Ekholm-Reed S, Chuang LC, Jackson PK, Reed SI (2007) Cyclin E overexpression impairs progression through mitosis by inhibiting APC Cdh1. J Cell Biol 178:371-385.

Koff A, Giordano A, Desai D, Yamashita K, Harper JW, Elledge S, Nishimoto T, Morgan DO, Franza SR, Roberts JM (1992) Formation and activation of a cyclin E-CDK2 complex during the G1 phase of the human cell cycle. Science 257:1689-1694.

Kowalska E, Ripperger JA, Hoegger DC, Bruegger P, Buch T, Birchler T, Mueller A, Albrecht U, Contaldo C, Brown SA (2013) NONO couples the circadian clock to the cell cycle. Proc Natl Acad Sci USA 110:1592-1599.

Lindqvist A, Rodriguez-Bravo R, Medema RH (2009) The decision to enter mitosis: feedback and redundancy in the mitotic entry network. Cell Biol 185:193-202.

Liu AC, Welsh DK, Ko CH, Tran HG, Zhang EE, Priest AA, Buhr ED, Singer O, Meeker K, Verma IM, Doyle FJ, Takahashi JS, Kay SA (2007) Intercellular Coupling Confers Robustness against Mutations in the SCN Circadian Clock Network. Cell 129, 605–616.

Mateyak MK, Obaya AJ, Sedivy JM (1999) c-Myc regulates Cyclin D-Cdk4 and –Cdk6 activity but affects cell cycle progression at multiple independent points. Mol Cell Biol 19:4672-4683.

Matsuo T, Yamaguchi S, Mitsui S, Emi A, Shimoda F, Okamura H (2003) Control mechanism of the circadian clock for timing of cell division in vivo. Science 302:255-259.

Matsuo T, Yamaguchi S, Mitsui S, Emi A, Shimoda F, Okamura H (2003) Control mechanism of the circadian clock for timing of cell division in vivo. Science 302:255-259.

Mazumder S, DuPree EL, Almasan A (2004) A dual role of Cyclin E in cell proliferation and apoptosis may provide a target for cancer therapy. Curr Cancer Drug Targets 4:65-75.

Miller BH, McDearmon EL, Panda S, Hayes KR, Zhang J, Andrews JL, Antoch MP, Walker JR, Esser KA, Hogenesch JB, Takahashi JS (2007) Circadian and CLOCK-controlled regulation of the mouse transcriptome and cell proliferation. Proc Natl Acad Sci U S A 104:3342-7.

Mohawk JA, Green CB, Takahashi JS (2012) Central and peripheral circadian clocks in mammals. Annu Rev Neurosci 35: 445-462.

Nagoshi E, Saini C, Bauer C, Laroche T, Naef F, Schibler U (2004) Circadian gene expression in individual fibroblasts: cell-autonomous and self-sustained oscillators pass time to daughter cells. Cell

119:693-705.

Norbury C, Nurse P (1992) Animal cell cycles and their control. Annu Rev Biochem 61:441-70.

Ohtsubo M, Theodoras AM, Schumacher J, Roberts JM, Pagano M (1995) Human Cyclin E, a nuclear protein essential for the G1-to-S phase transition. Mol Cell Biol 15:2612-2624.

Pagano M, Pepperkok R, Verde F, Ansorge W, Draetta G (1992) Cyclin A is required at two points in the human cell cycle. EMBO J 11: 961-971.

Panda S, Antoch MP, Miller BH, Su AI, Schook AB, Straume M, Schultz PG, Kay SA, Takahashi JS, Hogenesch JB (2002) Coordinated transcription of key pathways in the mouse by the circadian clock. Cell 109: 307–320.

Pines J (2006) Mitosis: a matter of getting rid of the right protein at the right time. Trends Cell Biol 16:55-63.

Pittendrigh CS (1960) Circadian rhythms and the circadian organization of living systems. Cold Spring Harb Symp Quant Biol 25:159-84.

Ralph MR, Foster RG, Davis FC, Menaker M (1990) Transplanted suprachi- asmatic nucleus determines circadian period. Science 247, 975–978.

Reppert SM, Weaver DR (2001) Molecular analysis of mammalian circadian rhythms. Annu Rev Physiol 63:647-76.

Resnitzky D, Reed SI (1995) Different roles for Cyclins D1 and E in regulation of G1-to-S transition. Mol Cell Biol 15:3463-3469.

Robles MS, Humphrey SJ, Mann M (2017) Phosphorylation is a central mechanism for circadian control of metabolism and physiology. Cell Metab 25:118-127.

Spruck CH, Won KA, Reed SI (1999) Deregulated cyclin E induces chromosome instability. Nature 401:297-300.

Stevens RG (2005) Circadian disruption and breast cancer: from melatonin to clock genes. Epidemiology 16: 254–258.

Takahashi JS, Hong HK, Ko CH, McDearmon EL (2008) The genetics of mammalian circadian order and disorder: implications for physiology and disease. Nat Rev Genet 10:764-75.

Takahashi JS, Hong HK, Ko CH, McDearmon EL (2008) The genetics of mammalian circadian order and disorder: implications for physiology and disease. Nat Rev Genet 9:764-775.

Tyson JJ, Novak B (2008) Temporal organization of the cell cycle. Curr Biol 18:759-768.

Welsh DK, Yoo SH, Liu AC, Takahashi JS, Kay SA (2004) Bioluminescence imaging of individual fibroblasts reveals persistent, independently phased circadian rhythms of clock gene expression. Curr Biol 14:2289-95.

Yagita K, Tamanini F, Yasuda M, Hoeijmakers JH, van der Horst GT, Okamura H (2002) Nucleocytoplasmic shuttling and mCRY-dependent inhibition of ubiquitylation of the mPER2 clock protein. EMBO J 21:1301-14.

Zhang R, Lahens NF, Ballance HI, Hughes ME, Hogenesch JB (2014) A circadian gene expression atlas in mammals: implications for biology and medicine. Proc Natl Acad Sci USA 111: 16219–16224.

Supplementary information

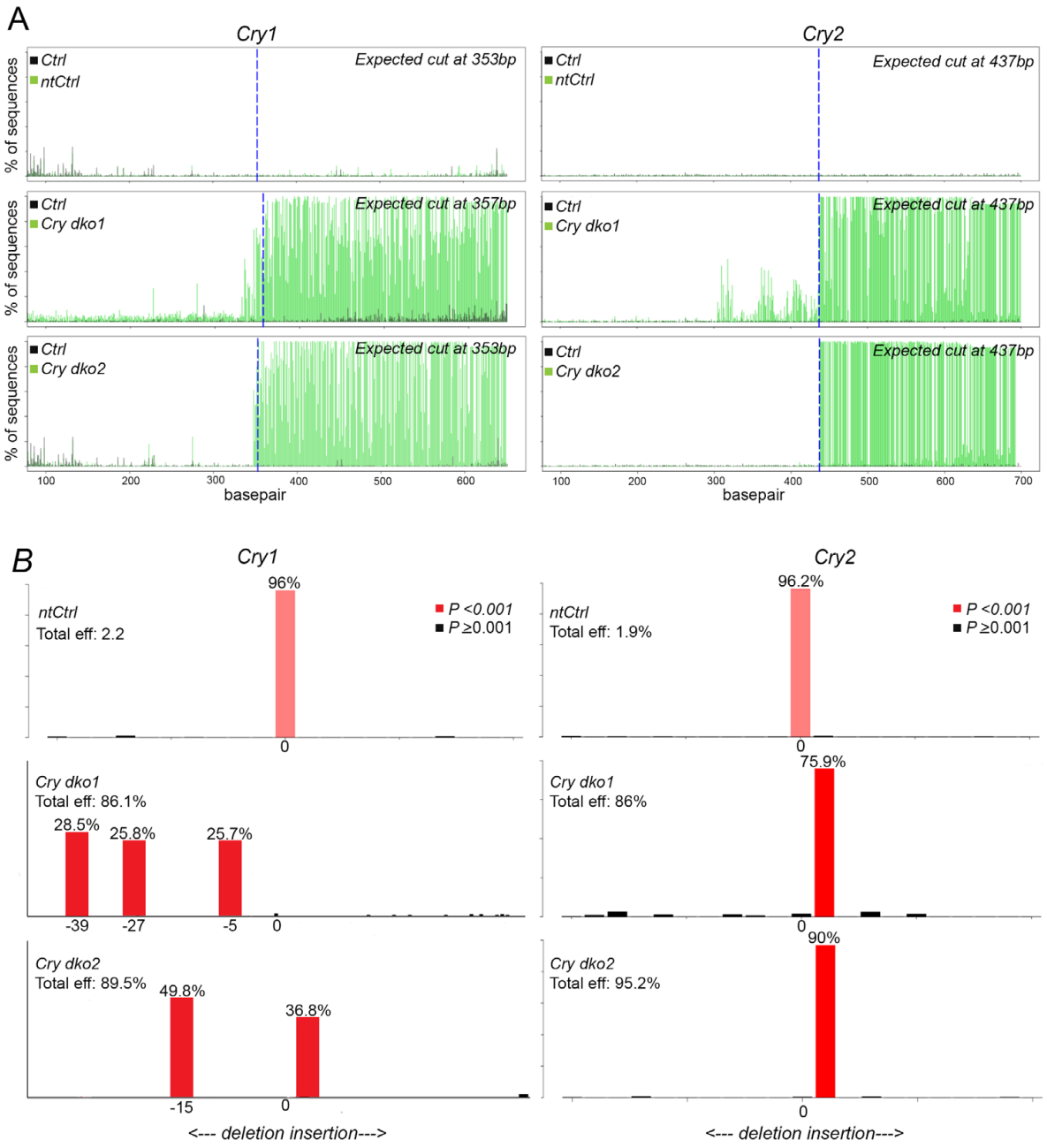

Fig.S1. Evaluation of genome editing using the TIDE algorithm. (A) Aberrant sequence signal in Control (black bars), and targeted cells (green bars). Expected cut site is shown by the vertical blue line. The right panels correspond to the *Cry1* locus and the left panels to the *Cry2* locus (shown are three different clones for each locus). B) Occurrence frequency of Insertions and deletions (Indels) is shown for the Cry1 locus (left panel) and Cry2 locus (right panel). p-value (statistical significance for each Indel) is calculated using the Tide algorithm.

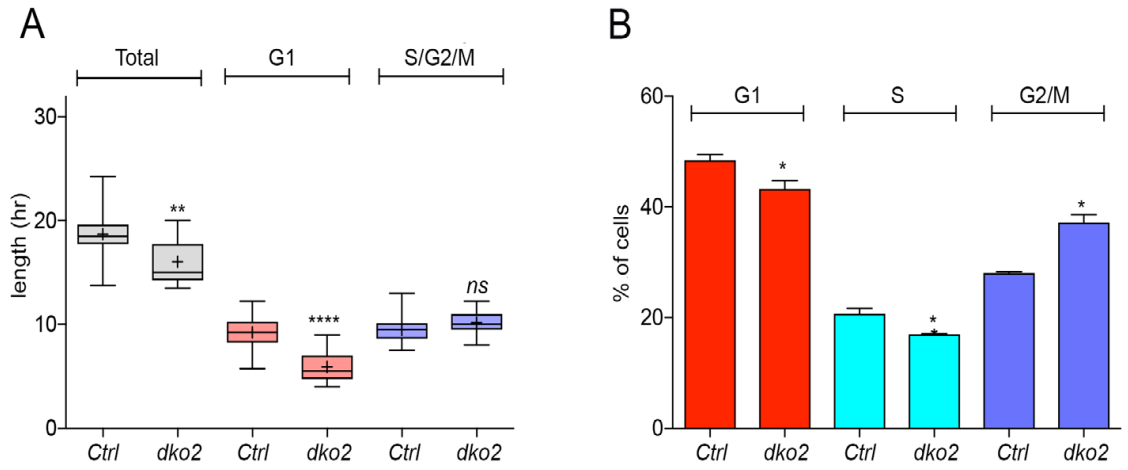

Fig.S2. Cell cycle dynamics in the absence of cryptochromes. (A) Box-whisker plot showing the length of the total cell cycle (grey), G1 (red) and S/G2/M (blue) in Ctrl and Cry dko2 cells (n= 20 cells per condition). The range between the highest and lowest values is shown. The solid line and cross within the box represent the median and mean value, respectively. The lowest and highest boundaries of the box indicate the 25 and 75 percentiles, respectively. ** $p<0.01$ and ****$p<0.0001$(Mann Whitney test). B) Quantification of cell cycle phase distribution of proliferating Ctrl and Cry dko2 cells. Shown is the average of 3 biological replicates (20000 cell counts/per sample). The data were analyzed using the two-tailed paired Student's t-test. Error bars indicate the SEM.

CHAPTER 4

Loss of coupling between the circadian clock and the cell cycle in a mouse breast carcinoma cell line

Names: Elham Farshadi , Esmee van der Ploeg , Conny van Oosterom , Gijsbertus T.J. van der Horst , Inês Chaves

Key words: Circadian clock, Cell cycle, Coupling, MBC399, Cancer

Abstract

Circadian control of cell division is well established in diverse organisms. Recent single cell studies on mouse fibroblast cells have shown that the circadian clock and cell cycle systems are robustly phase-coupled (Feillet et al., 2014; Bieler et al., 2014). The importance of clock-cell cycle coupling in timed mitosis and rhythmic DNA replication in healthy cells is evident (Scheving., 1983; Lévi et al., 2007). However, little is known about the interplay between these two oscillators in cancer cells, which often display de-regulated cell proliferation and circadian gene expression. In this study, we have investigated the reciprocal interaction between the circadian clock and the cell cycle in cancer cells. We introduced a fluorescent clock reporter into a *p53* mutant mouse breast cancer cell line and studied the clock-cell cycle coupling using live single cell imaging. We found that in the mouse breast cancer cell (MBC) line MBC399 the circadian clock is free running and that mitosis occurs independent of the circadian phase. We report here for the first time uncoupling between the circadian and cell cycle systems. Our observation illustrates the principle of chronotherapy that benefits from asynchrony in timed mitosis between the host and the malignant cells in order to predict the optimal time of treatment. Moreover, our study opens possibilities to further investigate the role of uncoupling in malignant cell growth.

Introduction

The circadian clock and cell cycle systems are two biological oscillators that are tightly connected to each other in different species, from unicellular organisms to mammals (Iwasaka et al., 2000; Mori et al., 2000., Reppert et al., 2001).

The circadian system is responsible to adjust the physiology and behaviour of an organism to the environmental changes such as the day/night cycle (Mohawk et al., 2012). The circadian clock is orchestrated in a hierarchy manner with the SCN at the top of hierarchy and peripheral clocks all over the body (Ko et al., 2006). The SCN clocks are entrained by the light signals that they receive from the photoreceptors located in the retinal ganglion (Meijer et al.,2007). Subsequently, the SCN transfers these entraining signals to the peripheral clocks via hormonal or neural cues (Welsh et al., 2004).

Circadian oscillations are generated by a circadian clock based on a network of transcriptional-translational feedback loops, which are governed by a set of clock genes including *Clock, Bmal1, Per (Per1, Per2),* and *Cry (Cry1, Cry2*) (Lowery et al., 2004). The CLOCK/BMAL1 heterodimer induces transcription of the *Per* and *Cry* genes via an E-Box enhancer element in their promoter. PER and CRY proteins heterodimerize and translocate to the nucleus where they inhibit CLOCL/BMAL1-mediated transcription, including their own transcription (Takahashi et al., 2008; Mohawk et al., 2012). *Rev-erbα* is another E-box clock gene that is under direct control of the CLOCK/BMAL1 complex, and plays an additional role in the circadian system to reinforce the strength of the primary negative feedback loop-driven oscillation (Preitner et al., 2002; Lowery et al., 2004). CLOCK/BMAL1 also drives transcription of so the called Clock Controlled Genes (CCGs), comprising at least 10% of the genome (Miller et al., 2007). Rhythmic expression of the CCGs brings rhythmicity to many metabolic and physiological events, including cell proliferation (Fu et al., 2013). Dividing cells copy their genome during S phase, and divide the genome into two daughter cells during mitosis (M phase). These two phases are separated by two gap phases (G1, and G2). During the G1 and G2 phases cells are prepared for the next step by cell growth, protein synthesis, and DNA repair (Norbury et al.,1992). Different cell cycle stages are triggered by a timed oscillation in the abundance of the important cell cycle regulatory molecules (Tyson et al., 2008).

Circadian control of cell proliferation has been shown in different studies. For instance, studies in human oral mucosa and skin have shown circadian rhythmicity in M and G1 phases of the cell cycle (Bjarnason et al., 2001). Bjarnason and co-workers analysed the correlation between rhythmic expression of clock genes and cell cycle markers in human oral mucosa and skin biopsies over the period of 24 hours. The highest level of Per1 mRNA was in the morning, and coincided with the peak expression of P53 as a G1 marker. In contrast, *Bmal1* transcript reached its highest expression at night, showing synchrony with the peak expression of CyclinB1, a marker of G2 and M phase. Rhythmicity in DNA synthesis and mitosis has been also demonstrated in epidermis, spleen, gastro-intestinal tract, and skin of rodent (Scheving., et al 1959; Burns et al., 1976; Scheving et al., 1983; Lévi et al., 2007). Moreover, in unicellular organisms, the circadian clock acts as an extra check point for mitosis, that only

allows the cells to divide at a specific time of the day (Mori et al., 2000).

Recent single cell studies on mouse fibroblast cell lines addressed the influence of the clock on the dynamics of the cell cycle (and vice versa) (Feillet et al., 2015; Bieler et al., 2014). By using the NIH3T3 cell line expressing a fluorescent clock reporter alone (Bieler et al., 2014) or in combination with two cell cycle markers (Feillet et al., 2014), dynamic interactions between the circadian clock and the cell cycle have been addressed. Both studies showed a robust coupling between the circadian clock and cell cycle with a ratio of 1:1 between their respective periods and mitosis always occurring at the same circadian clock phase. Feillet and co-workers proposed a bidirectional coupling between these two oscillators. Altering the cell cycle length, by changing the FBS concentration, impacted on the circadian period accordingly. Similarly, resetting the circadian clock, by the use of the clock synchronizer dexamethasone, clustered mitosis (Feillet et al., 2015). Considering the bi-directional interactions between the circadian oscillator and the cell cycle machinery in healthy cells, it may well be that this link is disrupted in the cancer cells.

Chemotherapy is often making use of cytotoxic drugs in conjugation with radiation therapy targeting dividing cells (Fu et al., 2013). These anti-cancer drugs do not discriminate between active growing host cells and tumor cells. Therefore, chemotherapy is always associated with some toxicity and side effects for the healthy cells. Thus, one of the challenges is to protect the host tissue and specifically target the malignant cells. Biological processes such as drug metabolism and cell proliferation follow a circadian rhythm (Philip et al., 2011; Levi et al., 2007). As a result, efficiency and toxicity of several anticancer drugs differs based on the time of drug administration during the day (Dallmann et al., 2016). On the other hand, dedifferentiated cells or fast growing cells often show different circadian rhythmicity, dampened amplitude, phase shifts and altered clock gene expression (Mormont et al., 1997; Fu et al., 2013). Chronotherapy is benefiting from the differences in circadian physiology between the host and cancer tissues in order to optimize the anti-cancer treatment, by reducing the toxicity of the treatment for the host cells and increasing the efficiency for the cancer cells (Levi et al., 2007). Gaining knowledge about the circadian clock and cell cycle coupling state in metastatic and fast growing cancer cells compared to host tissues may help us to strengthen the effect of chronotherapy.

In this study, we introduced a fluorescent clock reporter (Rev-Erbα-VNP) into a *p53* mutant mouse breast carcinoma cell line and studied the circadian clock and cell cycle progression using live single cell imaging. Our data for the first time show un-coupling between the circadian clock and cell cycle in a cell line.

Materials and Methods

Cell culture

NIH3T3^{3C} cells, containing the *Rev-Erbα-VNP* clock reporter and FUCCI *hCdt1-mKOrange* and *hGeminin-CFP* FUCCI cell cycle reporter genes (Feillet et al., 2015), were cultured in

Dulbecco's Modified Eagle's Medium (DMEM)/F10 (Lonza), containing 10% Fetal Bovine Serum (FBS) (Gibco), 100 U/ml Penicillin and 100 µg/ml Streptomycin (pH7.7) in a standard humidified incubator at 37°C and 5% CO_2). MBC-399 cells were cultured in DMEM/F12 GlutaMAX™ (Gibco), containing 10% FBS (Gibco), 100 U/ml Penicillin and 100 µg/ml Streptomycin, 5 µg/ml insulin (Sigma), 5 ng/ml EGF (Invitrogen), 5 ng/ml cholera toxin (Sigma) (pH 7.7), in a standard humidified incubator at 37°C and 5% CO_2.

To stably introduce a fluorescent circadian clock reporter, MBC-399 cells were seeded at 70% confluency and transfected with the Rev-Erbα-VNP construct (Nagoshi et al., 2004; kindly provided by Dr. Ueli Schibler; 1 µg per 6 well plate) and pcDNA3-neomycin (Invitrogen 200 ng per 6 well plate) using fuGENE transfection reagent (Roche) according to user's manual. Neomycin resistant clones were selected and kept for 2 weeks on 200 µg/ml G418.

Time-lapse Fluorescence Microscopy

For time-lapse imaging of circadian clock performance, cells were grown on glass bottom dishes and placed in the temperature (37°C), CO_2 (5%) and humidity controlled chamber of a live cell imaging Zeiss LSM510/Axiovert 200M confocal microscope, equipped with a 10x Ph objective. Images were recorded every 30 min for at least 72 hours using a Coolsnap HQ/Andor Neo sCMOS camera. Live cell imaging was conducted using the following parameters (as set up in Zeiss 200 software): Venus (yellow): 1000 ms (filter cube: Ex= 475/40 nm, DM= 500 nm, Em= 530/50 nm). Acquired images were concatenated and merged into a single file to generate a movie which was used for further analysis. Single cell numerical time series for the VNP fluorescent marker were generated using the LineageTracker plugin for ImageJ (https://github.com/pkrusche/lineagetracker.jsonexport). Time series were analyzed for circadian clock period. The clock period is defined as the mean intervals between the two peaks of Rev-Erbα-VNP.

Real time bioluminescence monitoring

In order to monitor the circadian clock rhythm, $2x10^5$ MBC399 cells were plated in ø35mm CELLSTAR® Tissue Culture dishes (Greiner Bio-One). Cells were transiently transfected with 1 µg *Bmal1::luciferase* reporter and 4 µl of X-tremeGene HP DNA Transfection Reagent (Roche Life Sciences) per dish, and grown to confluency at 37˚C and 5% CO_2. Confluent cells were circadian clock synchronized for one hour with 100 nM dexamethasone (Sigma). After one hour, the medium was replaced with medium buffered with 25mM HEPES (Lonza) and containing 0.1 mM luciferine (Caliper Life Sciences). The bioluminescence signal was monitored for 7 days (60 sec measurements at 10 min intervals) in a standard dry incubator using a LumiCycle 32-channel automated luminometer (Actimetrics), placed in a dry incubator at 37 °C. Prior to placing dishes in the LumiCycle, the lid was replaced by a glass coverslip and sealed with parafilm. The data were extracted using Actimetrics software and analyzed using Microsoft Excel.

Quantitative real time PCR

To analyze circadian clock gene expression, MBC 399 cells were seeded in triplicate in 6 well plates and grown to confluency, after which cellular clock were synchronized with a 1-hour pulse of 100 nM dexamethasone (Sigma). Cells were harvested at 24, 28, 32, 36, 40, and 44 hours after synchronization. Total RNA was isolated using TRIzol reagent (Life Technologies, Carlsbad, CA, USA) following manufacturer's protocol and first strand cDNA was synthesized using iScript cDNA Synthesis Kit (Bio-Rad) according to the manufacturer's protocol.

qPCR was performed in 384-well plates using iQ SYBR® Green Supermix (Bio-Rad) according to the manufacturer's protocol, using the following forward and reverse primers: *Rev-erbα*: Fwd 5'-ACC TTA CTG CTC AGT GCC TGG AAT-3' and Rev 5'-TGG ACC TTG ACA CAA ACT GGA GGT-3'. *Bmal1*: Fwd 5'-GAC ATA GGA CAC CTC GCA GA-3' and Rev 5'-GCC TTC CAG GAC ATT GGC TAA-3'. *Cry1*: Fwd 5'-CTC CAG CGG AAA CGA GAA CTG-3' and Rev 5'-GCT GTC CCC GAA TCA CAA ACA -3'. *Per2*: Fwd 5'-AGG ATC TTG ATG CCA ATC TAC GA-3' and Rev 5'-TTG GCA GAC TGC TCA CTA CTG-3'. *B2M*: Fwd 5'-ACC GGC CTG TAT GCT ATC CAG AAA-3' and Rev 5'- ATT TCA ATG TGA GGC GGG TGG AAC-3'.

All samples were analyzed in quadruplicate. Expression levels were normalized to the housekeeping gene beta-2-microglobulin (B2M) and plotted relative to the first time point. Relative gene expression was calculated using the comparative C(t) method described by Livak et al 2001.

Statistical analysis

For single cell studies, after performing the normality test, the two-tailed Mann-Whitney test was used to analyze the period of the circadian clock and of the cell cycle. Statistical analysis of circadian gene expression was performed using CircWave (R. Hut, University of Groningen).

Results

Clock performance in MBC399 cells

To study interactions between the circadian clock and the cell cycle in cancer cells, we used a mouse breast carcinoma cell line (MBC399) derived from a tumor obtained from a mammary epithelial cell specific $p53^{R270H/+}$ mouse (Wijnhoven et al., 2005; Van Dycke et al., 2015). First, we examined the circadian properties of the MBC399 cell line. To this end, MBC399 cells were transiently transfected with a *Bmal1* promoter-driven luciferase reporter construct (*Bmal1::Luc*), and bioluminescence was monitored in real time in clock synchronized cell cultures. As shown in Fig. 1A, MBC399 cells show robust bioluminescence rhythms with a

circadian period of 23.08 ± 0.11 hours, which well matches with that of established normal mouse cell lines such as NIH3T3.

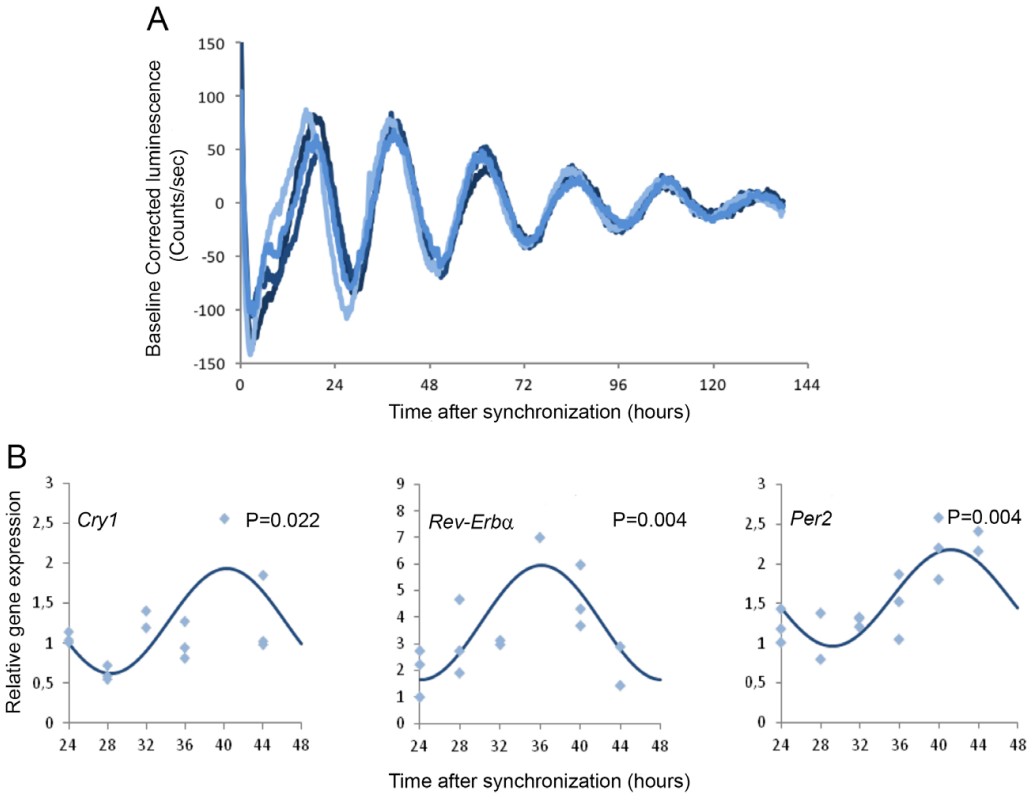

Figure 1. Circadian clock performance of MBC399 breast carcinoma cells. (A) Representative example of bioluminescence rhythms in clock synchronized confluent cultures of Bmal1::Luc transfected MBC399 cells. The Y-axis represents the baseline corrected oscillations in bioluminescence. The X-axis represents the time after synchronization. τ = 23.08 ± 0.11 hours (period of the oscillation; n=4). (B) Relative gene expression of the clock genes Cry1, Rev-erbα and Per2 over a period of 20 hours, starting 24 hour after clock synchronization. The line represents the fitted curve generated by CircWave, the dots represent the individual samples (n=3 per time point).

To analyze endogenous circadian clock gene expression, confluent MBC399 cell cultures were clock synchronized with dexamethasone, and total RNA was isolated 24, 28, 32, 36, 40, and 44 hours after synchronization. As shown in Fig. 1B, a significant circadian oscillation in gene expression of core clock genes has been observed (*Cry1* p=0.022, *Rev-erbα* p=0.0043, and *Per2* p=0.0045). Taken together, these data demonstrate that MBC399 cells contain a functional circadian oscillator that responds normally to clock synchronizing chemical cues.

The circadian clock-cell cycle coupling is lost in the MBC399 breast cancer cells

To follow the kinetics of the circadian clock in individual cells by live cell imaging, we stably introduced the fluorescent REV-Erbα-VNP reporter (previously described by Nagoshi

et al., 2004) in MBC399 cells and compared clock performance with that of NIH3T3^{3C} normal mouse fibroblasts previously generated in our lab (Feillet et al., 2014). Likewise, we followed cell division by phase contrast microscopy (as described by Nagoshi et al., 2004).

Fig. 2A shows time lapse fluorescence and phase contrast images of a representative single NIH3T3^{3C} cell, spanning one complete circadian cycle. In line with our previous observations, REV-ERBα-VNP fluorescence shows a robust oscillation, with mitosis (indicated by a red arrow) occurring consistently at the trough level of REV-ERBα-VNP expression, indicative for 1:1 phase coupling of the circadian clock and cell cycle (Fig. 2B). Consistent with circadian clock-cell cycle phase coupling, subsequent analysis of the circadian clock period (calculated from the interval between two peaks of Rev-ERBα-VNP) and cell cycle period (as calculated from the interval between two mitotic events) revealed statistically similar ($p=0.4$) cycle lengths of 17.6 ± 2.2 h (mean ± SD; Fig. 1*C* Lower panel) for the circadian clock and 17.1 ± 1.9 h (mean ± SD; Fig. 2*C* upper panel) for the cell cycle.

Next, we repeated this analysis for proliferating MBC399 cells. Fig. 2D shows a representative example of time lapse images of a single MBC399 cell, spanning a complete circadian cycle. Interestingly, and in marked contrast to NIH3T3^{3C} cells, mitosis in MBC399 cells occurs randomly and independent of the circadian phase (Fig. 2E). Moreover, whereas the mean cell cycle period of proliferating MBC399 cells is 15.9 ± 2.1 h (mean ± SD; Fig. 1F upper panel), we observed a significantly longer ($p<0.0001$) clock period spanning 25.8 ± 3.1 h (mean ± SD; Fig. 2F lower panel). The circadian period of proliferating MBC399 cells is similar to that of confluent MBC399 cells (23.08 ± 0.11). These findings suggest that the circadian clock in proliferating MBC399 cancer cells is free-running and that the circadian clock and cell cycle are no longer phase coupled.

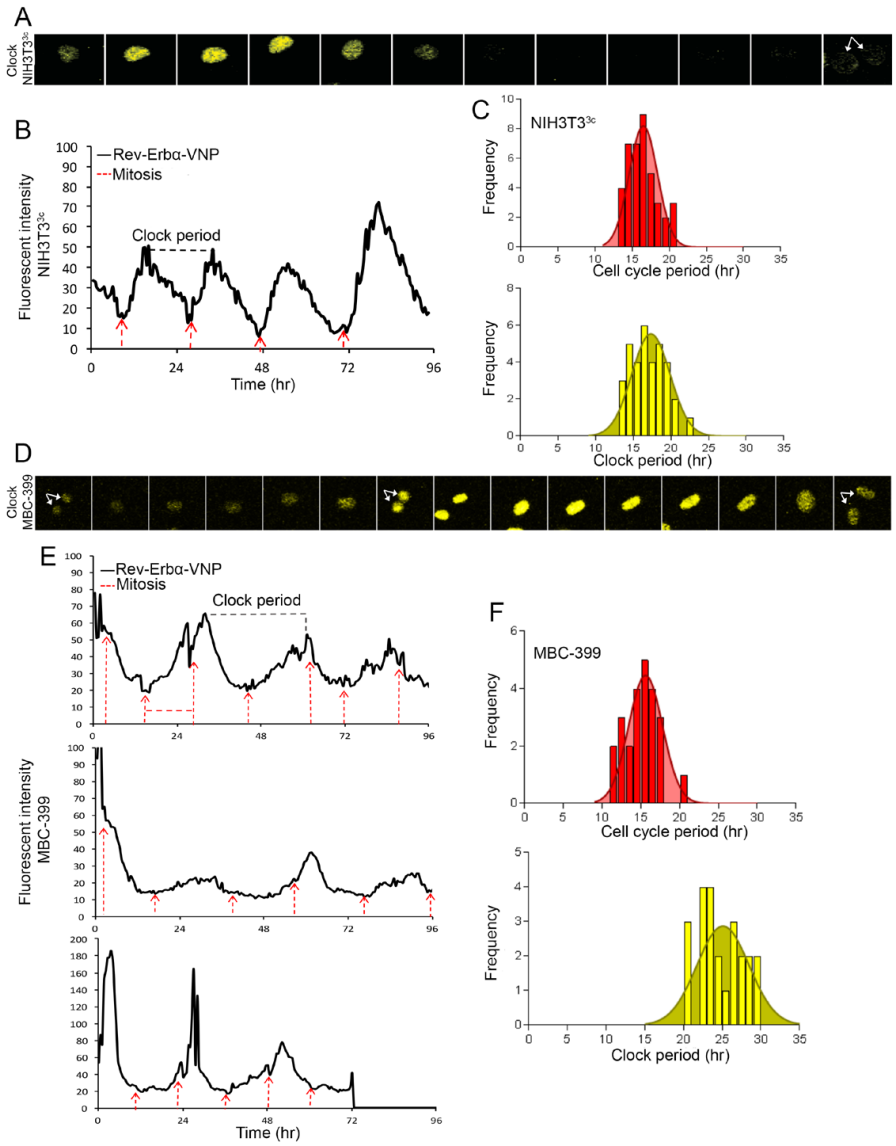

Figure 2. Circadian clock and cell cycle dynamics of MBC399 carcinoma cells. (A) Representative example of time series images of the nucleus of a proliferating NIH3T3^{3C} cell, stably expressing the circadian clock reporter (Rev-Erbα-VNP; yellow). Shown are images at 1.5 hour time intervals over a 18 h period, spanning one circadian cycle. The white arrows represent cytokinesis. **(B)** Representative example of fluorescence rhythms of Rev-Erba-VNP expression (NIH3T3^{3C}) during a period of 96 hours. Cell division is marked by the red arrows. **(C)** Frequency graph, showing cell cycle period (upper panel) and clock period (lower panel) of individual NIH3T3 cells (n=40). Mean and standard deviation are shown. **(D)** Representative example of time series images of the nucleus of a proliferating MBC399 cell, stably expressing the fluorescent circadian clock reporter Rev-Erbα-VNP (yellow). Shown are images at 2 hour time intervals over a 30 h period, spanning one circadian cycle. The white arrows represent cell division. **(E)** Representative examples (3 different cells) of fluorescence intensities of the Rev-Erbα-VNP signal (MBC399) during a period of 96 hours. Cell division is marked by the red arrows. **(F)** Frequency graph, showing cell cycle period (upper panel) and clock period (lower panel) of individual MBC399 cells (n=25).

Discussion

In this study, we have analyzed the relation between the circadian clock and cell cycle in the $p53^{R270H/+}$ mutant mouse breast carcinoma cell line MBC399 and observed that whereas the cell cycle period of MBC399 cancer is in the same range as that of proliferating normal $NIH3T3^{3C}$ fibroblasts, the circadian period is significantly higher. In proliferating $NIH3T3^{3C}$ cells, the circadian clock and the cell cycle are phase coupled at a 1:1 ratio, and accordingly synchronously oscillate with a period of approximately 17 hours. We have recently obtained first evidence that upon reaching confluency, the period of circadian oscillations in $NIH3T3^{3C}$ cells shifts to a free-running period close to 24 hours. This finding strongly suggests that the cell cycle can synchronize the circadian clock of cells in proliferating state. The circadian period of proliferating MBC399 cells, however, does not follow the cell cycle period and in fact resembles that of confluent cells. Moreover, mitosis in proliferating MBC399 cells occurs independent of the circadian phase. To our knowledge, this is the first example of a cell line in which clock and cell cycle systems are uncoupled and free-running. Importantly, further research involving other cell lines of the MBC mouse breast cancer cell panel, as well as other rodent and human tumor cell lines, should provide insight in whether the circadian clock - cell cycle uncoupling occurred incidentally, or is a common feature of cancer cells.

The obvious question arising is which key molecules mediate the coupling of these two intracellular oscillators. So far, the P53 tumor suppressor protein is the only identified cell cycle molecule that has mutual influences on both clock and cell cycle systems (Miki et al., 2013). As tumorigenesis in the $p53^{R270H/+}$ mouse model likely requires loss of the wild type *p53* allele (Olive et al., 2004**;** Wijnhoven et al., 2005) it would be interesting to correct the MBC399 cell line with a wild type p53 allele and investigate whether this would restore the coupling between the clock and cell cycle. We found that the cellular clock-cell cycle coupling is intact in a *P53* mutant human lung carcinoma cell line (H1299) (data is not shown). This indicates that P53 deficiency alone does not lead to loss of coupling. Genome and transcriptome analysis of proliferating MBC399 cells could be an effective way to identify key candidate coupling proteins and for uncovering the underlying mechanism behind the clock - cell cycle coupling.

Drugs used in cancer therapy often target specific cell cycle phases (Lévi et al.,2007). For instance, chemotherapeutic drugs such as 5-fluorouracil act on S-phase cells, whereas other drugs such as taxanes exert their highest toxicity on M-phase cells. The 24-hour rhythmicity in cell proliferation allowed the development of new cancer chemotherapeutic approaches which focus on the determination of the best treatment time (Levi et al.,2007). Extending the current knowledge of the circadian clock-cell cycle coupling mechanism in cancer cells will enable the development of new chronotherapuetic approaches in which the clock-cell cycle coupling in the normal tissue is used to predict the optimal time of treatment. For example, by choosing a time window in which normal cells are less sensitive to the treatment, while malignant cells undergo random cell division independent of the circadian phase. Our finding that in cancer cells the circadian clock and cell cycle can be uncoupled has shed new light on

the interplay between these two systems in cancer cells and may facilitate further improvement of cancer treatment.

References

Bieler J, Cannavo R, Gustafson K, Gobet C, Gatfield D, Naef F (2014) Robust synchronization of coupled circadian and cell cycle oscillators in single mammalian cells. *Mol Syst Biol* 10:739.

Bjarnason GA Jordan RCK, Wood PA Li Q, Lincoln DW, Sothern RB, Hrushesky WJM, Ben-David Y (2001) Circadian expression of clock genes in human oral mucosa and skin. *Am J Pathol* 158:1793-1801.

Burns ER, Scheving LE, Pauly JE, Tsai T (1976) Effect of altered lighting regimens, time-limited feeding, and presence of Ehrlich ascites carcinoma on the circadian rhythm in DNA synthesis of mouse spleen. *Cancer Res* 36:1538-44.

Dallmann R, Okyar A, Lévi F (2016) FDosing-Time Makes the Poison: Circadian Regulation and Pharmacotherapy. 22:430-445.

Feillet C, Krusche P, Tamanini F, Janssens RC, Downey MJ, Martin P, Teboul M, Saito S, Lévi FA, Bretschneider T, van der Horst GTJ, Delaunay F, Rand DA (2014) Phase locking and multiple oscillating attractors for the coupled mammalian clock and cell cycle. *Proc Natl Acad Sci USA* 111:9828-9833.

Feillet C, van der Horst GT, Levi F, Rand DA, Delaunay F (2015) Coupling between the Circadian Clock and Cell Cycle Oscillators: Implication for Healthy Cells and Malignant Growth. *Front Neurol* 6:96.

Filipski E, King VM, Etienne MC, Li X, Claustrat B, Granda TG, Milano G, Hastings MH, Levi F (2004) Persistent twenty-four hour changes in liver and bone marrow despite suprachiasmatic nuclei ablation in mice. *Am J Physiol Regul Integr Comp Physiol* 287: 844-51.

Fu L, Kettner NM (2013) The circadian clock in cancer development and therapy. *Prog Mol Biol Transl Sci* 119:221-282.

Gery S, Komatsu N, Baldjyan L, Yu A, Koo D, Koeffler HP (2006) The circadian gene Per1 plays an important role in cell growth and DNA damage control in human cancer cells. *Mol Cell* 22:375-382.

Geyfman M, Kumar V, Liu Q, Ruiz R, Gordon W, Espitia F, Cam E, Millar SE, Smyth P, Ihler A, Takahashi JS, Andersen B (2012) Brain and muscle Arnt-like protein 1 (BMAL1) controls circadian cell proliferation and susceptibility to UVB-induced DNA damage in the epidermis. *Proc Natl Acad Sci U S A* 109:11758-11763.

Iwasaki H, Kondo T (2000) The current state and problems of circadian clock studies in cyanobacteria. *Plant Cell Physiol* 41:1013-20.

Ko CH, Takahashi JS (2006) Molecular components of the mammalian circadian clock. *Hum Mol Genet* 2:271-7.

Lévi F (2002) From circadian rhythms to cancer chronotherapeutics. *Chronobiol Int* 19:1-19.

Lévi F, Filipski E, Iurisci I, Li XM, Innominato P (2007) Cross-talks between circadian timing system and cell division cycle determine cancer biology and therapeutics. *Cold Spring Harb Symp Quant Biol* 72:465-475.

Levi F, Schibler U (2007) Circadian rhythms: mechanisms and therapeutic implications. *Annu Rev Pharmacol Toxicol* 47:593-628.

Livak KJ, Schmittgen TD (2001) Analysis of relative gene expression data using real-time quantitative PCR and the 2(-Delta Delta C(T)) Method. Methods 25:402-8.

Lowery PL, Takahashi JS (2004) Mammalian circadian biology: elucidating genome-wide levels of temporal organization. *Annu Rev Genomics Hum Genet* 5:407-401.

Matsuo T, Yamaguchi S, Mitsui S, Emi A, Shimoda F, Okamura H. Control Mechanism of the Circadian Clock for Timing of Cell Division in Vivo. *Science*, 2003, 302 (5643): 255-259.

Meijer JH, Michel S, Vansteensel MJ (2007) processing of daily and seasonal light information in the mammalian circadian clock. *Gen Comp Endocrinol* 152:159-64.

Miki T, Matsumoto T, Zhao Z, Lee CC (2013) p53 regulates Period2 expression and the circadian clock. *Nat Commun* 4:24444.

Miller BH, McDearmon EL, Panda S, Hayes KR, Zhang J (2007) Circadian and CLOCK-controlled regulation of the mouse transcriptome and cell proliferation. *Proc Natl Acad Sci U* 104:3342–3347.

Mohawk JA, Green CB, Takahashi JS (2012) Central and peripheral circadian clocks in mammals. *Annu Rev Neurosci* 35: 445-462.

Mori T, Johnson CH (2000) Circadian control of cell division in unicellular organisms. *Prog Cell Cycle Res* 4:185-192.

Mormont MC, Lévi F (1997) Circadian-system alterations during cancer processes: a review. *Int J Cancer* 70:241-247.

Nagoshi E, Saini C, Bauer C, Laroche T, Naef F, Schibler U (2004) Circadian gene expression in individual fibroblasts: cell-autonomous and self-sustained oscillators pass time to daughter cells. *Cell* 119:693-705.

Norbury C, Nurse P (1992) Animal cell cycles and their control. *Annu Rev Biochem* 61:441-70.

Olive Kp, Tuveson DA, Ruhe ZC, Yin B, Willis NA, Bronson RT, Crowley D, Jacks T (2004) Mutant p53 gain of function in two mouse models of Li-Fraumeni syndrome. Cell 119:847-60.

Philip AK, Philip B (2011) Chronopharmaceuticals: hype or future of pharmaceutics. *Current pharm des* 17:1512–1516.

Preitner N, Damiola F, Lopez-Molina L, Zakany J, Duboule D, Albrecht U, Schibler U (2002) The orphan nuclear receptor REV-ERBalpha controls circadian transcription within the positive limb of the mammalian circadian oscillator. *Cell* 110:251–260.

Reppert SM, Weaver DR (2001) Molecular analysis of mammalian circadian rhythms. *Annu Rev Physi-o*l 63:647-76.

Scheving LE (1959) Mitotic activity in the human epidermis. *Anat* Rec 135:7-19.

Scheving LE, Tsai TH, Scheving LA (1983) Chronobiology of the intestinal tract of the mouse. *Am J Anat* 168:433-65.

Takahashi JS, Hong H.K, Ko C.H, McDearmon E.L (2008) The genetics of mammalian circadian order and disorder: implications for physiology and disease. *Nature* 9:764-775.

Tyson JJ, Novak B (2008) Temporal Organization of the Cell Cycle. *Curr Biol* 18:759-68.

Welsh DK, Yoo SH, Liu AC, Takahashi JS, Kay SA (2004) Bioluminescence imaging of individual fibroblasts reveals persistent, independently phased circadian rhythms of clock gene expression. *Curr Biol* 14:2289-95.

Wijnhoven SW, Zwart E, Speksnijder EN, Beems RB, Olive KP, Tuveson DA, Jonkers J, Schaap MM, van den Berg J, Jacks T, van Steeg H, de Vries A (2005) Mice expressing a mammary gland-specific R270H mutation in the p53 tumor suppressor gene mimic human breast cancer development. *Cancer Res* 65:8166-8173.

CHAPTER 5

Circadian clock genes differentially modulate the cancer properties of H1299 human non-small lung carcinoma cells

Names: Romana M. Nijman, Elham Farshadi, Cesar E. Payan Gomez, Cíntia R. Bombardieri, Roel Janssens, Stefanie Vester, Yanto Ridwan, Filippo Tamanini, Gijsbertus T.J. van der Horst and Inês Chaves *

Key words: circadian clock, cancer, proliferation, transcriptomics

Abstract

The circadian clock is an internal time-keeping system that generates near 24-hour rhythms in the physiology, metabolism and behavior of most organisms. At the cellular level, circadian rhythms are generated by a molecular oscillator, composed of clock genes and proteins, that act in transcription/translation based feedback loops. Several epidemiological and animal studies have demonstrated that disruption of the circadian system increases cancer risk and accelerates tumor progression. Furthermore, we have recently shown in a murine cell line that the positive (*Bmal1* and *Clock)* and negative (*Cry1* and *Cry2*) limb of the circadian oscillator differentially affect cell cycle length, and could therefore have opposite influence on cancer development. In the present study we have used the human small lung carcinoma cell line H1299 to investigate the impact of the circadian clock on cancer cell properties. To this end, we generated stable knockdown cell lines for the *BMAL1* and *CRY* genes and performed transcriptomics analysis. We subsequently measured cancer cell hallmarks such as proliferation rate, migration, invasion and tumor growth, all of which were altered according to the transcriptomics data. Our results demonstrate that clock genes *BMAL1* and *CRY* are involved in determining the proliferative capacity, cell migration and invasiveness of H1299 cells, and differentially regulate their tumor forming ability. A comparison with literature reveals that the impact of clock gene function on cancer properties could well be tumor cell specific and may vary with the spectrum of mutations in cell cycle and DNA damage response genes. Importantly, our data show that comparative transcriptome profiling is a good measure of the in vivo tumorigenic properties of cancer cell lines.

Introduction

As a consequence of the earth's rotation around its own axis, most forms of life are exposed to recurring light/dark and temperature changes (Dunlap et al., 1999). To anticipate to these daily environmental cycles, most organisms have developed an internal circadian clock with a near (circa) 24-hour (dies) periodicity that adjusts behavior, physiology and metabolism (e.g. body temperature, sleep-wake cycle, blood pressure, hormone secretion) to the needs across the day (Albrecht et al., 2003; Pittendrigh et al., 2003). In mammals, the circadian system is composed of a master clock in the neurons of the suprachiasmatic nuclei (SCN) in the anterior hypothalamus, and peripheral clocks in virtually all other cells and tissues. To keep synchrony with the light-dark cycle, the SCN clock is daily reset by light. In turn, the SCN synchronizes the peripheral clocks through neuronal connections and through the release of humoral factors (Reppert et al., 2002, Weaver et al., 1998, Welsh et al., 2010). Besides peripheral tissues, cells in culture also exhibit circadian rhythms (Yoo et al., 2004, Balsalobre et al., 1998).

At the molecular level, circadian rhythms are generated by a self-sustained oscillator composed of clock genes and proteins. The circadian oscillator consists of positive and negative transcription translation feedback loops (TTFL) that are rhythmically activated and repressed to maintain a 24-hour periodicity. The heterodimeric bHLH-PAS transcription factors CLOCK and BMAL1 drive the transcription of E-box promoter containing target genes such as the *Period* (*PER*) *1* and *2* and *Cryptochrome* (*CRY*) *1* and *2* genes and the *REV-ERB-α* gene. In the negative loop, the PER and CRY proteins form a heterodimeric complex that translocates to the nucleus and represses CLOCK/BMAL1-driven transcription, thereby inhibiting their own expression (Reppert et al., 2001; Ko et al., 2006). In the positive feedback loop, the REV-ERBα protein rhythmically inhibits RORα-mediated transcription of the *BMAL1* gene, thereby conferring robustness to the molecular oscillator (Preitner et al., 2002; Sato et al., 2004). Central and peripheral oscillators are composed of the same set of clock genes and proteins (Yagita et al., 2001).

Several studies have shown that approximately 10% of all genes are under circadian regulation (Panda et al., 2002, Storch et al., 2002). Such clock controlled genes (CCGs) are tissue-specific and couple circadian output processes to defined stages of the day. Interestingly, among the CCGs are genes involved in cell-cycle regulation and cell growth. Moreover, it has been proposed that the circadian system can act as a gatekeeper of cell cycle progression, as illustrated by the synchronization of cell divisions in epithelial tissues (Matsuo et al., 2003; Miller et al., 2007; Bjarnason et al., 2000; Feillet et al., 2014; Bieler et al., 2014).

Since loss of cell cycle control is the hallmark of a cancer cell, and given the intimate link between the circadian clock and the cell cycle, it is not surprising that genetic or environmental disturbance of the circadian system promotes carcinogenic events. Several epidemiological studies have shown that chronic disruption of the human circadian clock by shift work increases cancer incidence and negatively affects the prognosis of cancer patients (Hansen et al., 2006). Moreover, mutations in the core circadian clock genes *PER1* and *PER2* have

been identified in human breast and colon cancer (Sjöblam et al., 2006., Winter et al., 2007). Furthermore, several animal studies have demonstrated a link between disturbed circadian rhythmicity and enhanced tumor proliferation. Mice with a complete ablation of the SCN demonstrated not only a loss of rhythmic locomotor activity in constant darkness, but under these conditions also exhibit accelerated growth of implanted tumors (Filipski et al., 2002, 2003). Likewise, when chronically exposed to jet lag conditions, wild type mice exhibit accelerated tumor growth compared to mice kept in regular LD cycles (Filipski et al., 2004; Van Dycke et al., 2015). At the genetic level, mice lacking the *Per1*, *Per2*, *Cry1*/*Cry2* or *Bmal1*, demonstrated to be cancer prone after exposure to a single sub lethal dose of γ-radiation (Lee te al., 2010., Fu et al., 2002). The PER1 and PER2 proteins are also known to possess a tumor suppressor function by regulating cell-cycle genes that activate DNA damage checkpoints (Fu et al., 2002., Yang et al., 2009., Hua et al., 2006). A recent study contradicts this finding (Antoch et al., 2013), suggesting that the role of clock genes in cancer properties is not straightforward.

The involvement of the core clock genes in tumor progression is still poorly understood. In the present study, we investigated the impact of RNAi mediated clock gene knockdown in the well characterized human lung carcinoma cell line H1299. We focused on BMAL1 and CRY which are the dominant elements of the positive and negative limb of the circadian oscillator, respectively, and which we have shown to have opposite effects on cell cycle length (Farshadi et al., submitted for publication; Farshadi et al., manuscript in preparation). The initial step was to compare transcriptomics profiles by RNA sequencing. Significantly affected processes were further analyzed in vitro, notably proliferation rate, cell migration and invasiveness. Capacity of the knockdown cell lines to form tumors in vivo was analyzed using a xenograft model. Our data demonstrate that the core circadian clock genes *BMAL1* and *CRY1*/*2* have a significant effect on cancer progression. These findings may ultimately contribute to improving treatment of this type of lung cancer.

Materials and Methods

Cell culture

The human non-small-lung adenocarcinoma cell line H1299 was obtained from the American Type Culture Cell Collection (ATCC). The H1299 cell line was cultured in RPMI 1640 (Gibco) containing 10% fetal bovine serum (FBS) (Gibco) and 100 U/ml penicillin/streptomycin (Gibco) under the condition of 5% $C0_2$ at 37°C.

shRNA transfection

Initially, the H1299 cell line was transduced with a lentiviral construct expressing the firefly luciferase from the mouse *Per2* promoter (Oklejewicz *et a*l., 2008) to obtain a stable cell line. that allows real time recording of circadian oscillations.

In order to obtain a stable knock-down of clock genes, the *Per2::Luc* H1299 cell line was plated in a 24-well plate and grown to 50% confluency. Subsequently, the cells were transfected with pLKO.1-pura vectors (Sigma) expressing shRNA targeting *BMAL1* (TRCN0000095054), *CRY1* (TRCN0000011304), *CRY2* (TRCN0000078302), or a control non-targeting hairpin (SHC002). Cells were kept under puromycin selection for 2 weeks in order to obtain stable cell lines with inactivated core clock genes.

Real-time bioluminescence monitoring

In order to monitor circadian core clock performance, H1299 cells were cultured in RPMI 1640 medium buffered with 25 mM HEPES (Gibco) containing 0.1 mM luciferin (Sigma). After synchronization of intracellular clocks by treatment of confluent cultures with forskolin (Sigma) (dissolved in 100% ethanol, added to the culture medium at a final concentration of 10 μM, bioluminescence was recorded for 6 days (75 sec measurements at 10 min intervals) with a LumiCycle 32-channel automated luminometer (Actimetrics) placed in a dry, temperature-controlled incubator at 37°C. Data was analyzed with the Actimetrics software.

RNA isolation and quantitative PCR

Total RNA was isolated from cultured cells in triplicate using TRIzol (Invitrogen) following manufacturer's instructions. First-strand cDNA was synthesized from 1 mg of total RNA using oligo (dT) primers and SuperScript reverse transcriptase (Invitrogen) according to the manufacturer's protocol. Quantitative PCR amplification was performed using the iCycler iQ™ Real-Time PCR Detection System (BioRad), with SYBR-green and primer sets generating intron-spanning products of 150-300 bp. The following forward and reverse primers were used: *CRY1*: 5'-AGC TTT CAC GAT ATA GAG GAC-3' and 5'-CTT GAG AGC AAC TTC CAC TG-3'; *CRY2*: 5'-GGA CTA CAT CAG GCG ATA CC-3' and 5'-CTG GTA AAT CTG CTT CAT TCG T-3'; *BMAL1*: 5'-TCT TCT ATT CTT GGT GAG AAC CC-3' and 5'-TCC TTA TCC AGT AAG CTT CAC AG-3'; *CLOCK*: 5'-TTC CCT CAG TCA CAT CAC CAG CAA-3' and 5'-TGC TGG AAC TTT CCC TCC TTT CCT-3'; *PER1*: 5'-ATG ACC TCT GTG CTG AAG CAG GAT-3' and 5'-TCC ACA CAG GCC ATC ACA TCA AGA-3'; *PER2*: 5'-TGA GAA GAA AGC TGT CCC TGC CAT-3' and 5'-GAC GTT TGC TGG GAA CTC GCA TTT-3'; *β2M*: 5'-CTC TTG TAC TAC ACT GAA TTC A-3' and 5'-CCT CCA TGA TGC TGC TTA CA-3'; *HPRT*: 5'-TGG AGT CCT ATT GAC ATC GCC AGT-3' and 5'-AAC AAC AAT CCG CCC AAA GGG AAC-3'; *GAPDH*: 5'-AAG GTG AAG GTC GGA GTC AA-3' and 5'- ACC ATG TAG TTG AGG TCA ATG-3'. The generation of specific products was confirmed by melting curve analysis, and primer pairs were tested with a logarithmic dilution of a cDNA mix to generate a linear standard curve, which was used to calculate primer pair efficiencies. Expression levels were normalized to hypoxanthine guanine phosphoribosyl transferase (*HPRT*), β2 microglobulin (*β2M*) and Glyceraldehyde-3-phosphate dehydrogenase (*GAPDH*) mRNA levels.

Western Blot analysis

Whole cell extracts from H1299 core clock gene knockdown and control lines were obtained by lysing the cells with NP40 lysis buffer (1% Triton, 50 mM Tris-HCl pH8, 150 mM NaCl). Protein content was determined with the BCA Protein Assay Reagent (Thermo Scientific). Proteins were separated on a 4-12 gradient polyacryl amide gel (Invitrogen) and transferred to a nitrocellulose membrane (Schleicher and Schuell). Following incubation with blocking buffer (3% non-fat milk and 1% BSA) at RT for 2 hours, the membranes were incubated overnight with primary antibodies (1:1000 dilution) against core clock proteins at 4°C. After incubation with the secondary antibody (1:1000 dilution), bands were visualized using the ECL detection kit (Amersham) following the manufacturer's instructions. The bands were analyzed by Image Quant analysis software, using actin as a loading control. Primary antibodies against actin (sc10231), BMAL1 (sc48790), CRY1 (sc101006), and CRY2 (sc130731) were purchased from Santa Cruz Biotechnology Inc.

Transcriptomics analysis

To analyze circadian gene expression in the H1299 cell lines, cells were seeded in 35 mm dishes at a density of 2 x 105 cells and were harvested in log phase. RNA was isolated and purified with the NucleoSpin kit (Machery-Nagel) according to the manufacturer's protocol. Prior to processing samples for RNA Seq analysis, the quality of the experiment (i.e. synchronization) was confirmed by qPCR analysis of clock and clock-controlled gene expression as described above. For RNA sequencing, quality control and sequencing was performed at ServiceXS (Leiden, The Netherlands). FPKM values (FPKM + value1: a value of "1" was added to each value) were imported into OmniViz version 6.1.13.0 (Instem Scientific, Inc., UK). For each gene, the geometric mean of the value for all samples was calculated. The level of expression of a gene was determined relative to this geometric mean and log2-transformed. The geometric mean of the counts of all samples was used to ascribe equal weight to gene expression levels with similar relative distances to the geometric mean. Unsupervised cluster analyses was performed in Omniviz using Pearson's correlation in the Correlation View. Supervised analysis was done using statistical analysis of microarrays (SAM) to identify differentially expressed genes (DEG). Cutoff values for significantly expressed genes were a false discovery rate (FDR) of 0.05 or less and absolute fold change of 1.5. Functional annotation of the DEG was done using Ingenuity Pathway Analysis (Ingenuity, Mountain View, CA)

Proliferation, cell migration and cell invasion assays

To determine the proliferation rate of the H1299 core clock gene knockdown and control lines, $1x10^3$ cells were seeded in a 96-well plate. The cell growth was measured daily using the WST-1 assay (Roche) following the manufacturer's instructions. Assays were performed in triplicate.

In addition, we determined the cell cycle phase distribution over a 48 hour period after seeding $2x10^5$ cells. Cells were harvested at indicated time-points, washed with PBS and fixed with 70% ethanol. The fixed cells were washed with PBS and incubated with PBS containing 100 µg/ml RNase and 50 µg/mg propidium iodide (Sigma) for 30 min at 37°C. The cells were analyzed by a Becton Dickinson FACScan Flow Cytometer. The flow cytometry data were analyzed in FlowJo.

Cell migration and invasion were assayed in real time mode using the xCELLigence DP system (Roche diagnostics), in a 37°C incubator at 5% $C0_2$. For the migration assay, $5x10^4$ cells were seeded in the upper chamber containing RPMI 1640 medium without FBS. The lower chamber was filled with 160 µl RPMI 1640 medium containing 10% FBS as attractant. Cell migration of was monitored in real time for 30-hours. For the invasion assay, the upper chamber was coated with 0.2 µg/ml matrix gel prior to seeding $5x10^4$ cells. The upper chamber was filled with 160 µl RPMI1640 medium without FBS and the lower chamber was filled with 160 µl RPMI1640 medium supplemented with 10% FBS. The invasion was followed in real time for 48 hours.

Tumor xenograft studies

Male NMRI nude mice (age weeks) were obtained from Harlan and kept under a 12:12 hour light-dark cycle with ad libitum access to water and food. Mice were kept at the Animal Resource Center (Erasmus University Medical Center), which operates in compliance with the European guidelines (European Community 1986) and The Netherlands legislation for the protection of animals used for research, including ethical review. Animal studies at Erasmus University Medical Center were approved by DEC Consult, an independent Animal Ethical Committee (Dutch equivalent of the IACUC) under permit number 139-11-03 (EMC2360).

At the age of 6 weeks, mice were injected subcutaneously on the flank with 10^6 cells, suspended in a volume of approximately 200 µl RPMI 1640 medium supplemented with 50% FBS (6 animals per knockdown cell line). Tumor growth was monitored weekly and measured in two dimensions. The tumor size was calculated using the formula $V=a^2 b/2$, were a is the shortest and b the longest diameter. As all H1299 knockdown cell lines contained the for Per2::Luc reporter, development of metastasis was monitored three times during the experiment with an IVIS Spectrum *in vivo* imaging device (Caliper Life Sciences).

Formalin-fixed tumor samples were embedded in paraffin and stained with hematoxylin and eosin for general histopathological analysis. Immunohistochemical analysis was performed using antiphosphohistone (mitosis marker) and caspase-3 (apoptotic marker) antibodies as described (de Bruin et al., 2003; Jiang et al., 2005).

Statistical analysis

Data are presented as the mean SEM and the Student's t-test was used to compare between the groups. P-values < 0.05 were considered statistically significant.

Results

Stable shRNA-mediated downregulation of core clock genes in H1299 lung cancer cells

Prior to knocking down circadian clock genes, we transduced H1299 cells with a lentiviral mouse *Per2* promoter-driven luciferase reporter construct and selected a stable clone. This allows real time monitoring of clock performance in forskolin synchronized cell cultures.

To achieve stable down regulation of core clock genes, the parental *Per2::Luc* H1299 was transduced with shRNA constructs targeting *BMAL1*, *CRY1*, *CRY2,* or *CRY1/CRY2*. As a control, we also transduced H1299 cells with a non-targeting shRNA construct. For each shRNA construct, independent stable clones were selected for determining the relative mRNA expression levels after down regulation of clock genes by quantitative RT-PCR (Suppl. Fig S1A-C). Consistent with the reduction of mRNA levels, Western blot analysis of the shRNA expressing H1299 clones revealed reduced protein levels for the corresponding knockdown (Suppl. Fig. S1D-F). Based on the mRNA and protein levels we selected the two best shRNA responsive clones for further analysis. In the remainder of the paper, we show the data for clone 1, (similar data were obtained with clone 2 of all clock knockdown H1299 cell lines (data not shown)).

Given the molecular constitution of the circadian oscillator (i.e. interconnected positive and negative transcription-translation feedback loops), we also tested the relative expression levels of other clock genes in the various H1299 knockdown cell lines. As expected, down regulation of the transcription activator gene *BMAL1* resulted in a significant reduction of *PER* gene expression levels. However, the relative expression levels of *CRY* were not significantly reduced in the *BMAL1* H1299 knockdown cell lines (Suppl. Fig. S2). The relative expression level of *CLOCK* was reduced after shRNA mediated knockdown of either *CRY1* or *CRY2* (Suppl. Fig. S2), while relative *BMAL1* mRNA levels were slightly increased after down regulation of *CRY1* or *CRY2* (Supp. Fig. S2). In contrast, whereas knockdown of both *CRY* genes resulted in a small increase in the relative expression level of *CLOCK*, *BMAL1* mRNA levels were markedly elevated. The increased *BMAL1* expression levels after knockdown of the negative components TTFL contradicts previous studies (Shearman et al., 2000; Zhang et al., 2009), suggesting that this might depend on the cell type.

Next, we investigated the circadian performance of the panel of H1299 clock knockdown cell lines after treatment of the cell cultures with the clock synchronizing compound forskolin. Whereas the H1299 control cell line (stably expressing a non-targeting control shRNA) displayed a robust rhythm with a period of approximately 24.3 hour (Fig. 1A), knockdown of *BMAL1* attenuated the bioluminescence rhythm (Fig.1B). As expected, down regulation of *CRY1* or both *CRY1* and *CRY2* also blunted circadian oscillations (Fig. 1C and E) while, somewhat unexpectedly, knockdown of *CRY2* had a similar effect (Fig. 1D). In conclusion, knockdown of the core clock genes in H1299 lung cancer cells largely recapitulates the cir-

cadian phenotype of human U2OS osteosarcoma cells after knockdown of the corresponding gene(s) (Baggs et al., 2009).

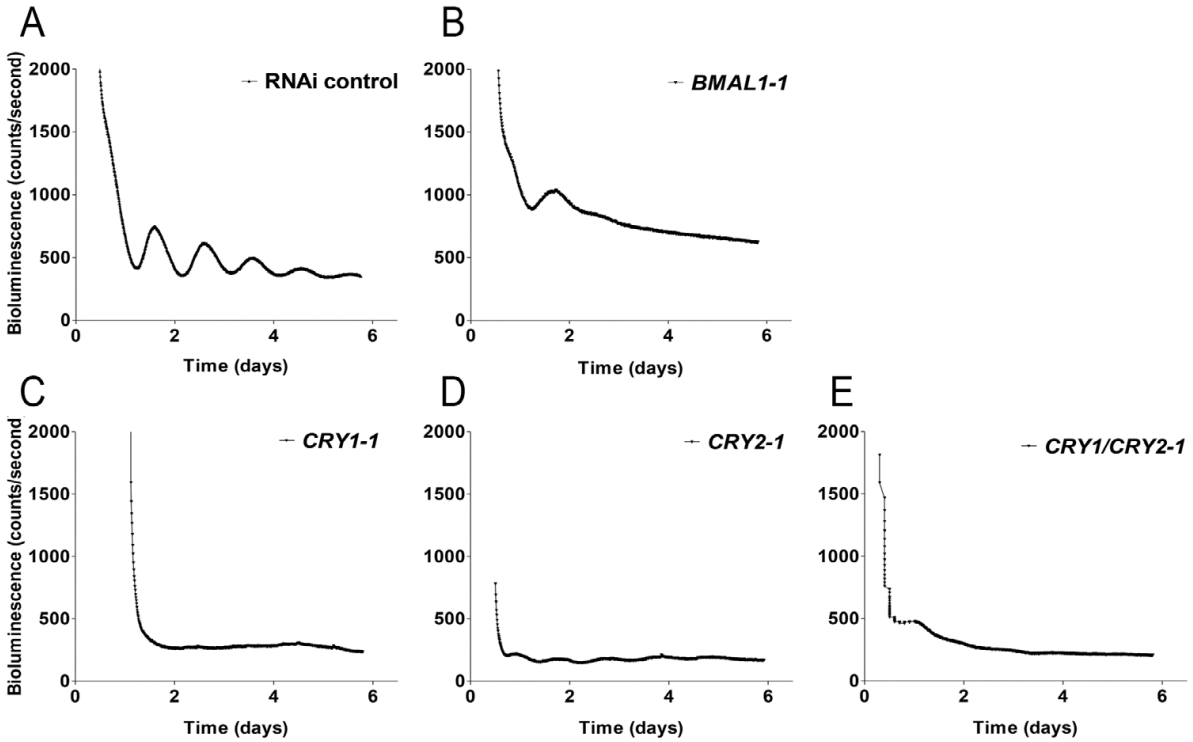

Figure 1. Clock performance of the H1299 cells after stable knockdown of core clock genes. Representative examples of real-time bioluminescence recordings of confluent cultures of forskolin synchronized H1299 *mPer2::Luc* cells, expressing a non-targeting shRNA (A), or shRNAs targeting *BMAL1* (B), *CRY1* (C), *CRY2* (D), *CRY1*/*CRY2* (E). The Y-axis represents the luminescence value, the X-axis represent time after synchronization (days).

Transcriptomics analysis of clock knock down cell lines

To investigate the effect of clock gene knock down on the properties of H1299 cells, gene expression analysis was performed on *CRY1*, *CRY2*, *CRY1*/*CRY2*, and *BMAL1* knockdown cells. Cells were harvested at log phase, and RNA isolation was performed for next generation sequencing. This experiment was performed in triplicate for each group of samples. Correlation analysis, based on expression of all the genes, shows the highest similarity in gene expression patterns between triplicate clusters (Fig. 2A). The high correlation between each of the triplicate samples within a group indicates the high quality of the data. *CRY2* and *CRY1*/*CRY2* knock down cells show the most similarities in the gene expression pattern, while the least correlation is seen in the gene expression profiles between these two cell lines compared to the rest of the groups (controls, *BMAL1* and *CRY1* knock down cells).

Gene expression levels were determined relative to the geometric mean, and non-significant values were excluded from further analysis. The threshold chosen was absolute fold-change

>1.5 and FDR < 0.05, and in total 7081 genes were detected as differentially expressed genes (DEGs) in all the groups. Among those, the highest number of DEGs are in *CRY1*/*CRY2* double knock down group, consisting of 2792 down-regulated genes and 2005 up-regulated genes (Fig.2B). OmniViz treescape represents a hierarchical clustering of the DEGs, where each row and column corresponds to one individual gene and one individual sample, respectively (Fig.2C). The most different gene expression pattern is observed in the *CRY1*/*CRY2* cluster versus control, and this difference is mostly coming from *CRY2* knock down, indicating a dominant effect of *CRY2* knock down in the *CRY1*/*CRY2* double knock down cell line.

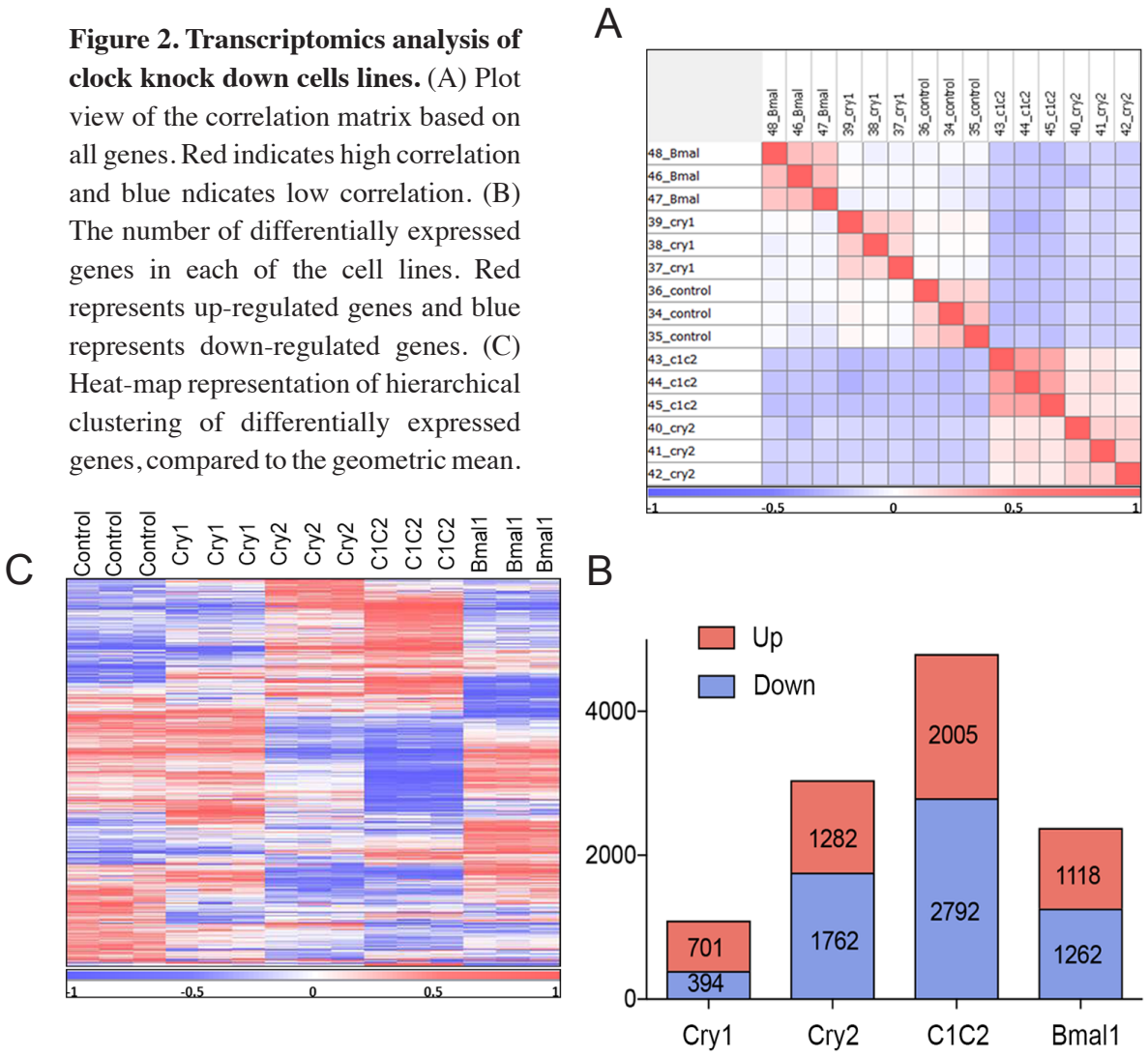

Figure 2. Transcriptomics analysis of clock knock down cells lines. (A) Plot view of the correlation matrix based on all genes. Red indicates high correlation and blue ndicates low correlation. (B) The number of differentially expressed genes in each of the cell lines. Red represents up-regulated genes and blue represents down-regulated genes. (C) Heat-map representation of hierarchical clustering of differentially expressed genes, compared to the geometric mean.

Identification of differentially regulated biological functions and diseases

Ingenuity pathway analysis (IPA) on differentially expressed genes revealed biological functions and diseases that are mostly related to each of the cell lines (**Fig. S1-S4**). Cancer is one of the top diseases and disorders which is significantly affected in all the knock down cell lines, indicating the strong involvement of the *BMAL1* and *CRY* in the regulation of the

cancer properties of the cells. We have selected the top 10 altered biological functions in each of the groups, sorted by the smallest p-value ($p<0.05$) (Fig. 3A).

A

Cry1 relevant biofunctions	p-value	Molecules
Cellular Movement	4,44E-16	193
Cancer	1,16E-14	602
Cellular Development	1,17E-14	268
Cell Death and Survival	4,25E-14	275
Tissue Development	5,16E-13	241
Cellular Growth and Proliferation	6,07E-13	266
Tumor Morphology	6,07E-13	104
Cellular Assembly and Organization	2,44E-12	131
Cellular Function and Maintenance	2,44E-12	229
Organismal Survival	3,48E-12	193

Cry2 relevant biofunctions	p-value	Molecules
Cancer	3,22E-22	1516
Cellular Movement	6,89E-19	418
Cellular Growth and Proliferation	7,54E-15	609
Embryonic Development	8,27E-14	417
Organismal Development	8,27E-14	556
Cellular Development	1,24E-13	604
Cardiovascular System Development and Function	3,02E-13	263
Gastrointestinal Disease	3,37E-13	673
Cellular Assembly and Organization	3,99E-13	293
Cellular Function and Maintenance	3,99E-13	400

Cry1/Cry2 relevant biofunctions	p-value	Molecules
Cancer	2,39E-26	2377
Cellular Assembly and Organization	2,83E-24	518
Cellular Function and Maintenance	2,83E-24	741
Cell Death and Survival	3,23E-21	949
Cellular Movement	3,69E-21	640
Cellular Growth and Proliferation	4,90E-21	945
Organismal Survival	4,21E-18	647
Cell Morphology	9,66E-18	737
Organismal Injury and Abnormalities	3,90E-15	1317
Reproductive System Disease	3,90E-15	1243

Bmal1 relevant biofunctions	p-value	Molecules
Cell Death and Survival	1,33E-20	547
Cancer	5,72E-19	1282
Cellular Assembly and Organization	7,25E-18	302
Cellular Function and Maintenance	7,25E-18	455
Organismal Survival	7,90E-18	380
Cellular Growth and Proliferation	4,27E-17	537
Cellular Development	2,08E-16	249
Cellular Movement	2,20E-15	343
Cell Morphology	9,98E-15	413
Tissue Morphology	1,70E-12	404

B

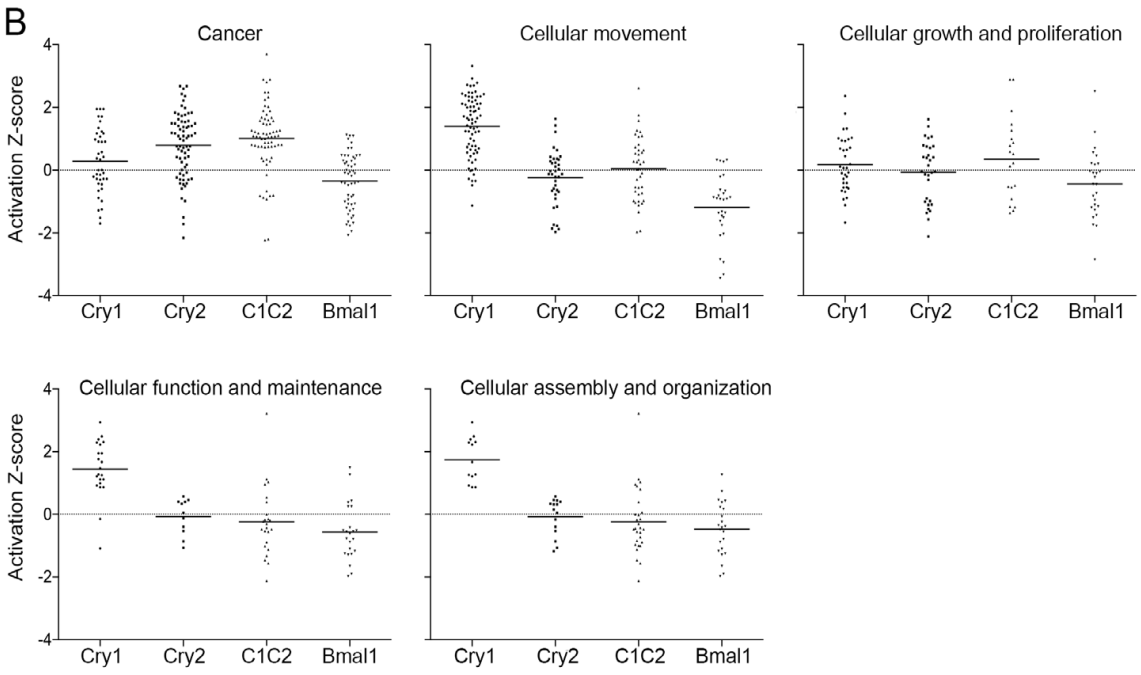

Figure 3. Differentially regulated biological functions and diseases. (A) Top 10 affected bio-functions in each of the knockdown cell lines, sorted by the smallest p-value (the most significantly altered functions are on top of the list). Commonly affected bio-functions are in boldface. The p-value and number of molecules affected in each bio-function are indicated. (B) Scatter plot of commonly affected bio-functions in each knock down cell line, relative to non-targeting control. The Y-axis represents the activation Z-score for each single disorder within a bio-function. Positive Z-scores indicate up-regulation, negative Z-scores indicate down-regulation.

Among these top 10 pathways, commonly affected functions between all the groups are cancer, cellular movement, cellular growth and proliferation, cellular function and maintenance, and cellular assembly, which are high-lighted in Fig. 3A. There are various types of disorders that are connected and relevant to each of the above biological functions. Fig. 3B, shows the normal distributions from the mean value (z-score) for all these relevant disorders in each category of biological function. Positive and negative expression values indicate up- and down-regulation of these disorders, respectively. In the category of cancer, the average grade for all the Z-scores is negative in the case of *BMAL1* knockdown, while the mean Z-score values for the other cell lines are positive, with the highest value in the *CRY1*/*CRY2* double knockdown cells. These data show that, in general, the trend for cancer development in *BMAL1* knockdown cells is decreased, while cancer development is increased in *CRY1*, *CRY2*, and *CRY1*/*CRY2* knockdown cells (Fig. 3B). Cellular movement is down regulated in *BMAL1* and *CRY2* knock down cells, and unaffected in the case of the *CRY1*/*CRY2* double knockdown. However, *CRY1* knockdown cells show up regulation of this function. Finally, cellular growth and proliferation for all knockdown cell lines show a slight down regulation or are unaffected (Fig. 3B).

Since cellular movement, proliferation, and cancer development are important characteristics of a cancer cell line, we took a closer look at the properties related to these categories of biological function (supplementary tables S1-S4). For a better comparison analysis we have selected common diseases and disorders in each of the categories of bio-functions, allowing to study the trend of change in gene expression profile for a specific disorder which is common among all the knockdown cell lines (Fig. 4). Interestingly, growth of malignant tumors was one of the cancer properties which was commonly and significantly (Zscore >2) affected in both *CRY1/CRY2* and *BMAL1* knockdown cells. Growth of malignant tumors was markedly increased in *CRY* double knockdown cells, whereas it was significantly reduced in the *BMAL1* knockdown condition (Fig. 4). Therefore, tumor growth as well as other properties such as cellular movement and proliferation were chosen to further be validated in vitro and in vivo studies.

Z Score

Decreasing -4 +4 Increasing

Cancer	Cry1	Cry2	Cry1/Cry2	Bmal1
Cancer	0,58	2,36	3,70	-0,80
breast or colorectal cancer	0,91	0,01	0,90	-0,19
epithelial neoplasia	-0,66	1,00	2,05	-0,09
solid tumor	-1,29	0,65	1,78	-0,37
metastasis	1,71	2,59	2,80	-0,80
carcinoma	-1,25	0,61	1,58	-0,40
breast or ovarian cancer	1,17	-0,28	1,08	0,48
breast cancer	1,17	-0,30	0,88	0,10
mammary tumor	0,34	-0,59	1,17	-1,10
precancerous condition	0,98	1,57	1,15	0,46
adenocarcinoma	-0,28	1,19	1,60	0,41
gastrointestinal tract cancer	-0,15	1,17	1,09	0,14
digestive organ tumor	0,01	0,76	0,75	0,70
growth of tumor	0,37	0,55	1,18	-1,65
proliferation of tumor cells	-0,21	0,76	1,00	-1,74
central nervous system cancer	1,34	1,83	0,76	0,30
head and neck tumor	1,23	1,24	1,05	0,25
neuroepithelial tumor	0,91	-0,30	0,29	-0,43
head and neck cancer	1,95	1,49	0,41	0,37
central nervous system tumor	1,95	0,43	1,08	1,09
glioma	0,91	-0,32	0,28	-0,43
proliferation of cancer cells	-0,88	1,02	1,47	-1,78
growth of malignant tumor	-0,98	1,30	2,25	-2,07
Cellular movement	**Cry1**	**Cry2**	**Cry1/Cry2**	**Bmal1**
cell movement	1,74	-0,66	-0,54	-2,85
cell movement of tumor cell lines	1,72	-0,35	-0,09	-3,33
invasion of tumor cell lines	2,00	0,22	1,09	-0,92
migration of cells	1,49	-0,91	-0,97	-2,94
migration of tumor cell lines	1,14	-1,16	-1,04	-3,44
invasion of cells	2,12	0,28	1,27	-0,66
cell movement of breast cancer cell lines	1,89		-0,55	-2,08
migration of breast cancer cell lines	1,42	-1,97	-1,33	-1,76
cell movement of brain cancer cell lines	2,02	0,64	-0,20	0,27
chemotaxis	2,12	-0,13	0,74	-1,47
chemotaxis of cells	2,08	-0,22	0,54	-1,62
migration of endothelial cells	1,87	0,33	0,03	-0,92
migration of neurons	0,64	-0,78	-0,99	-0,16
cell movement of endothelial cells	1,61	0,24	0,20	-1,32
cell movement of prostate cancer cell lines	0,77	-0,03	0,64	-0,87
leukocyte migration	2,34	0,42	-0,77	-1,36
migration of brain cancer cell lines	2,23	-0,22	-1,06	-0,22
Cellular growth and proliferation	**Cry1**	**Cry2**	**Cry1/Cry2**	**Bmal1**
proliferation of cells	0,68	-0,05	-0,49	-0,44
proliferation of tumor cell lines	1,31	-0,98	0,23	-0,23
proliferation of tumor cells	-0,21	0,76	1,00	-1,74
proliferation of connective tissue cells	0,63	-1,57	-1,18	-1,51
proliferation of embryonic cells	1,80	-0,31	-1,16	-1,11
formation of cells	-0,66	-1,00	-0,92	-2,85
proliferation of fibroblasts	-0,41	-1,24	-1,36	-0,74
proliferation of cancer cells	-0,88	1,02	1,47	-1,78
proliferation of endothelial cells	-0,55	1,10	0,13	-1,19

Figure 4. Comparison of affected diseases and disorders. Comparison analysis for common relevant diseases and disorders for each category of a bio-function (Cancer, Cellular movement, Cellular growth and proliferation). A Z-score of 0 means that the genes expression is comparable to the non-targeting control. The higher the absolute Z-score, the higher the significance of the genes expression change. Absolute Z-scores above 2 are considered significant.

Downregulation of core clock genes affects the *in vitro* tumorigenic properties of H1299 cells

Genetic defects in, as well as down regulation of core clock genes, have been shown to affect the cell proliferation rate *in vitro* (Antoch et al., 2008; Yang et al., 2008; Sun et al., 2009; Farshadi et al., submitted for publication; Farshadi et al., manuscript in preparation). Furthermore, our transcriptomics data suggest that cellular cancer related properties could be affected in the knockdown cell lines. We next examined the proliferation of the H1299 knockdown cell lines using the colorimetric WST-1 assay. Down regulation of either *CRY1*, *CRY2* or both resulted in a significant reduction ($p < 0.005$) of the proliferative capacity of H1299 cells by 28 to 75%, while knockdown of *BMAL1* did not have any effect (Fig. 5A). In addition, we analyzed the cell cycle distribution of proliferating control and knockdown H1299 cells. Within the time window analyzed, non-targeting shRNA expressing control H1299 cells accumulate in G2 phase while the percentage of S phase cells is reduced, which suggests that cells slowdown proliferation and reach confluency. However, the cell cycle phase distribution of all knockdown cell lines remained unaltered (Fig. 5B).

An important characteristic of a cancer cell is its ability to migrate to and invade surrounding tissues. These features should be affected in the knockdown cell lines, as suggested by the transcriptomics analysis. We therefore determined the cell migration as well as the invasive properties (Fig. 5C-D) of our H1299 knockdown cell lines *in vitro* in real time mode, using the xCELLigence system. After down-regulation of *BMAL1*, both cell migration and invasion were severely decreased by 80% ($p < 0.005$). The cell migration capacity was also significantly reduced after down regulation of *CRY1* or *CRY2,* and knockdown of both *CRY* genes further slowed down migration and repressed invasion capacity.

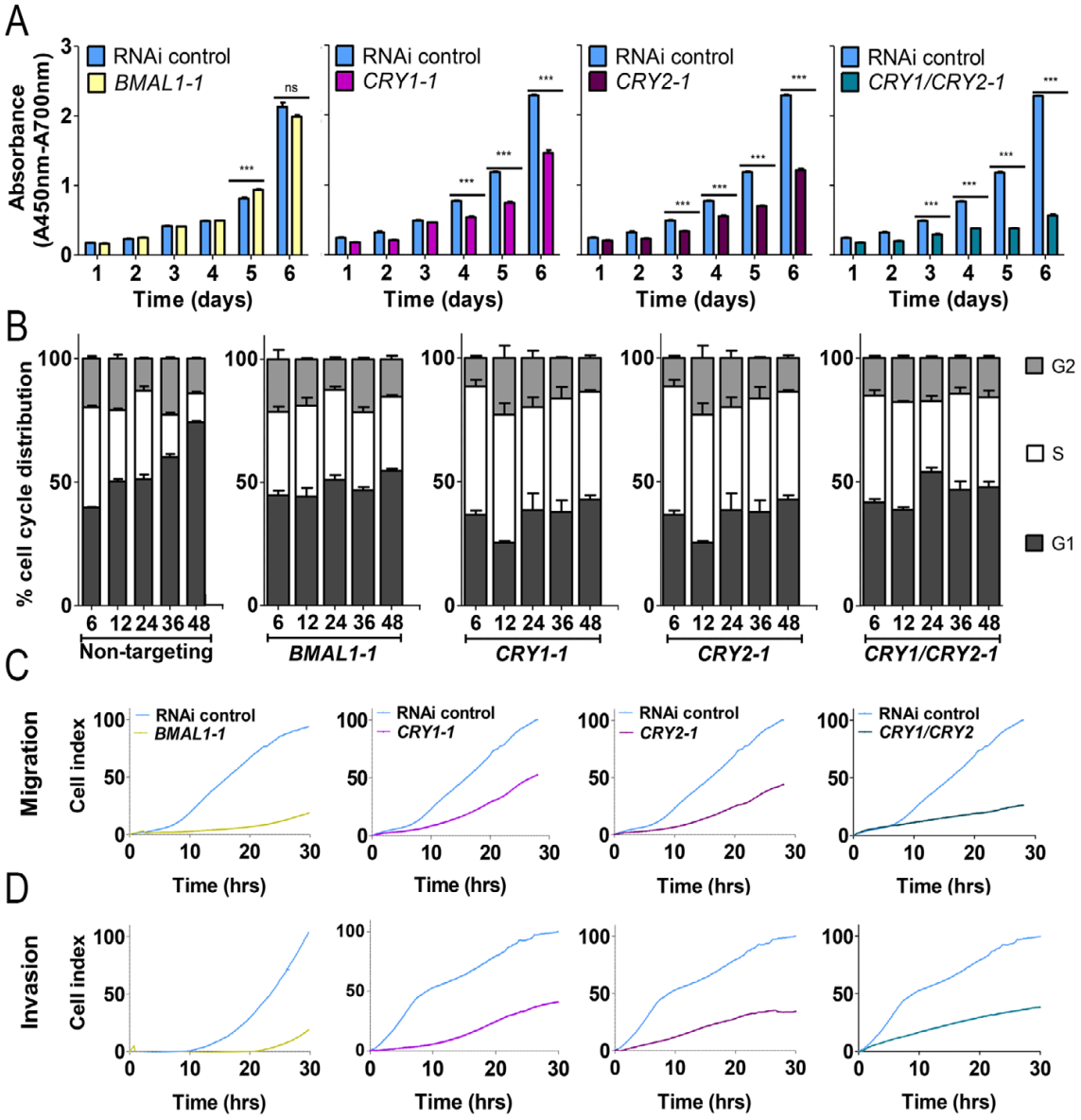

Figure 5. In vitro characterization of H1299 cells after knockdown of core clock genes. (A) Proliferation rate of H1299 cells stably expressing a shRNA targeting BMAL1 , *CRY*1, *CRY2*, and *CRY1*/*CRY2*. Cells (1x10^3/well) were seeded in quadruplicate in 96-well plates on day 0 and cell density was assayed on subsequent days using the colorimetric WST-1 assay. Blue bars represent the control H1299 cells stably expressing a non-targeting shRNA. Data are presented as mean ± SEM (NS = not significant, *** p<0.001; Student's t test). (B) Cell cycle phase distribution of proliferating of H1299 cells stably expressing a non-targeting shRNA or shRNAs targeting *BMAL1*, *CRY1*, *CRY2* or *CRY1*/*CRY2*. At indicated times cells were collected, stained with propidium iodide, and analyzed by flow cytometry. Data (n=3 experiments) are shown as mean ± SEM. (C and D) Cell migration and invasion properties of H1299 cells after stable knockdown of core clock genes. Representative examples of real-time recordings of cell migration (C) and invasion (D) of H1299 cells, stably expressing shRNAs targeting *BMAL1*, *CRY1*, *CRY2* or *CRY1*/*CRY2*. Migration and invasion were monitored for 30-hours using the xCELLigence DP system. Blue lines represent the control H1299 cells stably expressing a non-targeting shRNA.

Down regulation of *BMAL1* and *CRY* differentially affects H1299 tumor formation *in vivo*

The transcriptomics data of the knockdown cells lines suggests that knocking down *BMAL1* decreases the cancer properties of the H1299 cells, while knocking down CRY appears to have the opposite effect. However, the *in vitro* analysis of the different cell lines suggests that knocking down *CRY* or *BMAL1* should have a similar impact on the cancer properties of H1299 cells. We next set out to analyze the in vivo tumor formation properties of the knock down lines. To determine whether knockdown of core clock genes affects the tumor growth *in vivo*, we inoculated the non-targeting shRNA expressing control H1299 cells and core clock gene knockdown H1299 cells in NMRI-nude mice and followed tumor growth. Whereas control H1299 cell derived tumors became apparent 7 weeks after inoculation (Fig. 6), knockdown of *BMAL1* suppressed tumor formation, as evident from the absence of palpable tumors 16 weeks after inoculation (Fig. 8, right panel). Knockdown of *CRY1, CRY2,* or both *CRY1* and *CRY2* did not abolish tumor formation, and tumor growth appeared unaltered as compared to the control (non-shRNA expressing) H1299 xenografts (Fig. 6). Importantly, down regulation of *CRY2* or both *CRY1* and *CRY2* accelerated tumor appearance by two weeks (Fig. 6). As the H1299 cell lines contain the *Per2::Luc* reporter gene, we also subjected tumor bearing animals to *in vivo* bioluminescence imaging. Within the time span of the experiment, neither of the animals developed detectable metastasis (Suppl. Fig. S3). Tumors were analyzed for possible differences in morphology (HE staining), as well as in the expression of apoptosis and proliferation markers (caspase 3 and phospho-histone H3 staining, respectively). For all parameters tested, *CRY1*, *CRY2* and *CRY1/CRY2* knockdown H1299 cell derived tumors were indistinguishable from control (data not shown).

From these data, we conclude that BMAL1, and consequently high expression of E-box containing clock controlled genes, is required to maintain *in vivo* tumor formation properties of H1299 cells. Knocking down *CRY* did not affect the ability of the H1299 cells to form tumors, nor did it affect the growth rate of the tumor. Importantly, knockdown of CRY2 (alone or in combination with CRY1) reduced the tumor latency time by 2 weeks.

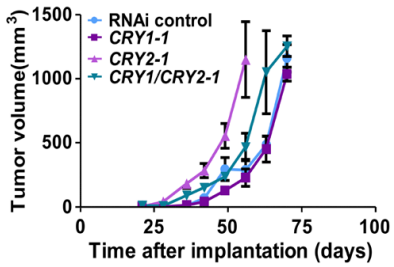

Cell lines	number of xenografts
H1299 Non-targeting control	4/6
CRY1	5/6
CRY2	4/6
CRY1/CRY2	5/6
BMAL1	0/6

Figure 6. In vivo tumor formation and growth rate of H1299 xenograft after knockdown of core clock genes. Nude mice were inoculated with 10^6 H1299 cell, stably expressing a non-coding shRNA or clock gene shRNAs. Animals were screened for the formation of tumors (bottom panel) and tumor volume (top panel). Data are presented as mean ± SEM (n=4).

Discussion

The circadian clock and the cell cycle are two fundamental mechanisms that are known to interact with each other and influence many biological processes (Feillet et al., 2014, Bieler et al., 2014). Disruption of the circadian clock has been shown to deregulate the cell cycle, leading to serious consequences such as cancer (Borgs et al., 2009; Lee et al., 2010). Several studies performed with circadian clock mutant mouse models and cell lines revealed a link between the circadian clock and cancer progression (Fu et al., 2002; Lee et al., 2010; Zheng et al., 2010; Van Dycke et al., 2015). However, the underlying mechanism is not fully understood.

In this study, we analyzed the transcriptome and systematically investigated the cancer properties of H1299 human non-small lung carcinoma cells after stable downregulation of the circadian core clock genes *BMAL1*, *CRY1* and *CRY2*. As expected, downregulation of the transcriptional activator *BMAL1* abolishes circadian rhythmicity in H1299 cells. In contrast to normal cells, where loss of negative limb genes may change period rather than abolish rhythms (e.g. *Cry2*) (Liu et al., 2007), but similar to U2OS osteosarcoma cells (Baggs et al., 2009), circadian rhythmicity of H1299 cells is heavily blunted after knockdown of any of the *CRY*. This finding strongly suggests that paralog compensation, a network feature that confers robustness to the molecular oscillator (Baggs et al., 2009) is altered in H1299 cells and that inactivation of a single transcriptional repressor gene is sufficient to demolish rhythmicity.

We have observed that inactivation of the *CRY* genes resulted in a reduction of the proliferation rate of H1299 cells, while inactivation of BMAL1 had no effect. Furthermore, while in control cells the cell cycle profile changed in time after seeding, no changes were observed in the knockdown cell lines. This observation contrasts the transcriptomics data, which suggested that cell growth and proliferation was only slightly affected. This could mean that, although the knockdown cell lines have a normal proliferation rate, they may have an extended lag phase.

Studies addressing the effect of clock gene inactivation on proliferation rate have yielded conflicting results. As an example, primary *Cry1*$^{-/-}$/*Cry2*$^{-/-}$ mouse embryonic fibroblasts (MEFs) display an increased growth rate (Destici et al., 2011), similar to the effect we observed in CRY deficient NIH3T3 cells (Farshdi et al., manuscript in preparation), while immortalized *Cry1*$^{-/-}$/*Cry2*$^{-/-}$ MEFs fibroblasts proliferate at wild type rate (Gauger and Sancar 2005). Likewise, primary *Bmal1* knockout mouse hepatocytes were reported to grow slower (Gréchez-Cassiau et al., 2008), an effect that we recapitulated by knocking down *Bmal1* or *Clock* in mouse NIH3T3 fibroblasts (Farshadi et al., submitted for publication). However, downregulation of *Bmal1* in murine fibroblasts increases the proliferation rate (Zeng et al.,2010). Apparently, the effect of down regulation of the core clock genes on cell proliferation may depend on cell type (e.g. cancer vs normal cells, hepatocytes vs fibroblasts, etc.), specific cell characteristics (e.g. status of cell cycle related genes), as well as on gene inactivation procedure (e.g. gene knockout, stable shRNA knockdown or transient shRNA or

siRNA transfection).

The malignancy of tumors not only depends the on growth rate of cancer cells, but also on their ability to migrate and invade surrounding tissue to form metastasis. We have shown that the cell migration and invasion capacity of H1299 cells was inhibited after down regulation of *BMAL1*, as well as by down regulation of the *CRY* genes. From the transcriptomics data we would expect CRY1 down regulation to increase the migration and invasion capacity, which is in contrast with the *in vitro* data. The ability of the H1299 cell lines to form tumors was tested in vivo, but, as no metastasis were observed, we cannot conclude what the effect is of *BMAL1* or *CRY* down regulation on the capacity of a tumor to metastasize.

As described above, changes in the *in vitro* cell proliferation, migration and invasion properties of H1299 cells after knockdown of core clock genes did not show a clear correlation with the transcriptomics data. In contrast, such correlation was largely observed in *in vivo* studies addressing tumor formation and growth of H1299 core clock gene knockdown cells. While knockdown of *BMAL1* abolished tumor formation, inhibition of the *CRY* genes did not affect the ability of H1299 cells to form tumors in xenograft studies. Importantly, down regulation of *CRY2* decreased the latency time of the tumors. We can conclude that, using the H1299 tumor cell line, high level expression of E-box genes is required for tumor development. This is the predicted outcome based on the analysis of the RNA sequencing results, indicating that omics-based approaches are valuable tools in determining the tumorigenic potential of cancer cell lines and appear more predictive than *in vitro* phenotyping.

Concluding remarks

At least to our knowledge, this is the first study that addresses the relation between circadian core clock genes and cancer properties of a tumor cell line in a systematical manner by stable shRNA-mediated gene inactivation and subsequent phenotypical characterization. ,Transcriptome analysis of a panel of H1299 cell lines revealed how clock genes impact on cancer related pathways. We have shown that clock genes *BMAL1* and *CRY* are involved in determining the tumor forming ability of the H1299 cells, and that the positive and negative circadian elements exert opposite effects . To what extent these findings are applicable to other tumor cell lines remains to be investigated, as tumor cell line specific mutations in cell cycle and DNA damage response genes may modulate the impact of clock genes. To obtain mechanistic insight in how these clock proteins link to the oncogenic properties of cancer cells more research is required.

Acknowledgements

This work was supported by grants from the Netherlands Organization for Scientific Research (ZonMW/ErasSysBio+ grant nr. 90.201.127) and the Netherlands Genomics Initiative/Netherlands Toxicogenomics Center (grant nr. 050-060-510) to GTJvdH.

References

Albrecht U, Eichele G (2003) The mammalian circadian clock. *Curr Opin Genet Dev.* 13:271-277.

Antoch M.P, Toshkov I, Kuropatwinski K.K, Jackson M (2013) Deficiency in PER proteins has no effect on the rate of spontaneous and radiation-induced carcinogenesis. *Cell Cycle* 12:3673-3680.

Baggs J.E, Price T.S, DiTacchio L, Panda S, FitzGerald G.A, Hogenesch J.B (2009) Network features of the mammalian circadian clock. *PLoS Biol* 7: e52.

Balsalobre A, Damiola F, Schibler U (1998) A serum shock induces circadian gene expression in mammalian tissue culture cells. *Cell* 93:929-937.

Bieler J, Cannavo R, Gustafson K, Gobet C, Gatfield D, Naef F (2014) Robust synchronization of coupled circadian and cell cycle oscillators in single mammalian cells. *Mol Syst Biol* 10:739.

Bjarnason G.A, Jordan R (2000) Circadian variation of cell proliferation and cell cycle protein expression in man: clinical implications. *Prog Cell Cycle Res* 4:193-206.

Borgs L, Beukelaers P, Vandenbosch R, Belachew S, Nguyen L, Malgrange B (2009) Cell "Circadian cycle: new role for mammalian core clock genes. *Cell Cycle* 8:832-837.

de Bruin A, Wu L, Saavedra H.I, Wilson P, Yang Y, Rosol T.J, Weinstein M, Robison M.L, Leone G (2003) Rb function in extra embryonic lineages suppresses apoptosis in the CNS of Rb-deficient mice. *Proc Natl Acad Sci USA* 100:6546-51.

Destici E, Oklejewicz M, Saito S, van der Horst G.T.J (2011) Mammalian cryptochromes impinge on cell cycle progression in a circadian clock-independent manner. *Cell Cycle* 10:3788-3797.

Dunlap J.C (1999) Molecular bases for circadian clocks. *Cell* 96:271-290.

Feillet C, Krusche P, Tamanini F, Janssens RC, Downey MJ, Martin P, Teboul M, Saito S, Lévi FA, Bretschneider T, van der Horst GTJ, Delaunay F, Rand DA (2014) Phase locking and multiple oscillating attractors for the coupled mammalian clock and cell cycle. *Proc Natl Acad Sci USA* 111:9828-9833.

Filipski E, King V.M, Li X, Granda T.G, Mormont M.C, Claustrat B, Hastings M.H, Lévi F (2003) Disruption of circadian coordination accelerates malignant growth in mice. *Pathol Biol* 51:216-219.

Filipski E, Delaunay F, King V.M, Wu MW, Claustrat B, Gréchez-Cassiau A, Cuettier C, Hastings M.H, Lévi F (2004) Effects of chronic jet lag on tumor progression in mice. Cancer Res 64:7879-85.

Fu L, Pelicano H, Liu J, Huang P, Lee C (2002) The circadian gene Period2 plays an important role in tumor suppression and DNA damage response in vivo. *Cell* 111:41-50.

Gauger M.A, Sancar A (2005) Cryptochrome, circadian cycle, cell cycle checkpoints, and cancer. *Cancer Res* 65:6828-6834.

Gréchez-Cassiau A, Rayet B, Guillaumond F, Teboul M, Delaunay F (2008) The circadian clock component BMAL1 is a critical regulator of p21WAF1/CIP1 expression and hepatocyte proliferation. *J Biol Chem* 283:4535-4542.

Hansen J (2006) Risk of breast cancer after night- and shift work: current evidence and ongoing studies

in Denmark. *Cancer Causes Control* 17:531-537.

Hua H, Wang Y, Wan C, Liu Y, Zhu B, Yang C, Wang X, Wang Z, Cornelissen-Guillaume G, Halberg F (2006) Circadian gene mPer2 overexpression induces cancer cell apoptosis. *Cancer Sci* 97:589-596.

Jiang Y, de Bruin A, Caldas H, Fangusaro J, Hayes J, Conway E.M, Robinson M.L, Altura R.A (2005) Essential role for survivin in early brain development. *Neurosci* 25:6962-6970.

Ko C.H, Takahashi J.S (2006) Molecular components of the mammalian circadian clock. *Hum Mol Genet* 15: R271-277.

Lee C, Donehower L.A, Herron A.J, Moore D.D, Fu L (2010) Disrupting circadian homeostasis of sympathetic signaling promotes tumor development in mice.*Plos One* 5: e10995.

Liu A.C, Welsh D.K, Ko C.H, Tran H.G, Zhang E.E, Priest A.A, Buhr E.D, Singer O, Meeker K, Verma I.M, Doyle F.J.3rd, Takahashi JS, Kay S.A (2007) Intercellular coupling confers robustness against mutations in the SCN circadian clock network. *Cell* 129:605-16.

Matsuo T, Yamaguchi S, Mitsui S, Emi A, Shimoda F, Okamura H (2003) Control mechanism of the circadian clock for timing of cell division in vivo. *Science* 302:255-259.

Miller B.H, McDearmon E.L, Panda S, Hayes K.R, Zhang J, Andrews J.L, Antoch M.P, Walker J.R, Esser K.A, Hogenesch J.B, Takahashi J.S (2007) Circadian and CLOCK-controlled regulation of the mouse transcriptome and cell proliferation. *Proc Natl Acad Sci USA* 104:3342-3347.

Panda S, Antoch M.P, Miller B.H, Su AI, Schook A.B, Straume M, Schultz P.G, Kay S.A, Takahashi J.S, Hogenesch J.B (2002) Coordinated transcription of key pathways in the mouse by the circadian clock. *Cell* 109:307-320.

Pittendrigh C.S (1993) Temporal organization: reflections of a Darwinian clock-watcher. *Annu Rev Physiol* 55:16-54.

Preitner N, Damiola F, Lopez-Molina L, Zakany J, Duboule D, Albrecht U, Schibler U (2002) The orphan nuclear receptor REV-ERBalpha controls circadian transcription within the positive limb of the mammalian circadian oscillator. *Cell* 110:251-260.

Reppert S.M, Weaver D.R (2001) Molecular analysis of mammalian circadian rhythms. *Annu Rev Physiol* 63:647-76.

Reppert S.M, Weaver D.R (2002) Coordination of circadian timing in mammals. *Nature* 418:935-941.

Sato T.K, Panda S, Miraglia L.J, Reyes T.M, Rudic R.D, McNamara P, Kinnery A, Naik K.A, FitzGerald G.A, Kay S.A, Hogenesch J.B (2004) A functional genomics strategy reveals Rora as a component of the mammalian circadian clock. *Neuron* 43:527-537.

Shearman L.P, Sriram S, Weaver D.R, Maywood E.S, Chaves I, Zheng B, Kume K, Lee C, van der Horst G.T.J, Hastings M.H, Reppert S.M (2000) Interacting molecular loops in the mammalian circadian clock. *Science* 288:1013-9.

Sjöblom T, Jones S, Wood L.D, Parsons D.W, Lin J, Barber T.D, Mandelker D, Leary R.J, Ptak, J, Silliman N, Szabo S, Buckhaults P, Farrell C, Meeh P, Markowitz S.D, Willis J, Dawson D, Willson J.K, Gazdar A.F, Hartigan J, Wu L, Liu C, Parmigiani G, Park B.H, Bachman K.E, Papadopoulos N,

Vogelstein B, Kinzler K.W, Velculescu V.E (2006) The consensus coding sequences of human breast and colorectal cancers. *Science* 314:268-274.

Storch K.F, Lipan O, Leykin I, Viswanathan N, Davis F.C, Wong W.H, Weitz C.J (2002) Extensive and divergent circadian gene expression in liver and heart. Nature 417:78-83.

Weaver D.R (1998) The suprachiasmatic nucleus: a 25-year retrospective. *J Biol Rhythms* 13:100-112.

Welsh D.K, Takahashi J.S, Kay S.A (2010) Suprachiasmatic nucleus: cell autonomy and network properties.*Annu Rev Physiol* 72:551-577.

Winter S.L, Bosnoyan-Collins L, Pinnaduwage D, Andrulis I.L (2007) Expression of the circadian clock genes Per1 and Per2 in sporadic and familial breast tumors. *Neoplasia* 9:797-800.

Yagita K, Tamanini F, van der Horst G.T.J, Okamura H. (2001) Molecular mechanisms of the biological clock in cultured fibroblasts. *Science* 292:278-281.

Yang X, Wood P.A, Oh E.Y, Du-Quiton J, Ansell C.M, Hrushesky W.J (2009) Down regulation of circadian clock gene Period 2 accelerates breast cancer growth by altering its daily growth rhythm.*Breast Cancer Res Treat* 117:423-431.

Yoo S.H, Yamazaki S, Lowrey P.L, Kazuhiro Shimomura K, Ko C.H, Buhr E.D, Siepka S.M, Hong H, Oh W.J, Yoo O.J, Menaker M, Takahashi J.S (2004) PERIOD2::LUCIFERASE real-time reporting of circadian dynamics reveals persistent circadian oscillations in mouse peripheral tissues. *Proc Natl Acad Sci USA* 101:5339-5346.

Zeng Z.L, Wu M.W, Sun J, Sun Y.L, Cai Y.C, Huang Y.J, Xian L.J (2010) Effects of the biological clock gene Bmal1 on tumour growth and anti-cancer drug activity. *J Biochem* 148:319-326.

Zhang E.E, Liu A.C, Hirota T, Miraglia L.J, Welch G, Pongsowakul PY, Lui X, Atwood A, Huss J.W, 3rd Janes J, Su A.I, Hogenesch J.B, Kay S.A (2009). A genome-wide RNAi screen for modifiers of the circadian clock in human cells. *Cell* 139:199-210.

Supplementary information

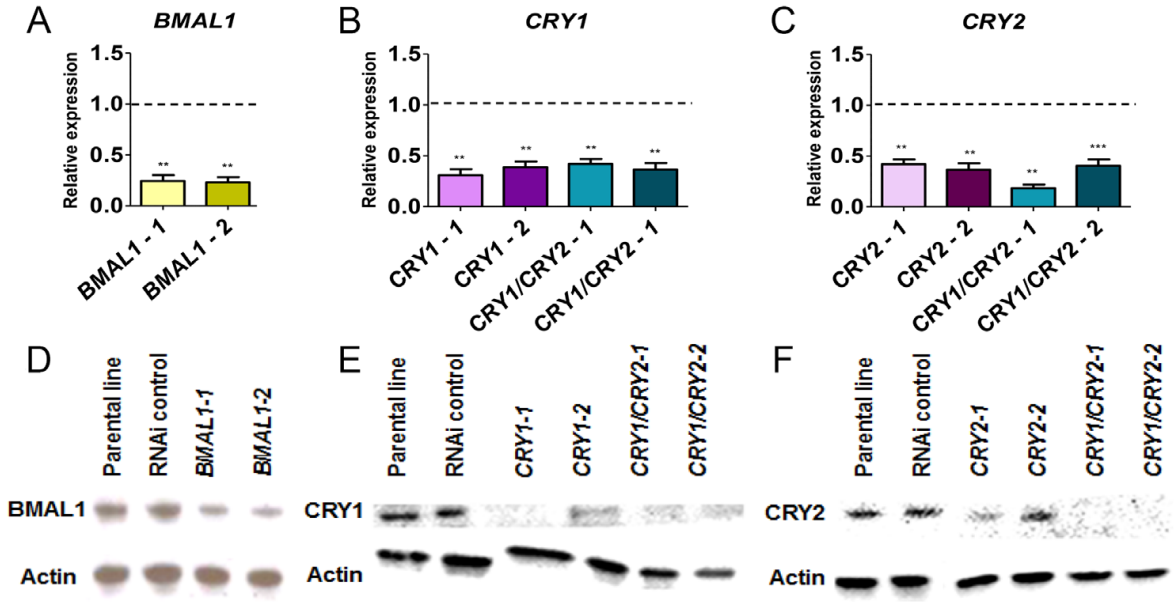

Figure S1. mRNA and protein levels after stable shRNA mediated knockdown of core clock genes in H1299 cells. Quantitative RT-PCR (A-C) and western blot analysis (D-F) of whole cell lysates of H1299 cells for the presence of BMAL1 (A,D), CRY1 (B,E), CRY2 (C,F) after stable knockdown of the corresponding mRNA. mRNA levels were normalized to *GAPDH* and expressed relative to the mRNA levels in control (non-targeting shRNA expressing) H1299 cells. In the western blot analysis, Actin was used as a loading control.

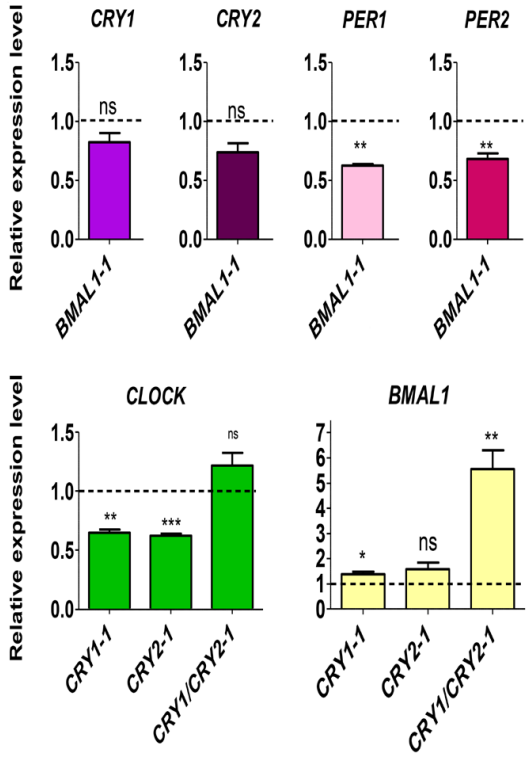

Figure S2. Relative core clock gene mRNA levels in H1299 clock gene knockdown cells. Quantitative RT-PCR analysis of *CRY1*, *CRY2*, *PER1*, *PER2*, *CLOCK*, or *BMAL1* mRNA levels in H1299 cells after stable knockdown of circadian core clock genes. mRNA levels were normalized to *GAPDH* and expressed relative to the mRNA levels in control (non-targeting shRNA expressing) H1299 cells. Data are presented as mean ± SEM (*$p < 0.05$, **$p < 0.01$, ***$p < 0.001$; Student's t test).

Figure S3. Visualization of tumors derived from xenografted circadian core clock gene knockdown H1299 cells. Nude NMRI mice were inoculated with 10^6 H1299 cell, stably expressing a non-coding shRNA or clock gene shRNA. Tumor developing mice were non-invasively monitored under isoflurane anesthesia for Per2::Luc derived bioluminescence using an IVIS® Spectrum imaging device (Caliper/Xenogen). Colors indicate signal intensity. Note the absence of metastasis.

Table S1

Cry1 relevant disease and disorders	p-value	Molecules
Cellular Movement	4.44E-16-6.1E-04	193
Cancer	1.16E-14-5.95E-04	602
Cellular Development	1.17E-14-5.95E-04	268
Cell Death and Survival	4.25E-14-6.14E-04	275
Tissue Development	5.16E-13-6.1E-04	241
Cellular Growth and Proliferation	6.07E-13-5.95E-04	266
Tumor Morphology	6.07E-13-5.95E-04	104
Cellular Assembly and Organization	2.44E-12-5.9E-04	131
Cellular Function and Maintenance	2.44E-12-5.9E-04	229
Organismal Survival	3.48E-12-1.15E-05	193
Cell Morphology	8.63E-12-5.87E-04	222
Cardiovascular System Development and Function	1.67E-10-6.14E-04	132
Gene Expression	2.49E-10-4.96E-04	167
Organismal Development	4.8E-10-5.95E-04	259
Tissue Morphology	1.07E-09-5.48E-04	219
Cardiovascular Disease	1.37E-09-1.81E-04	148
Neurological Disease	1.97E-09-3.7E-04	174
Gastrointestinal Disease	3.19E-09-1.46E-04	272
Skeletal and Muscular Disorders	3.39E-09-2.79E-04	184
Hereditary Disorder	4.18E-09-4.18E-09	63
Psychological Disorders	4.18E-09-1.85E-08	75
Embryonic Development	5.62E-09-5.95E-04	191
Cell-To-Cell Signaling and Interaction	2.26E-08-6.29E-04	141
Connective Tissue Development and Function	2.73E-08-5.95E-04	115
Organ Development	2.73E-08-5.95E-04	150
Organ Morphology	2.73E-08-6.14E-04	136
Skeletal and Muscular System Development and Function	2.73E-08-6.14E-04	162
Connective Tissue Disorders	3.33E-08-2.26E-04	93
Inflammatory Disease	3.33E-08-3.7E-04	116
Hematological System Development and Function	4.72E-08-5.67E-04	165
Immunological Disease	1.46E-07-3.11E-04	118
Nervous System Development and Function	1.78E-07-5.95E-04	131
Behavior	2.33E-07-5.84E-04	86

Organismal Injury and Abnormalities	4.47E-07-5.95E-04	312
Reproductive System Disease	4.47E-07-3.26E-04	285
Inflammatory Response	9E-07-6.29E-04	138
Immune Cell Trafficking	9.99E-07-5.67E-04	79
Respiratory System Development and Function	2.72E-06-4.75E-04	42
Cell Cycle	5.43E-06-2.1E-04	57
Developmental Disorder	7.5E-06-3.31E-04	130
Organismal Functions	7.59E-06-7.59E-06	21
Endocrine System Development and Function	9.27E-06-5.48E-04	23
Lipid Metabolism	9.27E-06-5.48E-04	66
Small Molecule Biochemistry	9.27E-06-5.48E-04	75
Vitamin and Mineral Metabolism	9.27E-06-1.22E-04	36
Infectious Disease	2.86E-05-2.46E-04	121
Digestive System Development and Function	3.65E-05-1.91E-04	39
Reproductive System Development and Function	3.66E-05-5.95E-04	22
Visual System Development and Function	3.74E-05-4E-04	45
Hematopoiesis	3.9E-05-5.29E-04	85
Hepatic System Disease	4.09E-05-1.46E-04	20
Lymphoid Tissue Structure and Development	5.15E-05-5.09E-04	78
Dermatological Diseases and Conditions	5.17E-05-5.81E-05	17
Renal and Urological Disease	5.29E-05-4.74E-04	64
Hematological Disease	5.81E-05-5.34E-04	15
Respiratory Disease	9.66E-05-4.83E-04	43
Drug Metabolism	1.04E-04-1.04E-04	12
Cellular Compromise	1.46E-04-1.46E-04	6
Renal and Urological System Development and Function	1.46E-04-5.48E-04	33
Carbohydrate Metabolism	2.26E-04-2.26E-04	3
Nutritional Disease	2.31E-04-2.31E-04	38
Cell Signaling	3.65E-04-5.61E-04	54
Amino Acid Metabolism	4E-04-4E-04	7
Molecular Transport	4E-04-4E-04	7
Post-Translational Modification	4.22E-04-4.22E-04	53
Cell-mediated Immune Response	5.09E-04-5.09E-04	40
DNA Replication, Recombination, and Repair	5.62E-04-5.62E-04	34
Ophthalmic Disease	6.24E-04-6.24E-04	8

Table S2

Cry2 relevant disease and function	p-value	Molecules
Cancer	3.22E-22-2.87E-04	1516
Cellular Movement	6.89E-19-3.18E-04	418
Cellular Growth and Proliferation	7.54E-15-2.45E-04	609
Embryonic Development	8.27E-14-3.18E-04	417
Organismal Development	8.27E-14-3.11E-04	556
Cellular Development	1.24E-13-3.12E-04	604
Cardiovascular System Development and Function	3.02E-13-2.65E-04	263
Gastrointestinal Disease	3.37E-13-2.87E-04	673
Cellular Assembly and Organization	3.99E-13-3.02E-04	293
Cellular Function and Maintenance	3.99E-13-3.02E-04	400
Organismal Survival	9.34E-13-1.03E-04	432
Cell Death and Survival	9.38E-13-3.04E-04	596
Tissue Development	1.99E-12-3.11E-04	524
Organismal Injury and Abnormalities	2.68E-12-2.53E-04	805
Reproductive System Disease	2.68E-12-2.53E-04	699
Gene Expression	2.68E-12-3.74E-06	378
Cell Morphology	2.78E-12-3.02E-04	461
Tumor Morphology	5.73E-11-3.73E-05	149
Skeletal and Muscular System Development and Function	7.12E-10-2.79E-04	204
Organ Development	8.12E-10-3.11E-04	348
Neurological Disease	1.09E-09-2.68E-04	435
Respiratory System Development and Function	2.59E-09-1.09E-05	95
Hereditary Disorder	3.19E-09-3.23E-04	272
Psychological Disorders	3.19E-09-9.9E-05	217
Skeletal and Muscular Disorders	3.19E-09-4.64E-05	288
Tissue Morphology	3.34E-09-3.18E-04	414
Connective Tissue Development and Function	3.81E-09-2.79E-04	247
Organ Morphology	3.81E-09-3.11E-04	345
Cell-To-Cell Signaling and Interaction	7.29E-09-2.18E-04	91
Cell Cycle	7.83E-09-1.8E-04	261
Cardiovascular Disease	9.26E-09-3.23E-04	251
Developmental Disorder	1.22E-08-3.23E-04	291
Nervous System Development and Function	1.22E-08-3.02E-04	301

Reproductive System Development and Function	1.23E-08-1.95E-04	122
Digestive System Development and Function	1.42E-08-2.56E-04	145
Connective Tissue Disorders	6.69E-07-4.64E-05	101
Visual System Development and Function	1.47E-06-1.88E-04	98
Auditory and Vestibular System Development and Function	1.55E-06-3.11E-04	48
Post-Translational Modification	1.87E-06-1.87E-06	124
Endocrine System Development and Function	3.72E-06-3.27E-05	33
Hair and Skin Development and Function	4.39E-06-1.75E-05	86
Carbohydrate Metabolism	6.73E-06-2.97E-04	125
Behavior	6.9E-06-2.05E-05	160
Hepatic System Disease	8.54E-06-2.49E-04	41
Renal and Urological System Development and Function	8.58E-06-2.93E-04	82
Infectious Disease	8.85E-06-2.79E-04	266
Cellular Compromise	1.26E-05-2.15E-04	81
Hepatic System Development and Function	1.96E-05-2.56E-04	12
Organismal Functions	1.96E-05-2.47E-04	69
Ophthalmic Disease	2.53E-05-3.19E-04	35
Lipid Metabolism	3.06E-05-3.06E-05	22
Small Molecule Biochemistry	3.06E-05-3.27E-04	69
Immune Cell Trafficking	3.74E-05-2.15E-04	146
Protein Synthesis	3.87E-05-3.87E-05	139
Hematological System Development and Function	5.44E-05-2.47E-04	256
Inflammatory Response	5.44E-05-2.15E-04	180
DNA Replication, Recombination, and Repair	8.13E-05-3.27E-04	82
Hematological Disease	8.33E-05-2.84E-04	229
Immunological Disease	8.33E-05-2.84E-04	96
Cell Signaling	8.62E-05-8.62E-05	75
Dermatological Diseases and Conditions	1.12E-04-1.12E-04	28
Respiratory Disease	1.34E-04-3.23E-04	53
Molecular Transport	1.87E-04-1.87E-04	41
Hypersensitivity Response	2.15E-04-2.15E-04	27
Hematopoiesis	2.45E-04-2.45E-04	45
Nucleic Acid Metabolism	3.27E-04-3.27E-04	20

Table S3

Cry1/Cry2 relevant diseases and functions	p-value	Molecules
Cancer	2.39E-26-2.82E-04	2377
Cellular Assembly and Organization	2.83E-24-2.86E-04	518
Cellular Function and Maintenance	2.83E-24-2.7E-04	741
Cell Death and Survival	3.23E-21-2.31E-04	949
Cellular Movement	3.69E-21-2.3E-04	640
Cellular Growth and Proliferation	4.9E-21-2.89E-04	945
Organismal Survival	4.21E-18-5.17E-09	647
Cell Morphology	9.66E-18-2.8E-04	737
Organismal Injury and Abnormalities	3.9E-15-1.87E-04	1317
Reproductive System Disease	3.9E-15-1.28E-04	1243
Cardiovascular System Development and Function	9.25E-15-2.8E-04	443
Gastrointestinal Disease	2.01E-14-1.02E-04	1000
Neurological Disease	1.25E-13-1.41E-04	612
Cellular Development	2.1E-13-2.89E-04	878
Organismal Development	1.3E-12-2.8E-04	851
Embryonic Development	1.4E-12-2.58E-04	663
Gene Expression	5.8E-12-7.08E-06	559
Nervous System Development and Function	9.15E-12-2.57E-04	528
Tissue Morphology	2.27E-11-2.8E-04	684
Hereditary Disorder	4.46E-11-5.7E-05	234
Psychological Disorders	4.46E-11-1.61E-04	252
Skeletal and Muscular Disorders	4.46E-11-2.17E-04	417
Tissue Development	6.07E-11-2.89E-04	814
Cell-To-Cell Signaling and Interaction	1.39E-10-2.7E-04	243
Cell Cycle	5.86E-10-1.96E-04	392
Organ Morphology	1.26E-09-2.8E-04	406
Developmental Disorder	1.82E-09-2.75E-04	436
Organ Development	2.99E-09-2.58E-04	480
Connective Tissue Development and Function	3.03E-09-2.58E-04	367
Skeletal and Muscular System Development and Function	3.03E-09-2.89E-04	410
Cardiovascular Disease	5.62E-09-2.75E-04	508
Tumor Morphology	8.3E-09-1.02E-04	248
Infectious Disease	1.72E-07-1.28E-04	419

Digestive System Development and Function	6.67E-07-8.53E-06	208
Respiratory System Development and Function	7.82E-07-2.42E-04	92
Cell Signaling	9.85E-07-2.69E-04	305
Behavior	1.49E-06-1.96E-04	269
Renal and Urological Disease	3.28E-06-1.7E-04	166
Renal and Urological System Development and Function	4.06E-06-9.7E-05	87
Protein Synthesis	4.11E-06-2.09E-04	283
Connective Tissue Disorders	5.31E-06-2.17E-04	122
Dermatological Diseases and Conditions	5.93E-06-5.93E-06	42
Hematological Disease	5.93E-06-5.93E-06	42
Cellular Compromise	1.52E-05-2.86E-04	105
Post-Translational Modification	1.8E-05-1.57E-04	216
Inflammatory Response	2E-05-2.7E-04	96
Reproductive System Development and Function	2.49E-05-1.51E-04	179
Visual System Development and Function	2.5E-05-1.22E-04	128
Lymphoid Tissue Structure and Development	3.63E-05-2.88E-04	163
Hematological System Development and Function	7.78E-05-2.88E-04	245
Lipid Metabolism	1.09E-04-1.22E-04	86
Small Molecule Biochemistry	1.09E-04-1.57E-04	148
Auditory and Vestibular System Development and Function	1.16E-04-2.58E-04	45
Molecular Transport	1.22E-04-2.09E-04	124
Endocrine System Disorders	1.28E-04-1.28E-04	120
Hematopoiesis	1.47E-04-2.88E-04	210
Organismal Functions	1.52E-04-1.85E-04	69
Protein Degradation	1.68E-04-1.68E-04	117
Ophthalmic Disease	2.06E-04-2.69E-04	58
Protein Trafficking	2.09E-04-2.09E-04	45
Immune Cell Trafficking	2.3E-04-2.3E-04	212

Table S4

Bmal1 relevant diseases and functions	p-value	Molecules
Cell Death and Survival	1.33E-20-4.71E-04	547
Cancer	5.72E-19-4.84E-04	1282
Cellular Assembly and Organization	7.25E-18-5.19E-04	302
Cellular Function and Maintenance	7.25E-18-5.19E-04	455
Organismal Survival	7.9E-18-1.15E-11	380
Cellular Growth and Proliferation	4.27E-17-5.19E-04	537
Cellular Development	2.08E-16-4.32E-04	249
Cellular Movement	2.2E-15-4.44E-04	343
Cell Morphology	9.98E-15-5.29E-04	413
Tissue Morphology	1.7E-12-3.55E-04	404
Gene Expression	6.96E-12-1.7E-05	344
Organismal Development	3.24E-11-5.23E-04	494
Cardiovascular System Development and Function	2.27E-10-3.55E-04	236
Tumor Morphology	2.38E-10-2.08E-04	142
Tissue Development	1.01E-09-5.23E-04	481
Connective Tissue Development and Function	1.26E-09-4.18E-04	239
Neurological Disease	1.27E-09-4.87E-04	414
Nervous System Development and Function	1.48E-09-5.23E-04	272
Gastrointestinal Disease	2.19E-09-3.52E-04	560
Developmental Disorder	3.03E-09-4.16E-04	284
Organismal Injury and Abnormalities	6.88E-09-4.16E-04	704
Reproductive System Disease	6.88E-09-1.54E-04	631
Embryonic Development	7.96E-09-5.23E-04	386
Organ Development	7.96E-09-5.23E-04	297
Skeletal and Muscular System Development and Function	7.96E-09-4.77E-04	249
Cell-To-Cell Signaling and Interaction	1.01E-08-4.44E-04	244
Infectious Disease	1.03E-08-3.06E-04	246
Connective Tissue Disorders	2.4E-08-4.16E-04	214
Inflammatory Disease	2.4E-08-3.46E-04	232
Skeletal and Muscular Disorders	2.4E-08-4.16E-04	346
Cardiovascular Disease	3.73E-08-2.59E-04	307
Hematological System Development and Function	4.48E-08-3.62E-04	259
Hematopoiesis	8.54E-08-3.62E-04	136

Behavior	1.67E-07-4.82E-04	152
Cell Signaling	1.79E-07-1.82E-04	137
Digestive System Development and Function	4.31E-07-3.45E-04	121
Organ Morphology	7.52E-07-4.88E-04	316
Psychological Disorders	1.38E-06-4.87E-04	178
Hereditary Disorder	2.22E-06-1.5E-05	119
Respiratory System Development and Function	2.22E-06-4.63E-05	72
Cell Cycle	2.28E-06-3.87E-04	170
Lymphoid Tissue Structure and Development	4.44E-06-3.55E-04	156
Inflammatory Response	1.05E-05-4.25E-04	259
DNA Replication, Recombination, and Repair	1.06E-05-1.06E-05	67
Immune Cell Trafficking	1.16E-05-3.44E-04	171
Metabolic Disease	1.19E-05-5.22E-04	140
Post-Translational Modification	1.83E-05-4.14E-04	128
Protein Synthesis	1.83E-05-2.03E-05	35
Dermatological Diseases and Conditions	1.85E-05-4.55E-04	140
Antigen Presentation	2.03E-05-2.03E-05	5
Cell-mediated Immune Response	2.52E-05-3.25E-05	79
Hematological Disease	2.64E-05-4.84E-04	189
Reproductive System Development and Function	3.34E-05-4.77E-04	111
Carbohydrate Metabolism	4.6E-05-1.9E-04	46
Molecular Transport	4.6E-05-4.6E-05	38
Small Molecule Biochemistry	4.6E-05-1.82E-04	84
Immunological Disease	4.69E-05-4.84E-04	209
Endocrine System Disorders	4.82E-05-5.22E-04	71
Free Radical Scavenging	5.12E-05-5.29E-04	73
Hair and Skin Development and Function	5.15E-05-2.06E-04	52
Lipid Metabolism	8.59E-05-8.59E-05	19
Protein Folding	9.51E-05-9.51E-05	6
Ophthalmic Disease	1.42E-04-3.11E-04	37
Cellular Compromise	2.08E-04-2.08E-04	4
Nutritional Disease	2.21E-04-2.21E-04	39
Renal and Urological Disease	3.24E-04-3.24E-04	24
Auditory and Vestibular System Development and Function	3.41E-04-3.41E-04	7
Visual System Development and Function	3.45E-04-3.45E-04	5
Cellular Response to Therapeutics	4.55E-04-4.55E-04	10

CHAPTER 6

General discussion

General discussion

Dividing cells are characterized by the presence of two clock systems: a circadian clock and a cell cycle clock. In mammalian cells, these two oscillatory systems are strongly coupled (Bieler et al., 2014; Feillet et al., 2014) and influence each other in a bi-directional way (Feillet et al., 2015). Synchronization of the circadian clock by the use of clock synchronizers, such as dexamethasone, clustered mitotic events. On the other hand, the circadian period in proliferating cells is adjusted to the cell cycle period. Although it is clear that these two oscillatory systems are robustly coupled and interact with each other, the details of these interactions remain to be fully determined. In the context of this bi-directional link, it is important to know how alteration in one of the oscillators impacts the other one. It is also important to verify how these two systems interact in cells displaying aberrant cell proliferation and a disrupted circadian system such as cancer cells.

In **Chapter two** of this thesis we studied the importance of the circadian clock in the regulation of cell cycle progression by genetic knockdown of the positive circadian elements of the molecular circadian oscillator. To this end, we have used a mouse fibroblast cell line (NIH3T3^{3C}) that expresses fluorescent reporters for the clock (Rev-Erb-VNP), and for the G1 phase (Cdt1:mKO2) and combined S, G2 and M phases (Geminin: E2crimson) of the cell cycle (Feillet et al., 2014). Using this system, we were able to quantify the kinetics of circadian oscillation and cell cycle progression in individual cells by live cell imaging. First, we analyzed the circadian oscillation in dividing versus non-dividing NIH3T3^{3C} cells. In line with our previous observation (Feillet et al., 2014), we observed circadian and cell cycle periods of approximately 17 hour in proliferating cells. Notably, after cells reached confluency, the circadian period was close to 23 hours. This suggests that the circadian clock in proliferating cells is no longer free running, but rather is entrained or reset by the cell cycle, likely each mitotic event.

Next, we analyzed the cell cycle progression in the absence of the positive circadian elements by silencing either the *Clock* or *Bmal1* gene, the gene products of which form the heterodimeric transcription activator CLOCK/BMAL1. Knockdown of these positive circadian regulators completely suppressed the circadian oscillation and induced an increase of 4 hours in the total cell cycle length, as determined by single cell imaging. Our results in particular demonstrate the importance of circadian regulation on the dynamics of cell division. Subsequent FACS analysis revealed that the increased cell cycle length was due to a lengthening of the G2 phase, which is suggestive for a role of the CLOCK/BMAL heterodimer in G2/M transition. Further, we have elucidated the molecular mechanism underlying CLOCK/BMAL1 mediated regulation of G2/M transition. Knockdown of *Bmal1* or *Clock* genes dampened Cyclin B1 protein levels in late G2 cells. High Cyclin B1 protein levels, as well as high Cyclin B1-Cdk1 kinase activity in late G2 cells, are essential for G2/M transition (Gavet & Pines, 2010). However, to avoid premature mitosis Cyclin B1-CDK1 complexes are initially kept in an inactive state by the inhibitory effect of WEE1 and MYT1 kinases (Mueller et al., 1995; Parker & Piwnica-Worms, 1992; Fung et al., 2005). It has been

well established that expression of WEE1 kinase is also under direct circadian control of the CLOCK/BMAL1 transcription factor (Matsuo et al., 2003). Thus, it appears that CLOCK/BMAL1 complex has a dual role in controlling G2/M check point by simultaneously regulating an activator (Cyclin B1) and an inhibitor (WEE1) of mitotic entry. However, the increased cell cycle length in *siClock* and *siBmal1* cells suggests that the regulatory effect of CLOCK/BMAL1 complex on the activator (Cyclin B1) of G2/M check point is dominant over the effect on the repressor (WEE1) of G2/M transition (See Fig. 1 for a schematic model of CLOCK/BMAL1 regulation on the G2/M cell cycle transition). This finding is supported by earlier reports showing a decreased cell proliferation in *Clock* or *Bmal1* knock out condition. For instance, after partial hepatectomy hepatocytes from *Clock* knock out mice showed delayed liver regeneration, which can be attributed to a delayed entry into mitosis (Matsuo et al., 2003). Moreover, primary hepatocytes from *Bmal1* knock out mice showed a decreased proliferation rate (Grechez-Cassaiu et al.,2008). Thus, our results suggest a novel regulatory mechanism of BMAL1/CLOCK on G2/M transition by modulating the G2 specific expression of Cyclin B1, explaining the observed slower cell cycle progression.

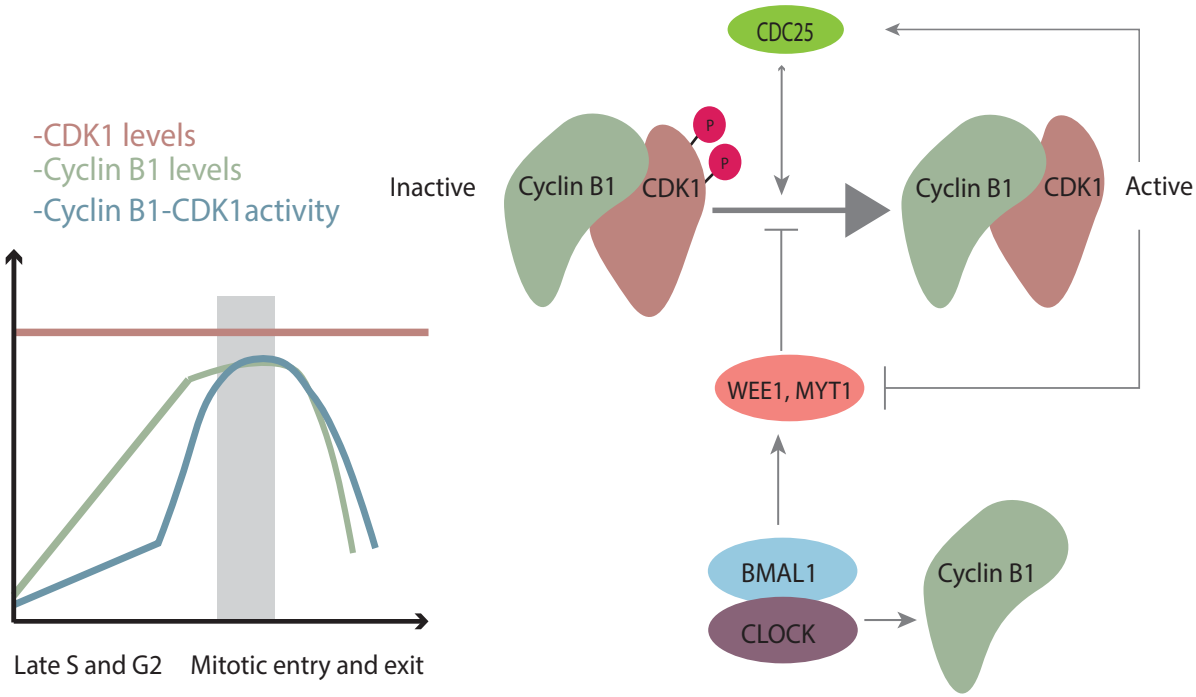

Figure 1. Schematic model. Activation of CyclinB1-CDK1 complex and role of CLOCK/BMAL1 in G2/M cell cycle transition (as it is described in the text).

In **Chapter three** we continued to investigate the role of the circadian clock in cell cycle regulation by studying the impact of CRISPR/Cas9 mediated inactivation of the negative circadian elements (*Cry1* and *Cry2*) in NIH3T3^{3C} cells. Using live cell imaging of cell cycle progression in individual cells and FACS analysis of proliferating cell cultures, we have shown that inactivation of both *Cry* genes shortened the G1 phase of proliferating cells by 2 hours, along with a significant increase in G2 and M phases.

To shed light on the underlying molecular mechanism, we also investigated Cyclin expression in the CRY deficient cells. We observed elevated levels of Cyclin E protein at G1/S transition in CRY deficient cells, which well explains the shortened G1 phase. In line with this finding, it has been shown that overexpression of Cyclin E decreases the time that cells spend to finish G1 phase and enter S phase (Ohtsubu et al., 1995; Resnitzky et al., 1995). Moreover, Cyclin A2 and Cyclin B1 protein levels remain high in early mitotic *Cry* double knock out cells, while these two cyclins are gradually degraded in the control cells. This observation is an indication of delayed degradation of these mitotic Cyclins. In line with this observation, there was higher phosphorylation of mitotic substrates (as detected by western blot analysis) and a larger mitotic cell population (flow cyctometry data). It has been reported that active Cyclin A2-CDK2 and Cyclin B1-CDK1 phosphorylate key mitotic substrates (Pines et al., 2006) and thereby regulate the stability and activity of mitotic proteins (Ptacek et al., 2006; Oslen et al., 2010). Subsequently, timed degradation of Cyclin A2 and Cyclin B1 allows phosphatases to reverse the phosphorylation of mitotic substrates and end mitosis (Domingo-Sananes et al., 2011). Therefore, our results suggest a prominent role of the negative circadian elements on phosphorylation of mitotic proteins, by modulating the degradation of important mitotic kinases. This in turn can have a high impact on mitotic progression. A comparative time course phosphoproteomics experiment in the Ctrl and *Cry dko* cell lines is needed to reveal the underlying mechanism involved in CRY-mediated post translational regulation and its effect on cell cycle progression.

Therefore, we have shown that the positive circadian elements (CLOCL/BMAL1) are involved in the regulation of G2/M transition, and that the negative circadian factors (CRY1 and CRY2) regulate G1/S, as well as mitotic progression. The positive and negative circadian elements increased and decreased the total period of the cell cycle respectively. The observed difference in phenotypes could be expected, considering the opposite regulatory effect of the positive and negative circadian elements on E-box transcription of clock controlled genes (CCG) participating in the regulation of cell cycle events.

The importance of the circadian clock-cell cycle coupling in healthy cells is well understood.

For instance, the cellular clock-cell cycle coupling has a major impact on timed mitosis at the tissue level (Scheving et al., 1959; Geyfman et al., 2012). Importance of the coupling was also shown to be necessary in tissue integrity (Janich et al., 2011). Regarding the significance of coupling in healthy cells, the interplay between the circadian clock and the cell cycle in cancer cells, that normally display de-regulated cell proliferation and disrupted clock gene expression, is of great interest. This raises the question whether the circadian clock/cell cycle coupling exists in the tumor cells. If not, what are the consequences of un-coupling between these two systems in the cancer cells.

In **Chapter four**, we have started to investigate the circadian clock - cell cycle coupling in a panel of $p53^{R270H/+}$ mutant mouse breast carcinoma (MBC) cell lines. To this end, we have stably introduced the fluorescent clock reporter Rev-Erbα-VNP to study the interaction between the circadian clock and cell cycle at the single cell level. Interestingly, whereas in proliferat-

ing NIH3T3^{3C} cells the circadian clock and cell cycle have comparable periods and are phase coupled in a 1:1 ratio, we observed that in proliferating MBC399 cells the circadian clock is free-running while mitosis occurs independent of the circadian phase. To our knowledge, this is the first example of a cell line in which the circadian clock and the cell cycle are uncoupled. The obvious question arising is which molecules are mediating the coupling between these two systems. One possible candidate could be P53 protein, which is the only identified cell cycle molecule that has mutual influences on both the circadian and cell cycle systems (Miki et al., 2013). Correcting the p53$^{R270H/+}$ mutant mouse breast carcinoma cell line could be an attractive strategy to study the role of P53 gene in the coupling between the circadian clock and cell cycle. Nonetheless, considering the complexity of circadian clock and cell cycle systems, P53 most likely is not the only mediating molecule. Therefore, transcriptome analysis of the MBC-399 cells in the proliferating state would provide us more details on probable coupling candidates. These molecules will be attractive targets for therapeutic purposes.

Chronotherapy benefits from desynchrony between cancer and normal cells in various processes that are under circadian control, such as drug metabolism and proliferation (Lévi et al., 2007). New cancer chronotherapeutic approaches for optimization of treatment time were developed based on the 24-hour rhythmicity in cell proliferation (Levi et al., 2007). Obtaining more knowledge about the circadian clock-cell cycle coupling in cancer cells will facilitate the improvement of chronotherapuetic approaches in which asynchrony in timed mitosis between the host and malignant tissues is used to predict the optimal time of treatment. For instance, by choosing a time window in which normal cells are least sensitive to the treatment, while malignant cells undergo random cell proliferation independent of the circadian phase.

In **Chapter five**, we aimed to understand how manipulation of core clock gene expression can affect the cancer properties of a cancer cell. To this end, we used the human lung carcinoma cell line H1299 and generated a panel of clock knockdown H1299 cell lines with attenuated expression of *CRY1*, *CRY2*, *CRY1/CRY2,* or *BMALl1*. We first analyzed the transcriptome of these cells. Ingenuity Pathway Analysis (IPA) on differential expressed genes revealed that cancer is one of the top significantly affected diseases and bio-functions in all the knockdown cell lines. Interestingly, categories related to the cancer properties of the cells, such as growth of malignant tumors and proliferation of tumor cells, were oppositely affected with a significant up regulation in *CRY1/CRY2* knockdown H1299 cells, and down regulation in *BMAL1* knockdown H1299 cells. Next, we validated our transcriptome profile using in vitro (cell culture) and in vivo (xenograft) studies. Our in vitro experiments showed that inactivation of the *CRY* genes resulted in a reduction of the proliferation rate of H1299 cells, while inactivation of BMAL1 had no effect. Therefore, this observation contrasts the transcriptomics data, which showed up regulation and down regulation of cell proliferation in *BMAL1* and *CRY* knock down cells. However, in line with the transcriptomics data, in vivo experiments showed accelerated tumor formation by about 2 weeks in *CRY/CRY2* knockdown cells. In contrast, tumor formation was entirely suppressed in *BMAL1* knock down cells. Therefore, a good correlation was observed between *in vivo* studies, addressing tumor formation and growth of H1299 core clock gene knockdown cells, and transcriptome data.

To understand the mechanisms involved, a detailed pathway enrichment analysis is required.

In conclusion, we have dissected the circadian clock/cell cycle coupling in healthy cells by genetically disrupting core circadian clock genes. By the use of Fuuci cell cycle system with the two cell cycle reporters (G1, and S/G2/M) we were able to study the cell cycle progression at the single cell level. Considering the broad impact of clock genes on different cell cycle phases further improvements of the Fucci system is required to discriminate between each of the S, G2, and M phases. Moreover, one of the questions that has not been firmly addressed is the bi-directionality in the interaction between the circadian and cell cycle systems. Previous reports in which the circadian clock and cell cycle are pharmaceutically manipulated are subject to debate since many of these drugs act on both systems. Therefore, an approach to manipulate only one of the oscillators without a direct influence on the other one is required. For instance, an optogenetic approach is an effective way to synchronize the circadian clock by light while cell cycle is not directly affected, and vice-versa. Such an approach, combined with a genome wide RNAi screen, will be a powerful means to identify molecules involved in the coupling between the circadian clock and the cell cycle. It will be important to determine the status of the coupling in various cancers in future studies, and to apply this knowledge to develop new therapeutic approaches. Gaining insight into the molecules mediating the coupling will help to design novel anti-cancer therapy targets.

References

Antoch MP, Gorbacheva VY, Vykhovanets O, Toshkov IA, Kondratov RV, Kondratova AA, Lee C, Nikitin AY (2008) Disruption of the circadian clock due to the Clock mutation has discrete effects on aging and carcinogenesis. *Cell Cycle* 7:1197–1204.

Bieler J, Cannavo R, Gustafson K, Gobet C, Gatfield D, Naef F (2014) Robust synchronization of coupled circadian and cell cycle oscillators in single mammalian cells. *Mol Syst Biol* 10:739.

Damiola F, Le Minh N, Preitner N, Kornmann B, Fleury-Olela F, Schibler U (2000) Restricted feeding uncouples circadian oscillators in peripheral tissues from the central pacemaker in the suprachiasmatic nucleus. *Genes Dev* 14: 2950-2961.

Destici E, Oklejewicz M, Saito S, van der Horst GT (2011) Mammalian cryptochromes impinge on cell cycle progression in a circadian clock-independent manner. *Cell Cycle* 10:3788-3797.

Domingo-Sananes MR, Kapuy O, Hunt T, Novak B (2011) Switches and latches: a biochemical tug-of-war between the kinases and phosphatases that control mitosis. *Philos Trans R Soc Lond B Biol Sci* 366:3584-3594.

Feillet C, Krusche P, Tamanini F, Janssens RC, Downey MJ, Martin P, Teboul M, Saito S, Lévi FA, Bretschneider T, van der Horst GTJ, Delaunay F, Rand DA (2014) Phase locking and multiple oscillating attractors for the coupled mammalian clock and cell cycle. *Proc Natl Acad Sci USA* 111:9828-9833.

Feillet C, van der Horst GT, Levi F, Rand DA, Delaunay F (2015) Coupling between the Circadian Clock and Cell Cycle Oscillators: Implication for Healthy Cells and Malignant Growth. *Front Neurol* 6:96.

Fu L, Kettner NM (2013) The circadian clock in cancer development and therapy. *Prog Mol Biol Transl Sci* 119:221-282.

Fu L, Patel MS, Bradley A, Wagner EF, Karsenty G (2005) The molecular clock mediates leptin- regulated bone formation. *Cell* 122:803-815.

Fung TK, Poon RYC (2005) A roller coaster ride with the mitotic cyclins. *Sem Cell Dev Biol* 16:335-342.

Gavet O, Pines J (2010) Progressive activation of CyclinB1-Cdk1 coordinates entry to mitosis. *Dev Cell* 18:533-543.

Geyfman M, Kumar V, Liu Q, Ruiz R, Gordon W, Espitia F, Cam E Millar SE, Smyth P, Ihler A, Takahashi JS, Andersen B (2012) Brain and muscle Arnt-like protein-1 (BMAL1) controls circadian cell proliferation and susceptibility to UVB-induced DNA damage in the epidermis. *Proc Natl Acad Sci U S A* 109:11758-11763.

Gréchez-Cassiau A, Rayet B, Guillaumond F, Teboul M, Delaunay F (2008) The circadian clock component BMAL1 is a critical regulator of p21WAF1/CIP1 expressionand hepatocyte proliferation. *J Biol Chem* 283:4535-4542.

Hoffman AE, Zheng T, Yi CH, Stevens RG, Ba Y, Zhang Y, Leaderer D, Holford T, Hansen J, Zhu Y (2010) The core circadian gene Cryptochrome 2 influences breast cancer risk, possibly by mediating

hormone signaling. *Cancer Prev Res* 3:539:548.

Matsuo T, Yamaguchi S, Mitsui S, Emi A, Shimoda F, Okamura H. Control Mechanism of the Circadian Clock for Timing of Cell Division in Vivo. *Science*, 2003, 302 (5643): 255-259.

Mazzoccoli G, Colangelo T, Panza A, Rubino R, De Cata A, Tiberio C, Valvano MR, Pazienza V, Merla G, Augello B, Trombetta D, Storlazzi CT, Macchia G, Gentile A, Tavano F, Vinciguerra M, Bisceglia G, Rosato V, Colantuoni V, Sabatino L, Piepoli A (2016) Deregulated expression of cryptochrome genes in human colorectal cancer. *Mol Cancer* 15:16.

Miki T, Matsumoto T, Zhao Z, Lee CC (2013) p53 regulates Period2 expression and the circadian clock. *Nat Commun* 4:24444.

Mueller PR, Coleman TR, Kumagai A, Dunphy WG (1995) Myt1: a membrane-associated inhibitory kinase that phosphorylates Cdc2 on both threonine-14 and tyrosine-15. *Science* 270:86-90.

Lévi F, Filipski E, Iurisci I, Li XM, Innominato P (2007) Cross-talks between circadian timing system and cell division cycle determine cancer biology and therapeutics. *Cold Spring Harb Symp Quant Biol* 72:465-475.

Ohtsubo M, Theodoras AM, Schumacher J, Roberts JM, Pagano M (1995) Human Cyclin E, a nuclear protein essential for the G1-to-S phase transition. *Mol Cell Biol* 15:2612-2624.

Oslen JV, Vermeulen M, Santamaria A, Kumar C, Miller ML, Jensen LJ, Gnad F, Cox J, Jensen TS, Nigg EA, Brunak S, Mann M (2010) Quantitative phosphoproteomics reveals widespread full phosphorylation site occupancy during mitosis. *Sci Signal* 3: ra3.

Parker LL, Piwnica-Worms H (1992) Inactivation of the p34cdc2-cyclin B complex by the human WEE1 tyrosine kinase. Science 257:1955-1957.

Pines J (2006) Mitosis: a matter of getting rid of the right protein at the right time. *Trends Cell Biol* 16:55-63.

Ptacek J, Snyder M (2006) Charging it up: global analysis of protein phosphorylation. *Trends Genet* 22:545-554.

Resnitzky D, Reed SI (1995) Different roles for Cyclins D1 and E in regulation of G1-to-S transition. *Mol Cell Biol* 15:3463-3469.

Rue P, Martinez Arias A (2015) Cell dynamics and gene expression control in tissue homeostasis and development. *Mol Syst Biol* 11:729.

Scheving LE (1959) Mitotic activity in the human epidermis. *Anat* Rec 135:7-19

Stokkan KA, Yamazaki S, Tei H, Sakaki Y, Menaker M (2001) Entrainment of the circadian clock in the liver by feeding. *Sience* 291:490-493.

Janich P, Pascual G, Merlos-Suarez A, Batlle E, Ripperger J, Albrecht U, Cheng HY, Obrietan K, Di Croce L, Benitah SA (2011) The circadian molecular clock creates epidermal stem cell heterogeneity. *Nature* 480:209-214.

APPENDIX

Summary
Samenvatting (Dutch summary)
PhD Portfolio
List of puplications
Curriculum vitae
Acknowledgments

Summary

Life on earth is exposed to a 24-hour light/dark cycle generated by the earth rotation around its own axis. Almost all living organisms have developed an internal timing system, called "the circadian clock", to adapt to the daily environmental changes. The circadian clock system gives a 24-hour rhythmicity to various physiological processes (such as behavior, metabolism, sleep wake cycle, and hormone secretion) to optimize them to an exact time of the day.

Mammalian circadian system is organized in a hierarchical manner with the superchiasmatic nucleus (SCN) as the master clock at the top of hierarchy, and peripheral clocks in almost all the single cells over the body. The SCN is located in the hypothalamus of brain and is composed of approximately 20,000 neurons. Light information is received by the photoreceptors located in the ganglion cells in the inner nuclear layer of the retina and transmitted to the SCN neurons. Subsequently, synchronizing signals coming from the SCN are transmitted to the peripheral clocks via hormonal and neural cues. Therefore, the whole organism is synchronized internally and synchronized to the external environment. At the molecular level, the circadian oscillator is based on autonomous and auto-regulatory feedback loops. The CLOCK/BMAL1 heterodimer induces E-box transcription of *Per (Per1, Per2)* and *Cry (Cry1, Cry2)* genes. PER and CRY proteins accumulate in the cytoplasm and after a delay of several hours translocate to the nucleus where they inhibit CLOCK/BMAL1-mediated transcription. The whole process follows a circadian periodicity close to 24-hours. CLOCK/BMAL1 heterodimer also induces E-box transcription of the so-called Clock Controlled Genes (CCG), composing 10% of the whole genome. Clock controlled genes are involved in the regulation of a variety of physiological events such as the cell cycle process. The cell cycle is another independent oscillatory system, governed by sequential events of transcription, and protein degradation. The circadian clock and cell cycle systems are tightly coupled and interact in a bi-directional way, meaning that synchronization of the circadian system using clock synchronizers, such as dexamethasone, will entrain mitosis. On the other hand, the circadian oscillator is reset by each mitotic event.

In chapter 2 we investigated the importance of these reciprocal interactions by knocking down the positive circadian elements (*Bmal1* and *Clock* genes). Using the NIH3T3^{3C} mouse fibroblast cell line (carrying fluorescent reporter genes for clock and cell cycle phase), we have shown an increased cell cycle length by about 4 hours in *Bmal1* knock down cells. We found that the slower cell cycle progression originated from a delayed G2/M transition caused by an impaired G2 specific expression of Cyclin B1.

In chapter 3, we knocked out the cryptochromes (*Cry1*$^{-/-}$, *Cry2*$^{-/-}$) in the NIH3T3^{3C} cells and investigated cell cycle progression in the absence of negative circadian elements. We have shown a decrease of 2 hours in the total cell cycle length, arising from a short G1 phase. Further molecular analysis revealed involvement of the cryptochromes on G1/S transition by regulating Cyclin E expression. Moreover, a high phosphorylation pattern of mitotic proteins in *Cry1*$^{-/-}$, *Cry2*$^{-/-}$ cells, together with a high percentage of mitotic cells, indicated impaired mitotic progression in cryptochrome deficient cells. Our data demonstrate that post-transla-

tional regulation of mitotic proteins is affected in the absence of cryptochromes.

In chapter 4, we studied the importance of coupling between the circadian clock and cell cycle machineries in cancer cells. We have stably introduced a circadian clock reporter (REV-ERBα promotor) into a mouse breast carcinoma cell line derived from heterozygous *p53-R270H/+ WAPCre* mice (MBC399). Using this system, we have followed the kinetics of circadian clock and cell cycle progression in real time and at the single cell level. We observed that the cellular clock/cell cycle coupling is lost in MBC399 cells. In contrast to the NIH3T3[3C] cells, cell division occurred independent of the circadian time in MBC399 cells. Our results highlight the importance of the cellular clock/cell cycle coupling in controlling the proliferation rate, which is lost in MBC399 cells.

In chapter 5, the effect of circadian clock gene knock-down on the cellular properties of human lung carcinoma cell lines (H1299 cell) was investigated. We have performed a transcriptome analysis on a panel of clock knock down H1299 cell lines. It appears that cancer and cellular growth are two of the top affected processes in all the clock knock down cell lines. Processes related to cancer, such as tumor formation and proliferation of malignant cells, were down regulated in Bmal1 knock down cells and up-regulated in cryptochrome deficient cells. In line with the transcriptome analysis, our in vivo study shows suppressed and accelerated tumor formation in *Bmal1* knock down and cryptochrome deficient cells, respectively. Overall, our transcriptome analysis, together with the in vivo studies, showed a prominent involvement of core circadian clock genes on the proliferation capacity of tumor cells, as well as tumor forming ability. The effect observed makes the circadian clock genes attractive targets in cancer therapy.

Samenvatting

Het leven op aarde wordt blootgesteld aan een 24-uurs licht/donker cyclus die wordt gegenereerd door de rotatie van de aarde om zijn eigen as. Bijna alle levende organismen hebben een intern timingsysteem ontwikkeld, "de circadiane klok" genoemd, om zich aan te passen aan deze 24-uurscyclus. Het circadiane kloksysteem geeft een 24-uursritme aan verschillende fysiologische processen (zoals gedrag, metabolisme, slaap-waakritme en hormoonafgifte), zodat ze optimaal zijn op een bepaald tijdstip van de dag.

Het circadiaans systeem van zoogdieren is georganiseerd op een hiërarchische manier. De superchiasmatische kern (SCN) als de hoofdklok aan de top van de hiërarchie en perifere klokken in bijna alle afzonderlijke cellen van het lichaam. De SCN bevindt zich in de hypothalamus van de hersenen en bestaat uit ongeveer 20.000 neuronen. Lichtinformatie wordt ontvangen door de fotoreceptoren die zich in de ganglioncellen in de binnenste laag van het netvlies bevinden en worden doorgegeven aan de SCN-neuronen. Vervolgens worden synchronisatiesignalen afkomstig van de SCN via hormonale en neurale signalen naar de perifere klokken verzonden. Hierdoor wordt het hele organisme intern gesynchroniseerd en tevens gesynchroniseerd met de externe omgeving. Op moleculair niveau is de circadiaanse oscillator gebaseerd op autonome en zelfregulerende feedbacklussen. Het KLOK/ BMAL1 heterodimeer induceert E-box-transcriptie van *Per* (*Per1, Per2*) en *Cry (Cry1, Cry2)* genen. PER en CRY eiwitten hopen zich op in het cytoplasma en verplaatsen zich na enkele uren naar de kern waar ze de KLOK/BMAL1 gemedieerde transcriptie remmen. Het hele proces volgt een circadiane periodiciteit, die bijna 24 uur duurt. KLOK/ BMAL1 heterodimeer induceert ook E-box-transcriptie van de zogenaamde Clock Controlled Genes (CCG), die 10% van het gehele genoom vormen. Klokgestuurde genen zijn betrokken bij de regulatie van een verscheidenheid aan fysiologische gebeurtenissen zoals het celcyclus proces. De celcyclus is een ander onafhankelijk oscillatiesysteem, die wordt beheerst door opeenvolgende gebeurtenissen van transcriptie en eiwitafbraak. De circadiane klok en celcyclus systemen zijn nauw gekoppeld en interageren op een bi-directionele manier met elkaar. Dit betekent dat synchronisatie van het circadiane systeem door middel van klok synchronizers, zoals dexamethason, de timing van de mitose meevoert. Aan de andere kant wordt de circadiane oscillator gereset bij elke mitose.

In hoofdstuk 2, onderzochten we het belang van deze reciproke interacties door de positieve circadiaanse elementen (Bmal1 en Klok genen) te verlagen. Met behulp van de NIH3T3^{3C}-fibroblastcellijn van muizen (die fluorescerende reportergenen draagt voor de klok en celcyclus fase) hebben we een toegenomen lengte van de celcyclus met ongeveer 4 uur in Bmal1 knockdown cellen aangetoond. We lieten zien dat de tragere voortgang van de celcyclus, als gevolg van een vertraagde G2/M overgang, werd veroorzaakt door een verminderde G2-specifieke expressie van Cyclin B1.

In hoofdstuk 3, hebben we de cryptochromen (Cry1 $^{-/-}$, Cry2 $^{-/-}$) in de NIH3T3^{3C}-cellen uitgeschakeld (knock out) en de voortgang van de celcyclus onderzocht in afwezigheid van negatieve circadiaanse elementen. We laten een afname van 2 uur in de totale lengte van de

celcyclus zien, voortkomend uit een korte G1-fase. Verdere moleculaire analyse onthulde de betrokkenheid van de cryptochromen op G1/S-transitie door de expressie van Cyclin E te reguleren. Bovendien duidde een hoog fosforyleringspatroon van mitotische eiwitten in Cry1 $^{-/-}$, Cry2 $^{-/-}$ cellen, tezamen met een hoog percentage mitotische cellen, op verminderde mitotische progressie in cryptochroom-deficiënte cellen. Onze gegevens tonen aan dat post-translationele regulatie van mitotische eiwitten wordt beïnvloed in afwezigheid van cryptochromen.

In hoofdstuk 4, hebben we het belang van de koppeling tussen de circadiane klok en de celcyclus in kankercellen bestudeerd. We hebben op stabiele wijze een circadiane klokreporter (REV-ERB-promotor) geïntroduceerd in een muizenborstcarcinoom cellijn afgeleid van heterozygote p53-R270H/+WAPCre muizen (MBC399). Met dit systeem hebben we de kinetiek van de circadiane klok en celcyclusprogressie in real time en op het niveau van een enkele cel gevolgd. We hebben vastgesteld dat de koppeling van de cellulaire klok/ celcyclus verloren gaat in MBC399 cellen. In tegenstelling tot de NIH3T3^{3C} cellen vond celdeling plaats onafhankelijk van de circadiane tijd in MBC399 cellen. Onze resultaten benadrukken het belang van de koppeling van de cellulaire klok/celcyclus, die verloren gaat in MBC399-cellen, bij het beheersen van de proliferatiesnelheid.

In hoofdstuk 5, onderzochten we het effect van de knockdown van circadiane klokgen op de cellulaire eigenschappen van menselijke long carcinoomcellijnen (H1299-cel). We hebben een transcriptoom analyse uitgevoerd op een panel van H1299 cellen met knock down klokgenen. Het blijkt dat kanker en cellulaire groei twee van de belangrijkst beïnvloede processen zijn in alle knock down cellijnen. Processen gerelateerd aan kanker, zoals tumorvorming en proliferatie van kwaadaardige cellen, werden neerwaarts gereguleerd in Bmal1 knockdown cellen en opwaarts gereguleerd in cryptochroom-deficiënte cellen. In lijn met de transcriptoom analyse, toont in vivo onderzoek ons vertraagde en versnelde tumorvorming in respectievelijk Bmal1 knockdown en cryptochroom-deficiënte cellen. Overall toonde onze transcriptoom analyse, in combinatie met de in vivo onderzoeken, een prominente betrokkenheid van de belangrijkste circadiane klokgenen op de proliferatiecapaciteit van tumorcellen, evenals het tumorvormende vermogen. Dit waargenomen effect maakt de circadiane klokgenen aantrekkelijke doelen in kankertherapie.

PhD Portfolio

Name PhD student: **Elham Farshadi**
Erasmus MC Department: **Molecular Genetics**
Research School: **Molecular Genetics Centre (MGC)**

PhD period: **July. 2012- Dec. 2017**
Promoter: **Prof. dr. G.T.J. van der Horst**
Supervisors: **Dr. I. Chaves**

1- PhD training	Year	Workload (ECTS)
General courses		
Biochemistry and Biophysics course	2012	3
Laboratory animal science (art 9)	2013	3
Cell and Developmental Biology course	2013	3
Genetics course	2013	3
Literature study course	2015	2
Biomedical scientific English writing	2016	4
Specific courses and workshops		
Photoshop and Illustrator CS 6 workshop	2014	0.3
Next generation sequencing (NGS) (Groningen)	2015	2
Posters		
20th MGC Phd workshop, Luxemburg.	2013	0.3
21th MGC Phd workshop, Munster, Germany.	2014	0.3
SRBR conference, Palm Harbor, United states.	2016	0.3
(Inter)national conferences		
Oral presentations in MGC DNA repair meetings	2012-2017	1
Oral presentation in CTR meeting, Rotterdam, NL	2015	1
Oral presentation in EBRS conference, Manchester, UK	2015	1
Oral presentation in MGC workshop, Dortmund, Germany	2016	1
Oral presentation in Gliwice Scientific meeting, Poland	2016	1

2-Teaching	Year	Workload (ECTS)
Teaching assistant for BSc Nano-biology students from Erasmus MC	2013-2016	
Supervising and training a second-year master student from the university of Nice Sophia Antipolis for 6 months	2015	36
Supervising and training a second-year master student from the university of Istanbul for 3 months	2016	
supervising and training a bio-medical master student from Erasmus MC for 6 months	2017	36

List of Publications

■ The positive circadian regulators CLOCK and BMAL1 heterodimer control G2/M cell cycle transition through Cyclin B1(Submitted).

Elham Farshadi, Jie Yan, Pierre Leclere, Albert Goldbeter, Inês Chaves, Gijsbertus T.J. van der Horst.

■ The circadian clock proteins CRY1 and CRY2 control the cell cycle G1/S transition and mitotic progression(To be submitted)

Elham Farshadi, Karlijn Houkes, Roel Janssens, Gijsbertus T.J. van der Horst, Inês Chaves.

■ Loss of coupling between the circadian clock and the cell cycle in a mouse breast carcinoma cell line (To be submitted).

Elham Farshadi, Esmee van der Ploeg, Conny van Oosterom, Gijsbertus T.J. van der Horst, Inês Chaves.

■ Circadian clock genes differentially modulate the cancer properties of H1299 human non-small lung carcinoma cells (Submitted)

Romana M. Nijman, Elham Farshadi, Cesar E. Payan Gomez, Cíntia R. Bombardieri, Roel Janssens, Stefanie Vester, Yanto Ridwan, Filippo Tamanini, Inês Chaves and Gijsbertus T.J. van der Horst.

Curriculum vitae

Name	Elham Farshadi
E-mail	elhamfarshadi@gmail.com
Date of birth	21. September. 1980
Place of birth	Ahvaz- Iran

Education

2012-2017 PhD candidate, Dept. of Molecular Genetics, Erasmus University Medical Center, Rotterdam, the Netherlands
Thesis: *'Circadian clock-cell cycle connection and its implication for cancer'*

2010-2012 MSc, Biomolecular Sciences, Faculty of life sciences, Vrije Universiteit Amsterdam, the Netherlands

Thesis 1*: 'Early Mitotic Inhibitor (EMI1) protein regulation during the cell cycle'*
Molecular Carcinogenic Department, the Netherlands Cancer Institution (NKI), Amsterdam, February 2011- August 2011

Thesis 2: *'Role of the matrix protein Slit and its receptor, Roundabout, in the regulation of hematopoietic stem cell polarity'*
Hematopoiesis Department, Sanquin Research Institute, Amsterdam, the Netherlands, October 2011- May 2012

2007-2009 Research assistant, Dept. of Molecular Medicine, Pasteur Institute of Iran, Tehran.

2003-2007 Bachelor of Science (Biology), Tehran, Iran.

Acknowledgement

My PhD was an immense learning opportunity. It was the best chance for a self-discovery to get aware of your strengths, weaknesses, desires and dreams. Also, a great chance to learn how to explore, to reach to your goals, and to get out of the failure cycle.

First of all, I would like to express my sincere appreciation to my promoter **Prof. dr. Bert van der Horst** who considered me as a PhD candidate in his lab. I am thankful to all his scientific supports, guidance, patience, and his fair criticisms that made me grow and learn during the entire PhD period. Thanks a lot Bert.

My sincere gratitude also goes to my co-promoter **Dr. Inês Chaves**. Inês, your smart and accurate suggestions had a major impact to bring the research to the right direction. I always enjoyed our brain storming which was a pure guidance for me. I highly appreciate your kind and professional supports that gave lots of confidence to me till the last day of my PhD. Muito obrigado Inês.

I am thankful to the reading committee of my thesis, **Prof. dr. Vermeulen, Prof. dr. Lêvi, Dr. de Bruin,** who have spent their precious time reading my thesis.

Also, it was a great pleasure collaborating with **Prof. dr. Albert Goldbeter**. Thanks Albert for the very useful skype meetings and scientific discussions.

Accordingly, I would also like to acknowledge the former head of department **Prof. dr. Hoeijmakers** who allowed me to begin my research in the molecular genetic department. My thankfulness also go to the present head of department **Prof. dr. Roland Kanaar** for all the supports.

Special thanks to my paranymphs: **Diana** and **Bharath. Diana**, your sociable, caring and kind manner makes you a wonderful person. I am blessed to have you as my friend. I wish you happiness in your life and a big success for the rest of your PhD carrier. You deserve the best. **Bharath,** I was so lucky to have met you 8 years ago. Not only you rocked my life, but also, I always enjoyed our private and scientific discussions. I wish the best of luck for you toward finishing your PhD. I know you will do great.

I am grateful to my lovely friends in the department "**Rana, Chiara, Diana, Akos, Marjolein**, and **Chang**" who turned the intense moments of my PhD into the fun working times. I am blessed by the fact that I can always count on your spiritual and scientific supports. Our dinner gatherings, (which was mostly began at "Hamburg" and end up at "Worm"), are unforgettable and the most pleasant for me. Thank you all and we should keep doing that.

Many thanks to our students who made a great contribution in this thesis: **Pierre, Karlijn, Mattijs, and Esmee**.

To my fellow PhD students: **Hester, Astrid, Joris** I wish you lots of success for the rest of your work. **Serena,** I wish you success with your new Post-doc carrier and all the best with your little baby. **Peter, Wilbert, Joris, Sylvia, Yvette, Nicole, Shanon** it was an honor to get to know you and have you as my colleagues. **Reneta, Sander, Yvonne** I am grateful for all

your technical helps and lab organizations. I also enjoyed all the game and movie sections you were organizing to bring the fun and cheerful faces to the lab.

I would also like to express my regards and special thanks to my former colleagues **Romana, Cezar.**

Roel I cannot thank you more for all the supports you gave to me particularly at the beginning of my PhD. Your supports assist me to find my way. Although we have worked for a short period of time together, but you were always open and welcome to me till the end of my work. Thank you for your useful guidance.

Yasemin, I could always talk to you and share my concerns and my happiness with you. I wish you success with finalizing your thesis. **Cristina, Franzi, Mariangela, Barbara, Maria Tresini** wish you all the best. **Hannes,** it was a great pleasure assisting you for Nanobiology courses. Thanks for this great experience. **Arjan** and **Karen** thanks for all the technical supports. With this I would also like to acknowledge all the people of **Vermeulen's**, **van Gent's**, and **Kanaar's** labs for their collaborations and assistances.

Michiel, it has been always fun talking to you that even in the saddest moment could bring a big smile on my face. I wish you all the best with finalizing your thesis. **Mateuses and Gosia** thanks for the wonderful fun and party times we had together. we should keep doing that. I also wish you both the best of luck for your thesis.

To the optical imaging center: **Gert van Capellen, Gert Kremers, and Martijn**; I am thankful for your immediate assistance at the microscopy to facilitate my work when needed. I *couldn't* have *done* this work *without your* expert help.

To the secretary ladies: **Jasperina** and **Sonja** I highly appreciate your kind helps to assist me filling in all the Dutch language forms ;) but also, all the administration works that you have done for me.

Special thank is devoted to **Job lassche** for his continuous support to take care of the renewal of my residence permit and my contract. This was a real help that facilitated my work particularly at the last year of my PhD. Thanks Job.

I must thank IT people of our department for all the technical supports: **Nils** and **Sjozef.**

I am grateful to **Dr. Behnaz Zarbakhsh** who opened the doors to me and guide me to reach to my carrier goals. **Khale Behnaz**, you are such a valuable person; not only to me, but also to all your other students.

Number of lovely family and friends who deserve some big hugs and thanks; **Ludwig and Klaasje** (Thanks to be like a real family to me)**, Annique and Wim, Reihane, Setare, Arian, Somi, Nasrin, Erfan, Sepehr, Tania, Faranak, Reza, Rick, Levien, Henry, Terry, Bita, Sanaz, Mandana.**

At the end, I want to thank my dear family:

My mother for her endless love, and support. **Maman Ziba** to you I am forever indebted. **Nooshin, Alireza, Neda, Soroush, Ronak, Ati, and Ebi** words cannot adequately express

how much you mean to me. I am truly lucky and blessed to have you in my life. **Marco,** you have supported me through all the intense times particularly associated with the last year of my study. I think even a higher than a doctorate degree should be devoted to you;). I am grateful to you for everything that you have done for me. You deserve the best of the world.

With love

Aida